2018

Investigating the Role of Nicotinic Acetylcholine Receptor Agonists in Lung Cancer Progression and Chemosensitivity in the Context of Treating Chemotherapy-Induced Peripheral Neuropathy

Sarah L. Kyte
Virginia Commonwealth University

Investigating the Role of Nicotinic Acetylcholine Receptor Agonists in Lung Cancer Progression and Chemosensitivity in the Context of Treating Chemotherapy-Induced Peripheral Neuropathy

A dissertation submitted in partial fulfillment of the requirements for the degree of Doctor of Philosophy at Virginia Commonwealth University

by

Sarah Lauren Kyte

Bachelor of Science, Christopher Newport University, 2014

Director: Dr. David A. Gewirtz, Professor,

Department of Pharmacology & Toxicology

Virginia Commonwealth University

Richmond, Virginia

July 2018

ACKNOWLEDGMENT

I would like to begin by thanking my doctoral committee: Dr. David Gewirtz, Dr. Imad Damaj, Dr. John Bigbee, Dr. Hamid Akbarali, and Dr. Xianjun Fang. Each of you have played a significant role in my education and in the progression of my project. I greatly appreciate your expertise and mentorship.

My participation in the CIPN project began when I rotated in Dr. Damaj's laboratory. Both him and his lab members, especially Dr. Deniz Bagdas and Dr. Wisam Toma, introduced me to animal research. I am incredibly grateful for their assistance and patience. As collaborators on the neuropathy project, Wisam and I have been on this journey together from the very first experiment. I have been blessed to work with a fellow scientist who is not only a great team player, but also a brother in Christ. The behavioral pharmacology skills that he shared strengthened my understanding and ability to perform *in vivo* studies, while his knowledge of God and His word provided great support. Most of all, I am thankful for the guidance of Dr. Damaj. He made great efforts to ensure that I continued learning about neuroscience and pain even as my project focused on cancer. I appreciate the time that he has devoted to my growth as a scientist and his continuous encouragement.

I first met my mentor, Dr. Gewirtz, when interviewing for the Biomedical Sciences Doctoral Portal at VCU. I recall being in awe of how passionate and optimistic he was about his work, traits that I admired and had hopes of acquiring. Dr. Gewirtz' love of science has only grown since then. I will never forget the valuable lessons that he has shared with me regarding both research and life. I have been truly blessed to have a

mentor who not only taught me to become an independent scientist, but who also cared for my well-being.

I cannot express how happy I am to be a part of the Gewirtz Lab family. It all began when I met Tareq Saleh on my first day. I remember finding him working in the hood when he asked me if I had any experience in cell culture, which I hadn't at the time. Tareq was enthusiastic to show me the ropes, teaching me every aspect of *in vitro* assays and cancer biology. I am grateful that I had the opportunity to work with such a passionate and intelligent scientist. Yet, I am most thankful for his friendship, as he is a constant source of laughter, a shoulder to lean on, and a creator of delicious food. Likewise, I have also enjoyed spending time with Liliya Tyutyunyk-Massey, a fellow scientist and friend with great resilience and grace.

I was fortunate to be in the Gewirtz lab when a visiting graduate student, Jingwen Xu, joined us. Not only was she a hardworking scientist, but it was a pleasure to be around someone who exuded so much joy and peace. I have also been lucky to work alongside my friend Nipa Patel, with her easygoing nature and good sense of humor. More recently, I have enjoyed mentoring one of our undergraduate lab members, Tammy Tran, who is quick to learn and always has a smile on her face. I couldn't have asked for a more dedicated and sweet lab mate. Although our time together has been short, it has been great getting to know Valerie Carpenter. Her spunk and candor will always be something that I admire. I'd also like to acknowledge our brother from another lab, Dr. Emmanuel Cudjoe, who always brings positive energy and his soothing singing voice. The time that I have spent with all of you, whether it be at a game night or in lab having long chats,

which usually turn into friendly debates, has meant so much to me. I am honored to be a part of such a remarkable group of people.

Lastly, I'd like to acknowledge my friends and family. Thank you to my best friends Sarah DeVed, Melissa Newman, and Eric Ginsburg, who have always been there to lend an ear and make me laugh. Thank you to my family for their unwavering support, especially my grandmother, Dr. Shirley Wiley, and my mom, Teresa West. You have been with me every step of the way and I wouldn't have been able to thrive without your words of wisdom, encouragement, and love. Most importantly, I thank God for equipping me with the gifts and determination necessary to succeed and for extending His loving kindness through the people who have been by my side throughout this journey.

TABLE OF CONTENTS

LIST OF TABLES

LIST OF FIGURES

LIST OF ABBREVIATIONS

ABC	Avidin-Biotin Complex
ACh	Acetylcholine
Akt/PKB	Protein kinase B
ANOVA	Analysis of variance
AO	Acridine orange
ATP	Adenosine triphosphate
AV/PI	Annexin V/Propidium Iodide
Bcl-2	B-cell lymphoma 2 protein
BrdU	Bromodeoxyuridine
CaMKII	Ca2+/calmodulin-dependent protein-kinase II
CCI	Chronic constriction injury
CCK-8	Cell counting kit-8
CFA	Complete Freund adjuvant
CGRP	Calcitonin gene-related peptide
CHAPS	3-((3-cholamidopropyl) dimethylammonio)-1-propanesulfonate
CIPN	Chemotherapy-induced peripheral neuropathy
CNS	Central nervous system
CRISPR	Clustered regulatory interspaced short palindromic repeats
DAB	3,3'-diaminobenzidine
DMEM	Dulbecco’s modified Eagle’s medium
DMSO	Dimethylsulfoxide
DRG	Dorsal root ganglia
EC	Endothelial cell
EC_{50}	Excitatory concentration to produce a half-maximal response
ELISA	Enzyme-linked immunosorbent assay
ENDS	Electronic nicotine delivery systems
ERK1/2	Extracellular signal-related kinase 1/2
FBS	Fetal bovine serum
FDA	U.S. Food and Drug Administration
FST	Forced swim test
GAPDH	Glyceraldehyde 3-phosphate dehydrogenase
Gy	Gray
HIF-1α	Hypoxia-inducible factor 1-alpha
HRP	Horseradish peroxidase
IC_{50}	Inhibitory concentration to produce a half-maximal response
IENF	Intraepidermal nerve fiber
IL	Interleukin
INFγ	Interferon-gamma

i.p.	Intraperitoneal
Jak-2	Janus kinase-2
JNK	Jun-amino terminal kinase
K_i	Inhibitory constant
LDB	Light/dark box
LDH	Lactate dehydrogenase
LLC	Lewis lung carcinoma
LPS	Lipopolysaccharide
LPS-RS	Lipopolysaccharide from *Rhodobacter sphaeroides*
MAPK	Mitogen-activated protein kinase
MEK	Mitogen-activated protein kinase kinase
MCP-1	Monocyte chemoattractant protein-1
MLA	Methyllycaconitine
MMP	Mitochondrial membrane potential
mPTP	Mitochondrial permeability transition pore
MTS	3-(4,5-dimethylthiazol-2-yl)-5-(3-carboxymethoxyphenyl)-2-(4-sulfophenyl)-2H-tetrazolium
MTT	3-(4,5-dimethylthiazol-2-yl)-2,5-diphenyltetrazolium bromide
NAB	N-nitrosoanabasine
nAChR	Nicotinic acetylcholine receptor
NADH	Nicotinamide adenine dinucleotide (reduced)
NAT	N'-nitrosoanatabine
NFκB	Nuclear factor-κB
NGF	Nerve growth factor
NNAL	4-(methylnitrosamino)-1-(3-pyridyl)-1-butanol
NNK	Nicotine-derived nitrosamine ketone
NNN	N-nitrosonornicotine
NRT	Nicotine replacement therapy
NSCLC	Non–small cell lung cancer
NSF	Novelty suppressed feeding
NSG	NOD *scid* gamma
PARP	Poly (ADP-ribose) polymerase
PBS	Phosphate-buffered saline
PG-VG	Propylene glycol – vegetable glycerin
PI	Propidium iodide
PI3K	Phosphoinositide 3-kinase
p-JNK	Phosphorylated Jun-amino terminal kinase
PKC	Protein kinase C
PLC	Phospholipase C
PNS	Peripheral nervous system
p-p38	Phosphorylated p38
PSNL	Partial sciatic nerve ligation
Rb	Retinoblastoma protein
ROCK	RHO-associated protein kinase
ROS	Reactive oxygen species
s.c.	Subcutaneous

SCLC	Small cell lung cancer
SDS-PAGE	Sodium dodecyl sulfate polyacrylamide gel electrophoresis
SNC	Sciatic nerve constriction
SNL	Spinal nerve ligation
SRC	Proto-oncogene tyrosine-protein kinase
STAT	Signal transducer and activator of transcription
TLR4	Toll-like receptor 4
TNFα	Tumor necrosis factor-alpha
trkA	Tyrosine kinase receptor A
TUNEL	Terminal deoxynucleotidyl transferase dUTP nick-end labeling
VCU	Virginia Commonwealth University
VEGF	Vascular endothelial growth factor
XTT	2,3-Bis(2-methoxy-4-nitro-5-sulfophenyl)-2*H*-tetrazolium-5-carboxanilide inner salt

ABSTRACT

INVESTIGATING THE ROLE OF NICOTINIC ACETYLCHOLINE RECEPTOR AGONISTS IN LUNG CANCER PROGRESSION AND CHEMOSENSITIVITY IN THE CONTEXT OF TREATING CHEMOTHERAPY-INDUCED PERIPHERAL NEUROPATHY

By Sarah Lauren Kyte, B.S.

A dissertation submitted in partial fulfillment of the requirements for the degree of Doctor of Philosophy at Virginia Commonwealth University.

Virginia Commonwealth University, 2018

Director: Dr. David A. Gewirtz, Professor, Department of Pharmacology & Toxicology

While cancer chemotherapy continues to significantly contribute to the number of cancer survivors, exposure to these drugs can often result in chemotherapy-induced peripheral neuropathy (CIPN), a consequence of peripheral nerve fiber dysfunction or degeneration. CIPN is characterized by sensory symptoms in the hands and feet, such as numbness, burning, and allodynia, resulting in an overall decrease in quality of life. Paclitaxel (Taxol), a microtubule poison that is commonly used to treat breast, lung, and ovarian cancers, has been found to cause CIPN in 59-78% of cancer patients. There is currently no effective preventative or therapeutic treatment for this side effect, which can be a dose-limiting factor for chemotherapy or delay treatment. Our collaborators in the laboratory of Dr. M. Imad Damaj have shown that nicotine, a nicotinic acetylcholine receptor (nAChR) agonist, and R-47, an α7 nAChR silent agonist, can prevent and reverse paclitaxel-induced peripheral neuropathy in mice. With regard to cancer, this work demonstrates that nicotine and R-47 do not enhance A549 and H460 human non-small

cell lung cancer cell viability, colony formation, or proliferation alone, and they do not attenuate paclitaxel-induced growth arrest, apoptosis, or DNA fragmentation. Most importantly, nicotine and R-47 do not increase the growth of A549 tumors or interfere with the antitumor activity of paclitaxel in tumor-bearing mice. These data suggest that targeting nAChRs may be a safe and efficacious approach for the prevention and treatment of CIPN in cancer patients.

INTRODUCTION

A. Chemotherapy-Induced Peripheral Neuropathy (CIPN)

Chemotherapy has played a significant role in the treatment and survival of cancer patients. However, this pharmacological approach can lead to long-term symptoms of drug toxicity, including chemotherapy-induced peripheral neuropathy (CIPN), a result of peripheral nerve fiber dysfunction or degeneration. CIPN is characterized by sensory symptoms in the hands and feet, including: numbness, tingling, burning pain, hyperalgesia, and allodynia. Despite various chemotherapy drug classes and dosing regimens, approximately 68% of cancer patients experience CIPN in less than a month following the completion of their treatment, whereas 30% suffer from symptoms of CIPN for 6 months or more after chemotherapy (Seretny *et al.*, 2014). There is currently no effective preventative or therapeutic treatment for CIPN; anticonvulsants, antidepressants, and anesthetics only perform modestly in relieving CIPN-induced neuropathic pain in cancer patients (Majithia *et al.*, 2016). CIPN can present during chemotherapy administration, thereby becoming a dose-limiting factor for chemotherapy or even delay treatment. Without the development of an efficacious therapy, CIPN will continue to negatively impact cancer patient survival and quality of life.

Paclitaxel, a taxane commonly used to treat breast, lung, and ovarian cancers, has been found to cause CIPN both acutely and chronically in 59-78% and 30% of cancer patients, respectively (Beijers *et al.*, 2012). Although much research has been performed to determine how paclitaxel and other cancer chemotherapy drugs (cisplatin, oxaliplatin, vincristine, bortezomib) can induce CIPN, the mechanism remains to be completely

understood. The predominant hypotheses for paclitaxel's mechanism of action in causing neuropathy are built upon the drug's ability to induce mitochondrial dysfunction and an inflammatory response.

A.1. Paclitaxel-Induced Mitochondrial Dysfunction

Atypical mitochondria, characterized as swollen and vacuolated, have been observed in the peripheral nerves of preclinical paclitaxel-induced neuropathy models and in the nerves of patients with peripheral neuropathy (Dalakas *et al.*, 2001; Flatters and Bennett, 2006). It is thought that paclitaxel can negatively impact mitochondrial function by opening the mitochondrial permeability transition pore (mPTP) after binding to β-tubulin, a protein within the mitochondrial membrane that is associated with the mPTP (**Figure 1**). The mPTP is formed along the inner mitochondrial membrane under pathological conditions and its opening is normally regulated by electron flux and the proton electrochemical gradient. mPTP opening can lead to mitochondrial swelling, when influx from the cytoplasm increases the volume-to-surface ratio, causing the rod-like shape of the organelle to become more spherical (Xie *et al.*, 2005). In addition, calcium is released into the cytoplasm and the mitochondrial membrane potential (MMP) decreases, a phenomenon that will ultimately close the mPTP. Atypical mitochondria present simultaneously with mechanical hypersensitivity, indicating that there may be a causal relationship between these two consequences of paclitaxel exposure.

Mitochondria produce reactive oxygen species (ROS) when the rates of electron entry into and transfer through the electron transport chain are not balanced. Paclitaxel induces an increase in intracellular calcium, which leads to insufficient calcium concentrations

inside the mitochondria and a decrease in adenosine triphosphate (ATP) production since calcium is required for the activation of dehydrogenase enzymes in the citric acid cycle (Hajnoczky *et al.*, 2002). Dysfunctional oxidative phosphorylation within the mitochondria results in ROS production, which can lead to the activation of caspases and apoptotic cell death (Alirezaei *et al.*, 2011). ROS generated by paclitaxel-induced atypical mitochondria may be contributing to CIPN since neurons have a high metabolic rate, low antioxidant supply, and are post-mitotic, making them more susceptible to the toxic effects of ROS (Lee *et al.*, 2012). For example, mitochondrial ROS are increased in the neurons of the dorsal horn of the spinal cord following spinal nerve ligation (SNL) in rats, which is thought to contribute to central sensitization and therefore sensory symptoms (Park *et al.*, 2006). In addition, administration of *N*-tert-butyl-α-phenylnitrone, a non-specific ROS scavenger, can reverse both SNL- and paclitaxel-induced mechanical allodynia in rats (Kim *et al.*, 2004; Fidanboylu *et al.*, 2011).

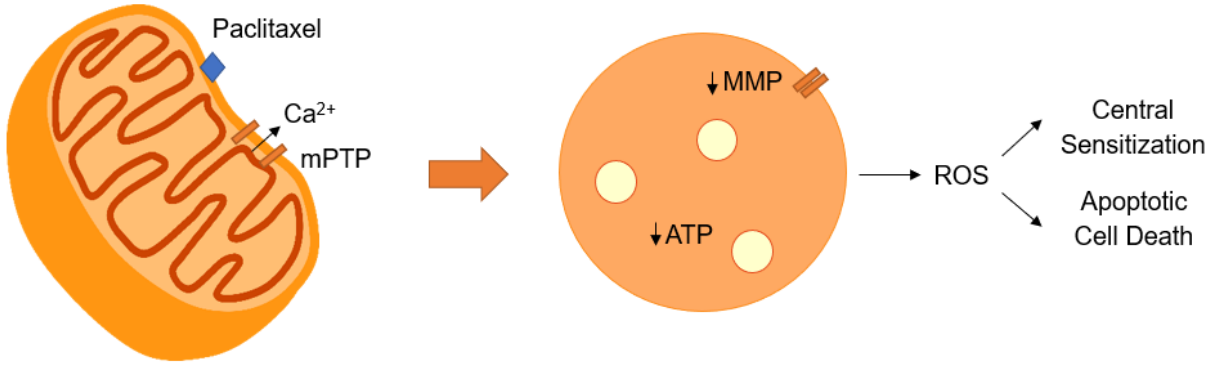

Figure 1. Paclitaxel induces mitochondrial dysfunction. When paclitaxel binds to the β-tubulin of the mitochondrial membrane, the associated mitochondrial permeability transition pore (mPTP) opens to release calcium into the cytoplasm; a reduction in intraorganelle calcium causes the mitochondrial membrane potential (MMP) to collapse, ultimately leading to closure of the mPTP. Influx through the mPTP causes mitochondrial swelling and vacuolization. The loss of calcium leads to reduced production of adenosine triphosphate (ATP) by the citric acid cycle. As a result, reactive oxygen species (ROS) are released by the dysfunctional organelle to ultimately initiate the intrinsic apoptotic pathway and possibly contribute to central sensitization proximal to the injured neuron.

A.2. Paclitaxel-Induced Inflammation

The second hypothesis relating to paclitaxel's neurotoxic mechanism of action involves an inflammatory response. The immune system consists of various cell types, one of which is the macrophage, a white blood cell that phagocytoses cellular debris and releases inflammatory mediators upon stimulation by various molecules, such as interferon-gamma (IFNγ) and lipopolysaccharide (LPS). Paclitaxel has been shown to mimic the agonistic activity of LPS at toll-like receptor 4 (TLR4) in macrophages, resulting in the production of pro-inflammatory cytokines (**Figure 2**). In preclinical models of paclitaxel-induced neuropathy, macrophages have been observed in the peripheral nervous system, specifically in the dorsal root ganglia (DRG), as well as in the central nervous system along with the resident microglia in the dorsal horn of the spinal cord (Polomano *et al.*, 2001; Liu *et al.*, 2010). In addition, paclitaxel increases the expression of TLR4 in both the DRG and the spinal cord. Mice and rats that do not possess TLR4 (knockout) or that have been treated with TLR4 antagonists exhibit decreases in hyperalgesia, spinal glial responses to inflammation, and macrophage infiltration (Zhang *et al.*, 2016). Paclitaxel also enhances the expression of monocyte chemoattractant protein-1 (MCP-1) in both the DRG and spinal cord. When this activity is inhibited by an anti-MCP-1 antibody or MCP-1 receptor knockout, paclitaxel-induced mechanical allodynia, macrophage recruitment, and loss of distal intra-epidermal nerve fibers are attenuated (Zhang *et al.*, 2013). Suppression of paclitaxel-induced peripheral neuropathy in rats with interleukin-10 (IL-10), an anti-inflammatory cytokine, is associated with a decrease in CD11b-positive (macrophage) immune cell recruitment, as well as reduced

tumor necrosis factor α (TNFα) and IL-1β expression in the lumbar DRG (Ledeboer *et al.*, 2007).

When paclitaxel binds to TLR4 in macrophages, DRG, and the dorsal horn of the spinal cord, downstream signaling cascades are initiated, including the mitogen-activated protein kinase (MAPK) pathway, which results in the activation of extracellular signal-related kinases (ERK1/2), p38 MAPK, and Jun-amino terminal kinase (JNK) (Y Li *et al.*, 2015). The phosphorylation and activation of these transcription factors causes synthesis and release of pro-inflammatory cytokines, such as IFNα/γ, TNFα, IL-1, and IL-6. Phosphorylated ERK1/2 and p38 MAPK have been found in the DRG following paclitaxel administration, and this effect was reversed by the TLR4 antagonist lipopolysaccharide from *Rhodobacter sphaeroides* (LPS-RS). Behavioral phenotypes of paclitaxel-induced neuropathy are reduced after the administration of MEK1/2 (upstream of ERK1/2) and p38 MAPK inhibitors (Y Li *et al.*, 2015). Ligation of the L5 spinal nerve induces p38 MAPK activation in both the spinal microglia and the DRG; an inhibitor of p38 MAPK activity, SB203580, abrogates SNL-induced mechanical allodynia (Jin *et al.*, 2003). In summary, it appears that paclitaxel could be inducing an inflammatory response via activation of macrophages, an action of the drug that is associated with CIPN.

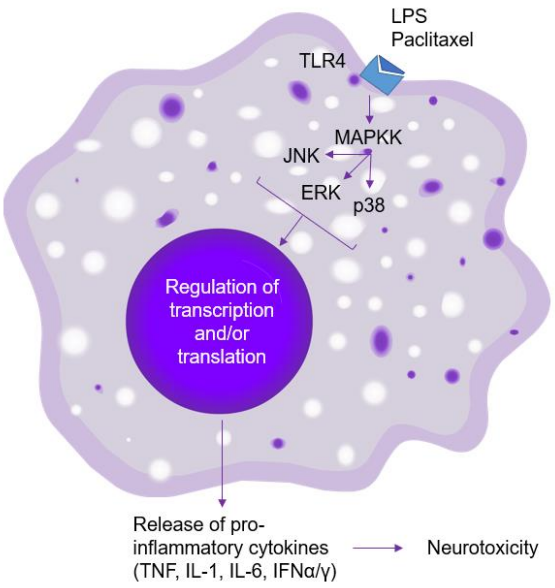

Figure 2. Paclitaxel induces pro-inflammatory cytokine release from macrophages. Toll-like receptor 4 (TLR4) agonists, including lipopolysaccharide (LPS) and paclitaxel, stimulate multiple mitogen-activated protein kinases (MAPKs) that regulate the transcription and translation of pro-inflammatory mediators, such as tumor necrosis factor (TNF), various interleukins (IL), and interferon (IFN). These cytokines can prevent neurogenesis and/or cause cytotoxicity in nearby neurons.

Overall, paclitaxel may be inducing mitochondrial dysfunction and/or a pro-inflammatory response, both of which can contribute to neuronal toxicity and sensitization. Continuing to determine how the neurotoxicity develops is important but can be a long and complex process. Therefore, we chose a different strategy, which was to identify a drug or class of drugs that could prevent and/or reverse CIPN due to its analgesic and perhaps anti-inflammatory properties. We could then deduce the specific mechanism of action (the receptor involved, the anatomical expression of said receptor, etc.) and further enhance efficacy of the CIPN therapy, if possible, by targeting a specific receptor subtype. This project was initiated in the laboratory of Dr. M. Imad Damaj at Virginia Commonwealth University, where a model of paclitaxel-induced peripheral neuropathy established in mice (**Chapter 1**) was utilized to test nicotinic acetylcholine receptor (nAChR) agonists as potential treatments for CIPN (**Chapters 2 and 4**).

B. Nicotinic Acetylcholine Receptors (nAChRs) as a Therapeutic Target for CIPN

Nicotinic acetylcholine receptors (nAChRs) are pentameric ligand-gated ion channels located on the membranes of various cell types within the central and peripheral nervous systems, including sensory neurons, as well as in muscle, tumor tissues, and immune cells. These receptors can be homo- or heteromeric, depending on the combination of the different subunits; for neuronal nAChRs, the possible subunits are α2-7, α9-10, and β2-4. When an agonist binds to a nAChR, a conformational change allows for the influx of sodium and calcium ions. In neurons, this ion flux results in depolarization of the cell and initiation of an action potential. However, other downstream signaling pathways of nAChRs may contribute to additional actions of the agonists, including analgesia.

Nicotine, an agonist of nAChRs, has been shown to produce analgesic and antinociceptive properties in humans and animals, respectively [see reviews by (Umana *et al.*, 2013; Flood and Damaj, 2014)]. For example, nonsmokers with spinal cord injuries reported lower complex pain scores (both neuropathic and musculoskeletal symptoms) following nicotine gum use (Richardson *et al.*, 2012). Likewise, patients receiving acute intranasal nicotine had lower post-operative pain scores and decreased their morphine consumption (Flood and Daniel, 2004). Similar observations with nicotine have also been made in rodents. For instance, nicotine has produced significant dose-dependent antinociceptive effects in mice during the tail-flick and hot-plate assays, as well as reductions in paw licking during both phases of the formalin test, signifying its ability to alleviate pain induced by both thermal and inflammatory stimuli (AlSharari *et al.*, 2012). With regard to neuropathic pain, nicotine has been shown to reverse mechanical allodynia

in a rat chronic constriction injury (CCI) model, and reverse both cold and mechanical allodynia following oxaliplatin treatment (Di Cesare Mannelli *et al.*, 2013). Nicotine and other nicotinic agonists are thought to relieve pain via nicotinic modulation, predominantly of the α7 subtype, in the descending pain transmission pathway (Umana *et al.*, 2017).

C. nAChRs and Cancer

Before nicotine could be thoroughly investigated as a potential CIPN therapy, we had to consider the actions of the drug in cancer models, those that would represent the cancer patient population suffering from CIPN. An ideal neuropathy treatment would be administered prior to and during cancer chemotherapy in order to protect the peripheral nerves from degeneration and/or alterations in function. In this scenario, the patients would have proliferating cancer cells; therefore, it would be beneficial for any adjuvant therapy to possess anti-tumor properties. If that were not possible, then it would be necessary to demonstrate that the neuroprotective compound does not enhance cancer progression or negatively impact chemosensitivity.

Taking these parameters into consideration, investigating nicotine as a CIPN therapy may be challenging since the scientific literature suggests that binding of nAChR agonists on the plasma membrane of a tumor cell activates the receptor, which could promote proliferative and anti-apoptotic signaling (**Figure 3**; Grando, 2014). Preclinical studies testing this hypothesis have been conducted, albeit under different experimental conditions. Our analysis of the literature on nicotine and its role in lung cancer in **Chapter 3** summarizes what is known relating to nicotine, cancer progression, and cancer chemotherapy, and compares the methodology and results of numerous studies in order

to identify remaining knowledge gaps. Overall, we discovered that various effects of nicotine in lung cancer cell lines and lung tumor-bearing mice have been reported in the literature, ranging from enhancing growth to having no significant effect to even decreasing proliferation. With regard to human studies, it has been reported that nicotine replacement therapy (NRT), specifically nicotine gum, is not a significant predictor of any cancer type, which is in contrast with cigarette smoking that is predictive of lung cancer (Murray *et al.*, 2009). While it can be assumed that this finding would be the most reliable when considering how nicotine would impact patients in the clinic, it is important to consider that the study participants began NRT when cancer-free. Therefore, our work with nicotine in cell culture and in animal models of cancer are necessary to predict if nicotine and other nAChR agonists could be viable CIPN treatments.

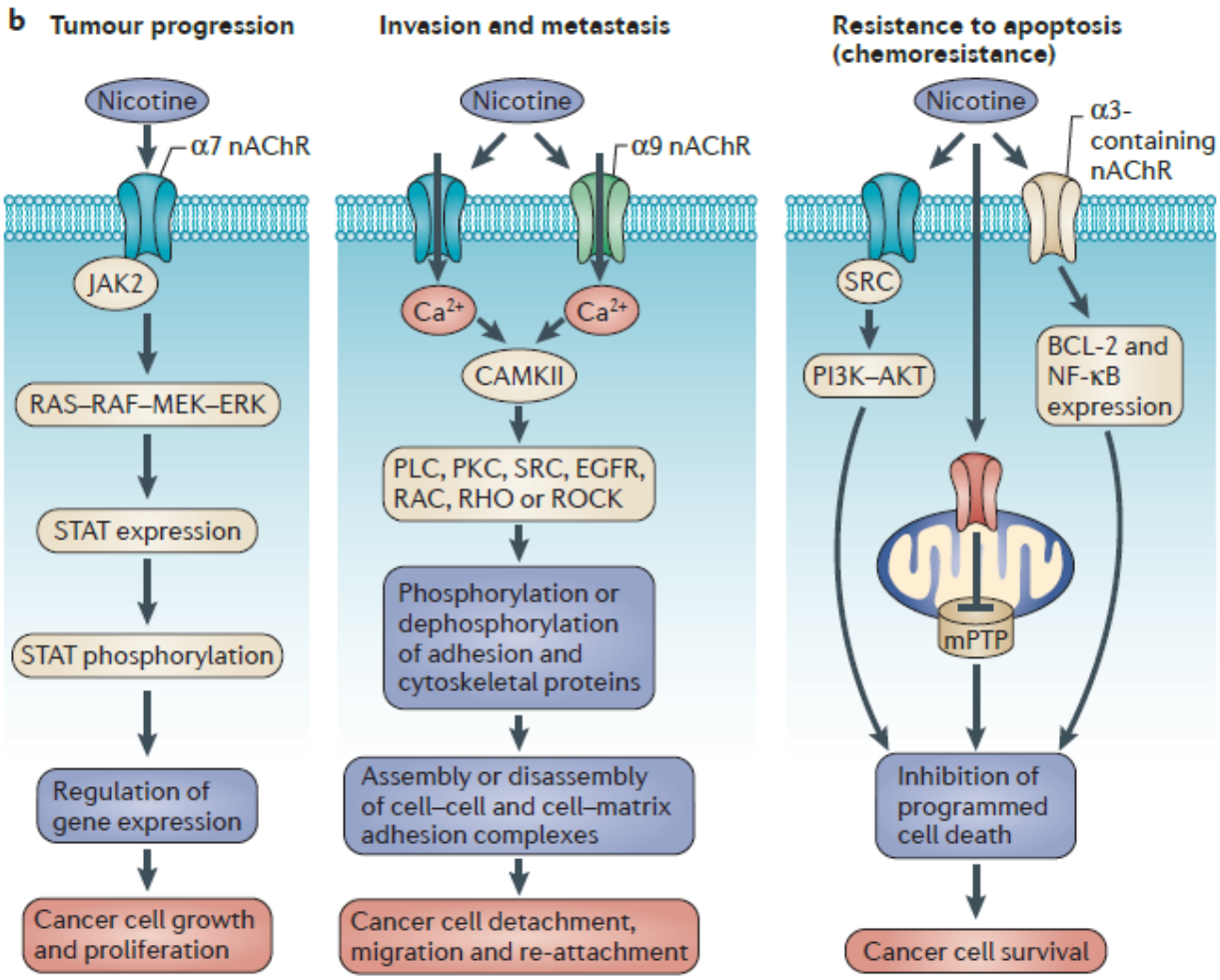

Figure 3. Nicotinic acetylcholine receptor downstream signaling pathways thought to facilitate the pro-tumor effects of nicotine in cancer. Akt, protein kinase B; Bcl-2, B-cell lymphoma 2 protein; CaMKII, Ca2+/calmodulin-dependent protein-kinase II; Jak2, Janus kinase 2; MEK, mitogen-activated protein kinase kinase; mPTP, mitochondrial permeability transition pore; NF-κB, nuclear factor-κB; PI3K, phosphoinositide 3-kinase; PKC, protein kinase C; PLC, phospholipase C; ROCK, RHO-associated protein kinase; STAT, signal transducer and activator of transcription. Adapted from (Grando, 2014).

D. Dissertation Aims

We hypothesize that nicotine, and specific nicotinic acetylcholine receptor (nAChR) agonists, may be effective in preventing and reversing chemotherapy-induced peripheral neuropathy without enhancing lung tumor growth or interfering with the antitumor efficacy of the chemotherapy drug paclitaxel.

Specific Aim 1: To determine if nAChR agonists enhance the proliferation of lung cancer cells. In order to test if nicotine and selective nAChR agonists, such as the α7 nAChR silent agonist R-47, are capable of enhancing the proliferation of lung cancer cells, we evaluated the effect of these drugs on cell viability, colony formation, and rate of growth in two human non-small cell lung cancer (NSCLC) cell lines, A549 and H460. These cell lines were chosen since paclitaxel is commonly used to treat NSCLC and because they express nAChRs (Dasgupta *et al.*, 2006; Ettinger *et al.*, 2010; Yoo *et al.*, 2014). To assess if these findings translate to an animal model, we administered the nAChR agonists in two lung tumor-bearing mouse models, murine Lewis lung carcinoma (LLC) cells in C57BL/6J mice and human A549 cells in NOD *scid* gamma (NSG) mice, to determine their influence on tumor volume and tumor weight.

Specific Aim 2: To ensure that nAChR agonists do not interfere with the antitumor properties of paclitaxel in lung cancer. We determined if nAChR agonists would cause any interference with the effectiveness of the cancer chemotherapy drug paclitaxel by evaluating the extent of NSCLC cell growth arrest, apoptosis, and DNA fragmentation. The tumor-bearing mice described in Aim 1 were also treated with nAChR agonists and

paclitaxel in combination to determine if the former would prevent or attenuate paclitaxel-induced reductions in tumor volume and tumor weight. In addition, tumors were excised from mice treated with paclitaxel alone or in combination with the nAChR agonist in order to assess intratumoral apoptosis with immunohistochemical staining for the apoptotic marker cleaved poly (ADP-ribose) polymerase (PARP).

As an introduction to our CIPN animal model, Chapter One describes the establishment and characterization of paclitaxel-induced peripheral neuropathy in the mouse. This model reflects the physical and behavioral aspects of CIPN observed in cancer patients and was therefore utilized in Chapters Two and Four when testing the effects of nicotinic acetylcholine receptor agonists on the development and maintenance of CIPN. The results of these neuropathy studies provided the rationale for investigating the influence of said drugs on cancer progression and chemosensitivity, as shown in Chapters Two, Three, and Four, which is crucial if these compounds are to be used as preventative and/or therapeutic treatments for CIPN in cancer patients.

CHAPTER ONE

Effects of Paclitaxel on the Development of Neuropathy and Affective Behaviors in the Mouse

Wisam Toma[1], S. Lauren Kyte[1], Deniz Bagdas, Yasmin Alkhlaif, Shakir D. Alsharari, Aron H. Lichtman, Zhi-Jian Chen, Egidio Del Fabbro, John W. Bigbee, David A. Gewirtz, M. Imad Damaj

[1]These authors contributed equally to this work.

Departments of Pharmacology and Toxicology (W.T., S.L.K., D.B., Y.A., A.H.L., D.A.G., M.I.D.), Neurology (Z.C.), Internal Medicine (E.D.), Anatomy and Neurobiology (J.W.B.), and Massey Cancer Center (D.A.G.), Virginia Commonwealth University, Richmond, Virginia; Experimental Animals Breeding and Research Center (D.B.), Uludag University, Bursa, Turkey; Department of Pharmacology and Toxicology (S.D.A.), King Saud University, Riyadh, Saudi Arabia

Disclosure #1: The work included in this chapter has been published in Neuropharmacology (117:305-315, February 2017).

Disclosure #2: The experiments included in this work were performed in the laboratory of Dr. M. Imad Damaj, primarily by Dr. Wisam B. Toma. S. Lauren Kyte performed the nesting and novelty suppressed feeding assays.

A. Introduction

Various neoplastic diseases, such as breast, lung, and ovarian cancer, are commonly treated with paclitaxel, a chemotherapeutic drug in the taxane class. The anti-tumor effect of paclitaxel is mediated through its binding to microtubules of the cytoskeleton and enhancement of tubulin polymerization, thereby resulting in cell cycle arrest, and ultimately apoptotic cell death (Jordan and Wilson, 2004). Although paclitaxel effectively increases both progression-free survival and overall survival in cancer patients, it also produces painful sensory and emotional deficits (Seretny *et al.*, 2014; Dranitsaris *et al.*, 2015). Specifically, paclitaxel causes chemotherapy-induced peripheral neuropathy (CIPN), a result of peripheral nerve fiber dysfunction or degeneration, acutely in 59-78% of cancer patients and chronically in 30% of cancer patients (Beijers *et al.*, 2012). CIPN is characterized by sensory symptoms such as numbness, tingling, cold and mechanical allodynia, as well as an overall decrease in quality of life. In addition, cancer patients receiving chemotherapy experience behavioral symptoms including fatigue, anxiety, and depression. For example, approximately 58% of cancer patients suffer from depression, while anxiety is prevalent in approximately 11.5% of the cancer patient population (Massie, 2004; Mehnert *et al.*, 2014). Importantly, patients with comorbidities of depression and anxiety suffer from increased severity of symptoms and experience delayed recovery, which may interfere with positive outcomes (Massie, 2004). In

comparison, 34% and 25% of the general population of patients experiencing neuropathic pain report respective feelings of depression and anxiety (Gustorff *et al.*, 2008).

It is clear that there is a critical need to determine the mechanisms underlying these behavioral symptoms elicited by cancer chemotherapy drugs, as well as to identify new targets to prevent or treat these side effects. A necessary requisite to accomplish these aims is to establish relevant preclinical models of chemotherapy-induced side effects. However, to our knowledge there are presently no published preclinical studies that have characterized paclitaxel-induced affective-like behaviors. Thus, the objectives of the current study were to develop a mouse model of paclitaxel-induced side effects. Multiple assessments of nociceptive and affective-related behaviors were performed in mice treated with one cycle of paclitaxel (i.p., every other day for a total of four injections). After determining the dose-response curve and time-course of paclitaxel-induced mechanical and cold allodynia following systemic administration in mice, the impact of paclitaxel was assessed on multiple affective behavioral phenotypes in individual cohorts of mice, such as nest building, anxiety- (light/dark box test, novelty suppressed feeding), depression- (forced swim test), and anhedonia- (sucrose preference test) related behaviors. In addition, studies investigated the nociceptive effect of carboplatin treatment alone and in combination with paclitaxel due to the use of the carboplatin-paclitaxel combination in the clinic.

B. Materials and Methods

Animals. Adult male C57BL/6J mice (8 weeks at beginning of experiments, 20-30 g) were purchased from The Jackson Laboratory (Bar Harbor, ME). A total of 197 mice were used,

with 84 used to assess nociceptive effects and 113 used to assess affective-like behaviors. Mice were housed in an AAALAC-accredited facility in groups of four, then individually housed for the duration of the nesting, novelty suppressed feeding (NSF), and sucrose preference assays in order to accurately assess the ability of each individual mouse to nest, and to measure the food or sucrose consumed by each individual mouse. Mice were group-housed for all other behavioral assays. Food and water were available ad libitum, except when under the food restrictions of the NSF assay. The mice in each cage were randomly allocated to different treatment groups. All behavioral testing on animals was performed in a blinded manner; behavioral assays were conducted by an experimenter blinded to the treatment groups. Experiments were performed during the light cycle (7:00 am to 7:00 pm) and were approved by the Institutional Animal Care and Use Committee of Virginia Commonwealth University and followed the National Institutes of Health Guidelines for the Care and Use of Laboratory Animals. Animals were euthanized via CO_2 asphyxiation, followed by cervical dislocation. Any subjects that showed behavioral disturbances unrelated to chemotherapy-induced pain were excluded from further behavioral testing. Animal studies are reported in compliance with the ARRIVE guidelines (Kilkenny *et al.*, 2010).

Drugs. Paclitaxel and carboplatin were purchased from Tocris (Bristol, United Kingdom). Paclitaxel was dissolved in a mixture of 1:1:18 [1 volume ethanol/1 volume Emulphor-620 (Rhone-Poulenc, Inc., Princeton, NJ)/18 volumes distilled water]. Carboplatin was dissolved in 0.9% saline. All injections were administered intraperitoneally (i.p.) in a volume of 1 ml/100 g body weight.

Induction of CIPN model. In the clinic, low-dose paclitaxel therapy consists of administering 80 mg/m^2 intravenously once every week; the duration of treatment is dependent upon disease progression and limiting toxicity (Seidman *et al.*, 2008). To mimic this low-dose regimen, our studies involved i.p. injections of 2, 4, or 8 mg/kg paclitaxel every other day for a total of four injections (1 cycle), resulting in a cumulative human equivalent dose of 28.4-113.5 mg/m^2 (Reagan-Shaw *et al.*, 2008). A low-dose regimen (8 mg/kg, 1 cycle) results in long-term mechanical allodynia, which better represents the clinical manifestation of peripheral neuropathy, and allows for affective-related behavioral measures to not be obscured by severe motor deficits and weight loss. When referring to the time at which affective behavioral assays were conducted, "post-paclitaxel injection" refers to the time after the first of four paclitaxel injections.

Immunohistochemistry and quantification of intra-epidermal nerve fibers (IENFs). The staining procedure was based on a previously described method of Bennett *et al.*, (2011) with modifications. The glabrous skin of the hind paw was excised, placed in freshly prepared 4% paraformaldehyde in 0.1 M PBS (pH 7.4), and stored overnight at 4˚C in the same fixative. The samples were embedded in paraffin and sectioned at 25 µm. Sections were deparaffinized, washed with PBS, and incubated at room temperature for 30 min in blocking solution (5% normal goat serum and 0.3% Triton X-100 in PBS). Sections were incubated with a 1:1000 dilution of the primary antibody, PGP9.5 (Fitzgerald - cat# 70R-30722, MA, USA) overnight at 4˚C in a humidity chamber. Following phosphate buffer saline (PBS) washes, sections were incubated for 90 min at

room temperature with a 1:250 dilution of goat anti-rabbit IgG (H+L) secondary antibody conjugated with Alexa Fluor® 594 (Life Technologies - cat# A11037, OR, USA). Sections were mounted in Vectashield (Vector Laboratories, Burlingame, CA, USA) and examined using a Zeiss Axio Imager A1 – Fluorescence microscope (Carl Zeiss, AG, Germany). Sections were examined in a blinded fashion under 63x magnification. The IENFs in each section were counted in a blinded fashion and the density of fibers is expressed as fibers/mm. An individual cohort consisting of 6 mice per group was used.

Cycles of paclitaxel. To investigate the impact of paclitaxel treatment on peripheral sensitization following repeated cycles, we used the lowest paclitaxel dose in this study for a total of two cycles. Mice were injected with vehicle or paclitaxel (2 mg/kg) for each cycle. Mechanical thresholds were evaluated between the days of injection and subsequently once per week. The second cycle of treatment began one week after the first cycle. An individual cohort consisting of 6 mice per group was used.

Carboplatin-paclitaxel treatment. In this study, we first investigated if carboplatin, which is often used in combination with paclitaxel for chemotherapeutic intervention, would induce allodynia in mice on its own after systemic administration. To explore the effect of carboplatin on changes in nociceptive behavior, mice were injected with carboplatin (0, 5, or 20 mg/kg) for 1 cycle and tested for 7 days. In a separate experiment, we studied the impact the carboplatin treatment on paclitaxel-induced allodynia using the sequence of carboplatin-paclitaxel administration. Mice were first injected with carboplatin (5 mg/kg, 1 cycle), then another cycle of injections was administered with a low dose of paclitaxel

(1 mg/kg). The second cycle of treatment (paclitaxel, 1 mg/kg) began one week following the first cycle (carboplatin, 5 mg/kg). Mechanical thresholds were evaluated between the days of injection. An individual cohort consisting of 6 mice per group was used.

Assessment of nociceptive behavior. An individual cohort consisting of 6 mice per group was used for the assessment of mechanical and cold allodynia; the mice had a resting period of 24 hours between assays. An additional cohort consisting of 6 mice per group was used for the locomotor activity test to assess potential paclitaxel-induced motor deficits.

Mechanical allodynia evaluation (von Frey test). Mechanical allodynia thresholds were determined using von Frey filaments according to the method suggested by Chaplan *et al.*, (1994) and as described in our previous report (Bagdas *et al.*, 2015). The mechanical threshold is expressed as log10 (10 £ force in [mg]).

Cold allodynia evaluation (acetone test). This test was conducted as previously described (Otrubova *et al.*, 2013), but with slight modifications. Briefly, mice were placed in a Plexiglas cage with mesh metal flooring and allowed to acclimate for 30 min before testing. 10 µl of acetone was projected via air burst from the pipette onto the plantar surface of each hind paw. Time spent licking, lifting, and/or shaking the hind paw was recorded by a stopwatch over the course of 60 s.

Locomotor activity test. The test was performed as described previously in Bagdas *et al.*, (2015). Briefly, mice were placed into individual Omnitech (Columbus, OH) photocell activity cages (28 x 16.5 cm) containing two banks of eight cells each. Interruptions of the photocell beams, which assess walking and rearing, were then recorded for the next 30 min. Data are expressed as the number of photocell interruptions.

Assessment of affective behaviors

Nesting procedure. The nesting procedure was adapted as previously described by Negus *et al.*, (2015) with some modifications. Briefly, mice were housed individually in cages containing corn cob bedding and all previous nesting material was removed from the home cage prior to conducting the nesting assay. For each cage, one compressed cotton nestlet was weighed and cut into 6 rectangular pieces of equal size. The mice were then relocated to a quiet, dark room. After an acclimation period of approximately 30 min, the nestlet pieces were then placed on top of the wire cage lid, parallel to the wire and evenly spaced. The mice were allowed 120 min to nest, after which the weight of the nestlet pieces remaining on the cage lid and the nest quality (0-2; 0 = no nest formed, 1 = some nesting activity, 2 = established nest) was recorded. The percentage of animals that did nest, the amount of nesting material acquired (percent weight used), and the ability to participate in innate murine nesting behavior (nest quality) were determined. The nesting assay was conducted with three individual cohorts of mice: one at 1 week (n = 6 per group), one at 2 weeks (n = 6 per group), and another at both 8 and 11 weeks (n = 6 Veh, n = 7 PAC) post-paclitaxel (8 mg/kg, i.p) or vehicle injection. These specific cohorts

were used for both the nesting and NSF assays, since nesting is not thought to be a stress-inducing task. The mice had a resting period of one week between assays.

Novelty suppressed feeding (NSF). The NSF test measures a rodent's aversion to eating in a novel environment. It assesses stress-induced anxiety by measuring the latency of an animal to approach and eat a familiar food in an aversive environment (Bodnoff *et al.*, 1988). Mice were housed individually in cages with wood-chip bedding and were deprived of food for 24 h. At the end of the deprivation period, the mice were relocated to a quiet, dark room. After an acclimation period of approximately 30 min, the mice were allowed access to an unused, pre-weighed food pellet in a clean test cage containing fresh wood-chip bedding, which was placed directly under a bright light. Each mouse was placed in a corner of the test cage, and a stopwatch was immediately started. The latency to eat (s), defined as the mouse sitting on its haunches and biting the pellet with the use of forepaws, was recorded. The amount of food (g) consumed by the mouse in 5 min was measured, serving as a control for change in appetite as a possible confounding factor. The NSF assay was conducted with two individual cohorts of mice, one at 3 weeks (n = 6 per group) and another at both 9 and 11 weeks (n = 6 Veh, n = 7 PAC) post-paclitaxel (8 mg/kg, i.p.) or vehicle injection. These specific cohorts were used for both the nesting and NSF assays, since nesting is not thought to be a stress-inducing task. The mice had a resting period of one week between assays.

Light/dark box (LDB) test. The light/dark box test is based upon a conflict between the innate aversion to brightly illuminated areas and spontaneous exploratory activity

(Crawley and Goodwin, 1980). The test was adapted as previously described (Wilkerson *et al.*, 2016) with minor modifications. Briefly, the LDB apparatus consisted of a small, enclosed dark box (36 x 10 x 34 cm) with a passage way (6 x 6 cm) leading to a larger, light box (36 x 21 x 34 cm). The mice were acclimated to the testing room for 30 min prior to testing. Mice were placed in the light compartment and allowed to explore the apparatus for 5 min. The number of entries into the light compartment and the total time spent (s) in the light compartment were recorded for 5 min by a video monitoring system and measured by ANY-MAZE software (Stoelting Co., Wood Dale, IL). Individual cohorts of mice (n = 6 per group) were tested at 3, 6, and 9 weeks post-paclitaxel (8 mg/kg, i.p.) or vehicle injection.

Forced swim test (FST). The forced swim test was performed as described previously by Damaj *et al.*, (2004), the common method for assessing depression-like behavior in mice (Bogdanova *et al.*, 2013). Briefly, mice were gently placed into individual glass cylinders (25 x 10 cm) containing 10 cm of water, maintained at 24°C, and left for 6 min. Immobility was recorded (s) during the last 4 min. A mouse was considered to be immobile when floating in an upright position and only making small movements to keep its head above water, but not producing displacements. An individual cohort of mice (n = 6 per group) was tested throughout the FST study at 1, 2, 3, and 4 weeks post-paclitaxel (8 mg/kg, i.p) or vehicle injection.

Sucrose preference. The sucrose preference test is used as a measure of anhedonia-like behavior (Thompson and Grant, 1971). Mice had access to two, 25 ml sipper tubes,

one containing normal drinking water and the other containing a 2% sucrose solution. Mice were housed individually, with access to food, water, and 2% sucrose 24 h per day. Mice were acclimated to the cages with sipper tubes for 3 days prior to injection (days 1-3), during which baseline measurements were taken. Paclitaxel (8 mg/kg, i.p.) or vehicle injections started on day 4. Water and sucrose intake were measured on days 1, 2, 3, 4, 5, and 6, as well as on days 10, 11 and 12. The location of both sipper tubes was switched daily to avoid place preference. Sucrose preference was calculated as a percentage of the volume of 2% sucrose consumed over the total fluid intake volume. An individual cohort of mice (n = 8 per group) was tested during the vehicle/paclitaxel treatment.

Statistical analyses. In the current study, a power analysis calculation was performed with the Lamorte's Power Calculator (Boston University Research Compliance) to determine the sample size of animals for each group (Charan and Kantharia, 2013). For assessing the nociceptive behaviors, the calculation showed that an n of 5 was required to achieve a power of 90% with an alpha error of 0.05; we used 6 mice per group. For the behavioral assays, the calculations showed that an n of 5 for novelty suppressed feeding, an n of 5 for nesting, an n of 8 for the light/dark box test, an n of 6 for the forced swim test, and an n of 8 for sucrose preference was required to achieve a power of 90% with an alpha error of 0.05; we used 6 to 8 mice per group. The data were analyzed with GraphPad Prism software, version 6 (GraphPad Software, Inc., La Jolla, CA) and are expressed as mean ± SEM. Before conducting statistical analyses, normality and variance tests were performed; normality of residuals was determined by the Shapiro-Wilk test for $n > 6$ or the Kolmogorov-Smirnov test for $n \leq 6$, and equal variance was

determined by the F test. Data that did not pass the normality test were analyzed by non-parametric tests, and data that did not have equal variance were analyzed without the assumption of equal standard deviations. Data were normalized to initial vehicle measurements when appropriate. Unpaired t tests were performed to compare behaviors of vehicle- and paclitaxel-treated mice at a single time point. Two-way repeated measure analysis of variance (ANOVA) tests were conducted, and followed by the Bonferroni post hoc test, when behavioral outcomes of vehicle- and paclitaxel-treated mice were being compared over multiple time points. Differences were considered to be significant at $P < 0.05$.

C. Results

Paclitaxel induced changes in nociceptive behaviors in mice

Initial experiments determined the effect of paclitaxel on the development of mechanical and cold allodynia as a function of the drug dose. As anticipated, increased nociceptive responses and duration of effects were related to dose of paclitaxel. However, no significant changes in body weight gain or spontaneous activity were observed. As seen in **Figures 4A and B**, paclitaxel induced both mechanical allodynia [$F_{dose \times time}$ (21, 105) = 9.481, $P < 0.0001$] and cold allodynia [$F_{dose \times time}$ (9, 45) = 14.76, $P < 0.0001$] in dose- and time-related manners, respectively. At 8 mg/kg paclitaxel, mechanical allodynia was observed on day 1 post-paclitaxel injection, and this effect was sustained for more than 90 days (data not shown). On the other hand, 2 and 4 mg/kg paclitaxel induced mechanical allodynia beginning on day 3, and the effects did not differ in terms of magnitude or time to recover. With regard to cold allodynia, paclitaxel presented a clear

dose-dependent induction on day 8 post-paclitaxel injection. However, mice that received 2 or 4 mg/kg paclitaxel recovered by day 22, whereas the 8 mg/kg group continued to exhibit cold allodynia. In regard to general body condition, even the highest dose of paclitaxel (8 mg/kg) did not significantly alter body weight [$F_{\text{dose x time}}$ (5, 25) = 1.093, P > 0.05; **Supplementary Fig. 1A**], or motor coordination [$F_{\text{dose x time}}$ (4, 40) = 0.5204, P > 0.05; **Supplementary Fig. 1B**].

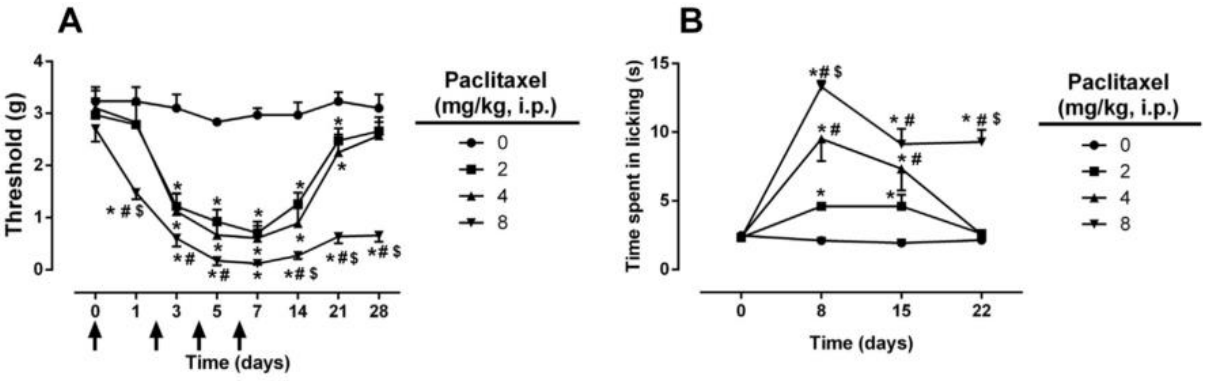

Figure 4. Paclitaxel induces nociceptive behaviors. Paclitaxel doses of 2, 4, and 8 mg/kg (i.p., every other day for a total of 4 injections) induce both mechanical (A) and cold (B) allodynia in a dose and time dependent manner. Arrows indicate vehicle/paclitaxel injections on days 0, 2, 4, and 6. Baseline measurements were taken before vehicle/paclitaxel administration on day 0. The same cohort was tested for both mechanical and cold allodynia; n = 6 per group (data expressed as mean ± SEM). *P < 0.05 vs vehicle; $^{\#}$P < 0.05 vs paclitaxel (2 mg/kg); $^{\$}$P < 0.05 vs paclitaxel (4 mg/kg). BL, baseline.

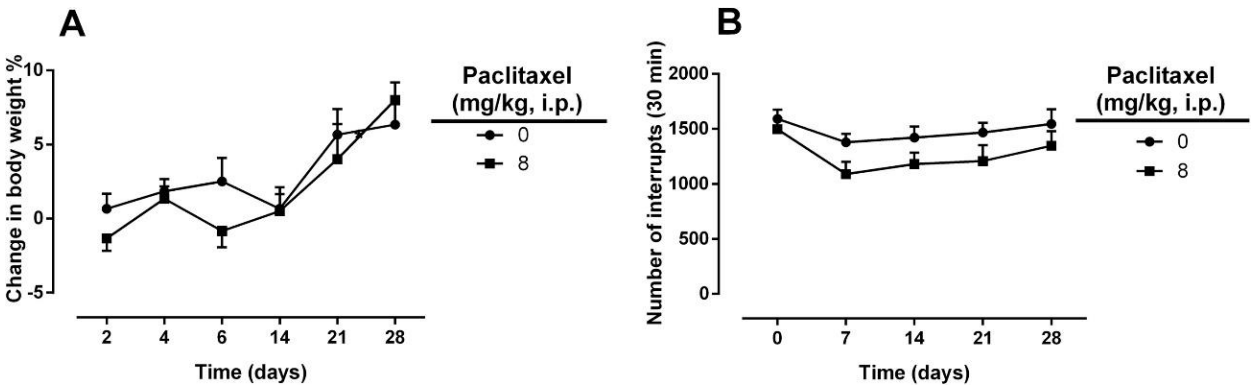

Supplementary Figure 1. Paclitaxel has no effect on body weight and spontaneous activity in mice. One cycle of paclitaxel (8 mg/kg, i.p., every other day for a total of 4 injections) did not cause significant loss of body weight (A) or alteration in motor coordination (B) compared to vehicle-treated mice. Vehicle/paclitaxel injections were administered on days 0, 2, 4, and 6. Baseline measurements were taken before vehicle/paclitaxel administration on day 0. One cohort was tested (n = 6 per group); data expressed as mean ± SEM.

Paclitaxel decreased the density of intra-epidermal nerve fibers (IENFs)

Because changes in the density of peripheral nerve fibers represent a hallmark of CIPN, we studied the changes in peripheral nerve fiber density following paclitaxel treatment using immunohistochemistry. At 28 days post-paclitaxel injection, mice treated with paclitaxel (8 mg/kg, 1 cycle) demonstrated significant reductions in the density of IENFs when compared to vehicle-treated mice [$t = 3.736$, $df = 10$, $P < 0.01$; **Figure 5A**]. Representative immunostained sections of foot pads from vehicle- (**Figure 5B**; upper panel) and paclitaxel-treated mice (**Figure 5B**; lower panel) show the reduction in IENFs following paclitaxel treatment.

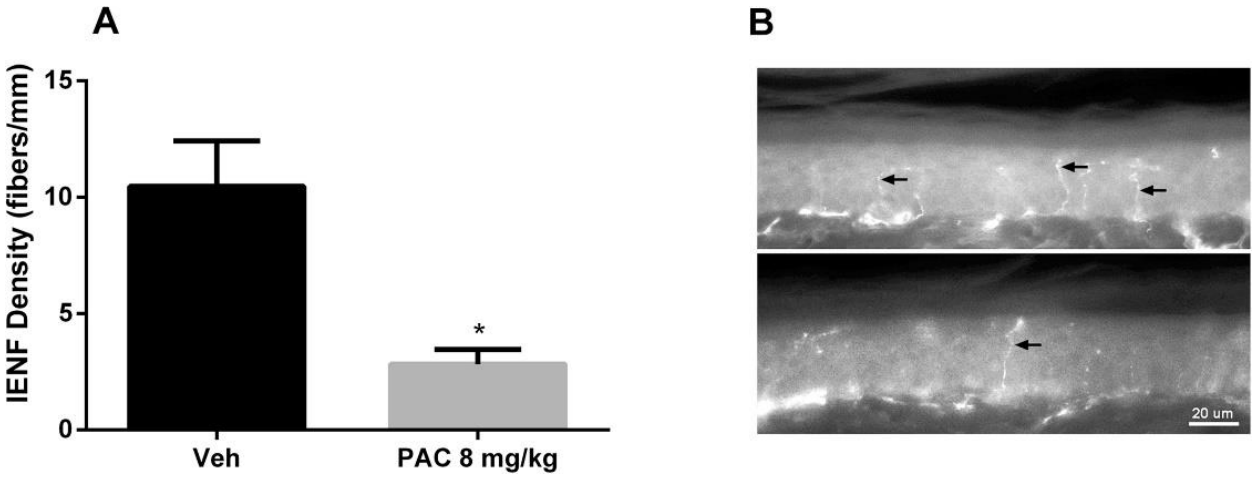

Figure 5. Paclitaxel induces a reduction in intra-epidermal nerve fiber (IENF) density at 28 days post-paclitaxel injection. A) Quantification of IENF density in mice treated with one cycle of paclitaxel (8 mg/kg, i.p., every other day for a total of 4 injections) shows a significant reduction compared to vehicle. One cohort was tested; n = 6 per group (data expressed as mean ± SEM). *P < 0.05 vs vehicle. Veh, vehicle; PAC, paclitaxel. B) Immunostained sections of vehicle- (upper panel) and paclitaxel-treated (lower panel) hind foot pad skin showing the reduction of IENFs (arrows) following paclitaxel treatment. Bar represents 20 microns in both images.

Impact of repeated drug cycles on paclitaxel-induced mechanical allodynia

To investigate the effect of repeated cycles of paclitaxel on mechanical allodynia, mice were injected with two cycles of a low dose of paclitaxel (2 mg/kg). As expected, the first cycle of paclitaxel (2 mg/kg) was capable of inducing mechanical allodynia. Indeed, paclitaxel (2 mg/kg) induced a significant reduction in mechanical threshold that lasted for at least 14 days after the first injection of paclitaxel [$F_{\text{dose x time}}$ (7, 35) = 8.436, P < 0.0001; **Figure 6A**]. After a one-week wash-out period, mice received another cycle of paclitaxel (2 mg/kg). Surprisingly, the effects of paclitaxel were significantly enhanced in the mice subjected to a second cycle, which was demonstrated by a further decrease in mechanical threshold [$F_{\text{dose x time}}$ (3, 15) = 48.61, P < 0.0001; **Supplementary Fig. 2**]. In addition, mice that received a second cycle of paclitaxel treatment (2 mg/kg) displayed a

much longer duration of allodynia (**Figure 6B**) compared to one cycle of treatment (**Figure 6A**) [$F_{\text{dose x time}}$ (13, 65) = 10.97, P < 0.0001; **Figure 6B**]. Whereas mice given one cycle recovered by day 21 post-paclitaxel injection, mice given two cycles recovered by day 63 after the first injection of paclitaxel. Calculation of the area under the curve (AUC) threshold for the initial 28 days of both the first and second cycles of paclitaxel treatment revealed significant differences (2.5-fold difference) between cycles [$F_{\text{treatment}}$ (3, 20) = 60.35, P < 0.0001; **Figure 6C**].

Paclitaxel induced allodynia following carboplatin treatment

We further investigated the impact of carboplatin treatment on paclitaxel-induced allodynia. Mice given one cycle of carboplatin alone did not demonstrate significant mechanical nociceptive changes. As shown in **Supplementary Figure 3**, one cycle of 5 or 20 mg/kg carboplatin did not significantly reduce the mechanical threshold [$F_{\text{dose x time}}$ (8, 40) = 0.4526, $P > 0.05$]. However, in a separate cohort of mice, a low-dose paclitaxel (1 mg/kg) cycle administered one week following the completion of the carboplatin (5 mg/kg) cycle led to a significant reduction of mechanical threshold compared to the vehicle-paclitaxel group [$F_{\text{dose x time}}$ (12, 60) = 16.65, $P < 0.0001$; **Figure 6D**].

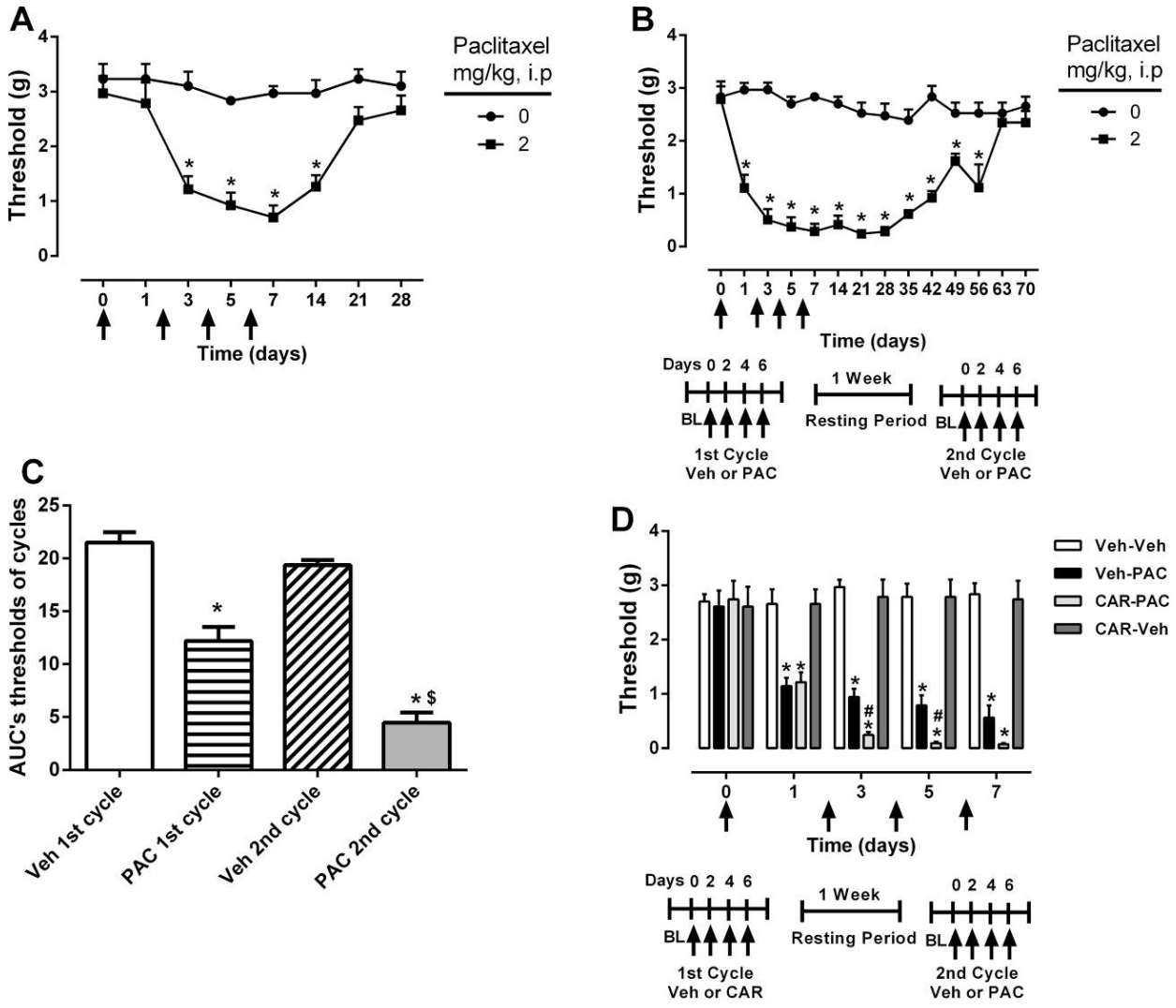

Figure 6. Mice are sensitized to cutaneous stimulation after second cycle of paclitaxel treatment. A) Mice treated with one cycle of paclitaxel (2 mg/kg) or vehicle (i.p., every other day for a total of 4 injections). B) Mice from 3A treated with a second cycle of paclitaxel (2 mg/kg) or vehicle (i.p., every other day for a total of 4 injections). C) AUC mechanical threshold for initial 28 days of first and second cycles of paclitaxel treatment. D) Comparison of mechanical thresholds during the second cycle of treatment between mice treated with carboplatin (5 mg/kg) alone and with carboplatin followed by a low dose of paclitaxel (1 mg/kg). Arrows indicate vehicle/paclitaxel/carboplatin injections on days 0, 2, 4, and 6 of each cycle. Baseline measurements were taken before vehicle/paclitaxel/carboplatin administration on day 0. One cohort was tested; n = 6 per group (data expressed as mean ± SEM). *$P < 0.05$ vs vehicle; $^{\$}P < 0.05$ vs first cycle of paclitaxel (2 mg/kg), $^{\#}P < 0.05$ vs carboplatin (5 mg/kg). Veh, vehicle; PAC, paclitaxel; CAR, carboplatin.

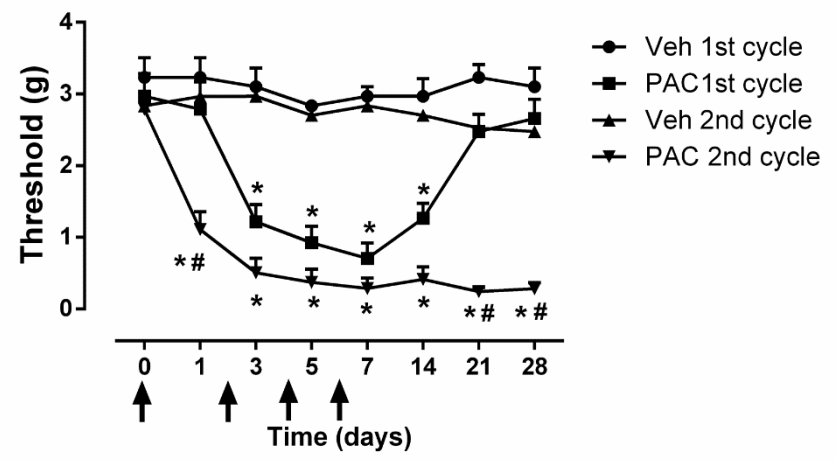

Supplementary Figure 2. Paclitaxel sensitizes mice to cutaneous stimulation after second cycle. Comparison of mechanical threshold during the initial 28 days of one- or two-cycle paclitaxel (2 mg/kg, i.p.) or vehicle treatment. Arrows indicate vehicle/paclitaxel injections on days 0, 2, 4, and 6. Baseline measurements were taken before vehicle/paclitaxel administration on day 0. One cohort was tested (n = 6 per group); data expressed as mean ± SEM. *P < 0.05 vs vehicle; #P < 0.05 vs first cycle of paclitaxel (2 mg/kg). Veh, vehicle; PAC, paclitaxel.

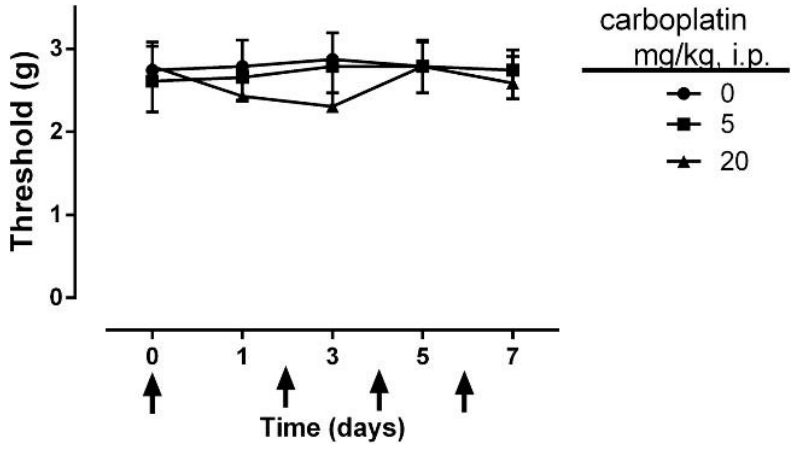

Supplementary Figure 3. Carboplatin alone does not induce mechanical allodynia. Dose-response curve for mice treated with one cycle of carboplatin at doses of 0, 5, and 20 mg/kg, i.p., every other day for a total of 4 injections. Arrows indicate vehicle/carboplatin injections on days 0, 2, 4, and 6. Baseline measurements were taken before vehicle/carboplatin administration on day 0. One cohort was tested (n = 6 per group); data expressed as mean ± SEM.

Paclitaxel induced changes in affective-related behaviors in mice

To assess whether paclitaxel interferes with the natural behavior of mice, a nesting assay was conducted at various time points after paclitaxel treatment was initiated. However, paclitaxel did not interfere with nesting activity [z = 0.856, $P > 0.05$; $z = 1.000$, $P > 0.05$], the quantity of nesting material used [$t = 0.08655$, df = 10, $P > 0.05$; $t = 0.03402$, df = 10, $P > 0.05$], or nest quality [$t = 0.4152$, df = 10, $P > 0.05$; $t = 0.2033$, df = 10, $P > 0.05$] at 1 and 2 weeks post-paclitaxel injection, respectively (**Figure 7**). Similar results were observed at 8 and 11 weeks post-paclitaxel injection, in which nesting activity was not significantly affected by paclitaxel [z = 0.926, $P > 0.05$; **Figure 7A**]. The use of nesting material [$F_{\text{treatment x time}}$ (1,11) = 1.157, $P > 0.05$] and nest quality [$F_{\text{treatment x time}}$ (1,11) = 0.0094, $P > 0.05$] were also not found to be significantly altered (**Figures 7B and C**).

With regard to affective-related changes, we assessed anxiety-, depression-, and anhedonia-like behaviors at various time points in mice treated with paclitaxel, according to the aforementioned treatment regimen. Alterations in anxiety were assessed utilizing the novelty suppressed feeding (NSF) assay. Paclitaxel significantly increased the latency to eat in a novel environment at 3 and 9 weeks post-paclitaxel injection (**Figure 8A**). A significant increase in latency to eat occurred at 3 weeks post-paclitaxel treatment [$t = 2.224$, df = 12, $P < 0.05$, **Figure 8A**]. In addition, significant differences in latency to eat between vehicle- and paclitaxel-treated mice occurred at 9 weeks post-paclitaxel injection ($P < 0.05$), which dissipated by week 11. The amount of food consumed in the test cage was not impacted by paclitaxel treatment (**Figure 8B**).

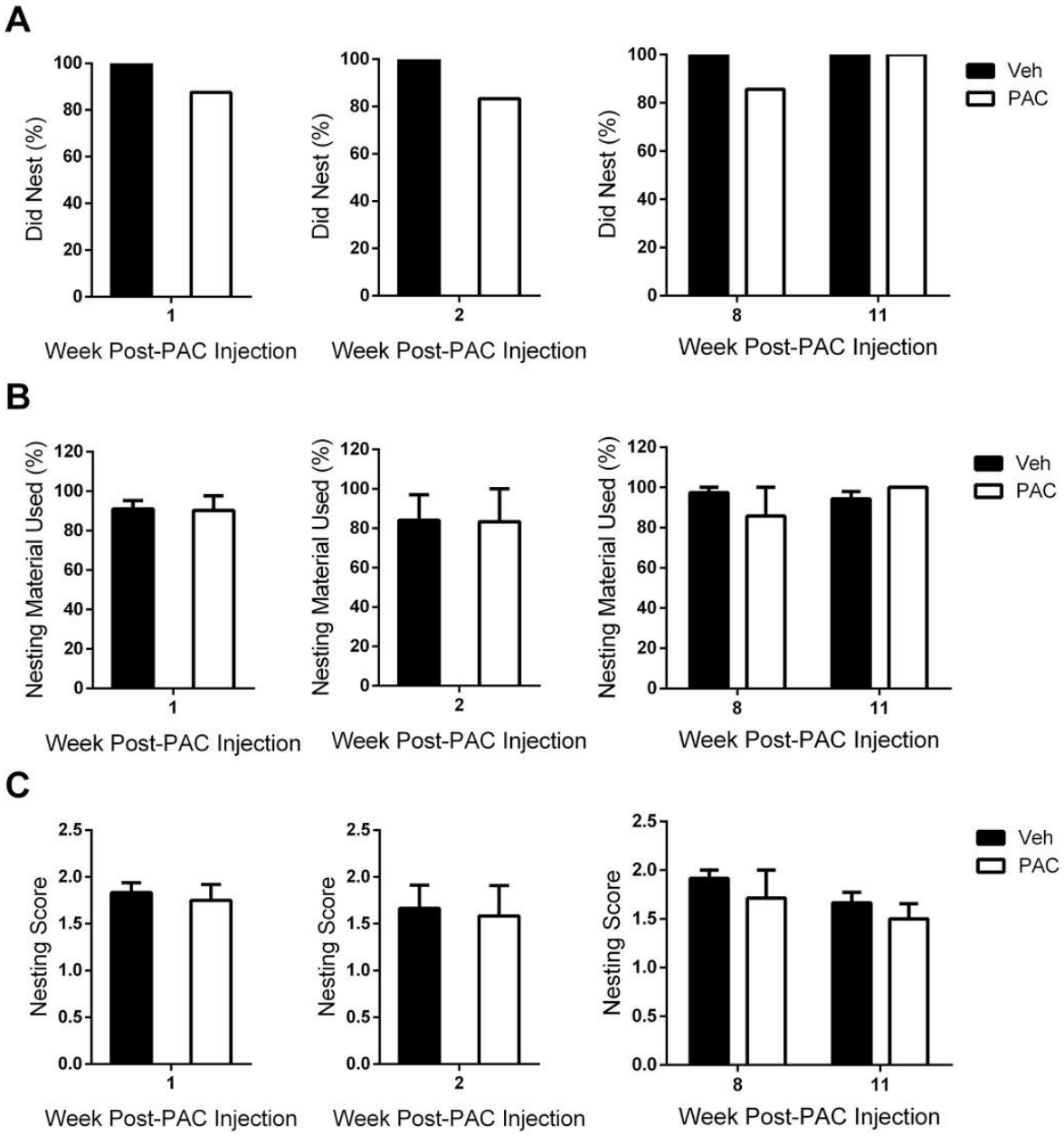

Figure 7. Paclitaxel does not influence the nesting behavior of mice. Mice were allowed 120 minutes to nest at weeks 1, 2, 8, and 11 post-paclitaxel (8 mg/kg, i.p.) or vehicle injection. A) It was determined that mice had participated in nesting activity if at least one nestlet piece had been chewed or pulled into the home cage. A comparison of proportions via z-tests between vehicle- and paclitaxel-treated mice was not significant at any time point. B) The percentage of nesting material used was determined by the following equation: (weight of initial nestlet pieces – weight of remaining nestlet pieces)/weight of initial nestlet pieces. C) The quality of each nest was evaluated on a scale ranging from 0 to 2 (0 = no nest formed, 1 = some nesting activity, 2 = established nest). Individual cohorts were tested at 1 week (n = 6 per group), 2 weeks (n = 6 per group), 8 and 11 weeks (n = 6 Veh, n = 7 PAC) post-paclitaxel (8 mg/kg, i.p.) or vehicle injection; data expressed as mean ± SEM. Post-PAC injection refers to the time following the first of four paclitaxel injections. Veh, vehicle; PAC, paclitaxel.

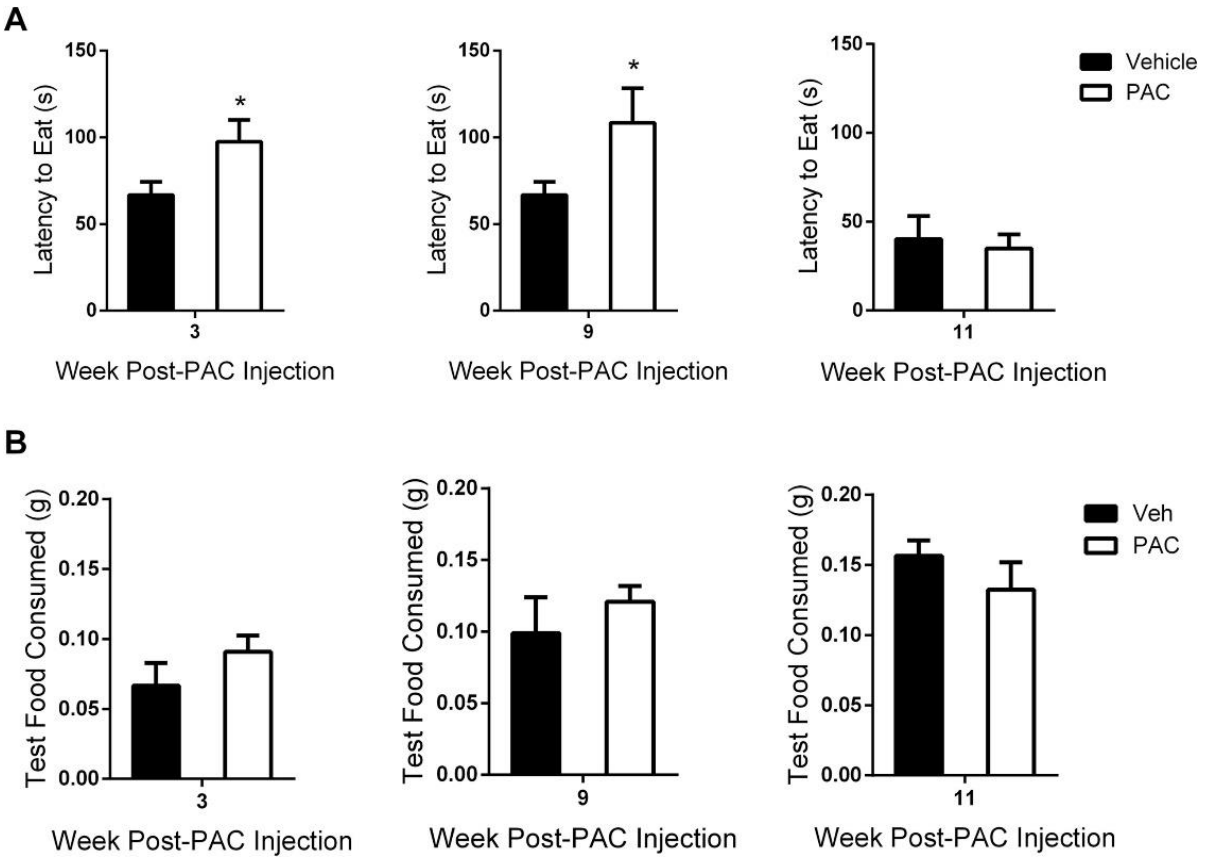

Figure 8. Paclitaxel induces anxiety-like behavior in the novelty suppressed feeding assay. (A) Latency to eat test cage food was determined as the time in seconds from the when the mouse was placed inside the test cage until the mouse sat on its haunches while holding and biting the food pellet. (B) Consumption of test cage food was calculated with the following equation: (initial weight of food pellet – weight of food pellet after 5 min eating period in test cage). Individual cohorts were tested at 3 weeks (n = 6 per group), 9 and 11 weeks (n = 6 Veh, n = 7 PAC) post-paclitaxel (8 mg/kg, i.p.) or vehicle injection; data expressed as mean ± SEM. **P* < 0.05 vs vehicle. Post-PAC injection refers to the time following the first of four paclitaxel injections. Veh, vehicle; PAC, paclitaxel.

Paclitaxel was also found to induce anxiety-like behavior in the light/dark box (LDB) test, in which time spent in the light compartment of the LDB apparatus was significantly decreased at 3 weeks [$t = 2.277$, df = 14, $P < 0.05$], 6 weeks [$t = 2.350$, df = 14, $P < 0.05$], and 9 weeks [$t = 2.309$, df = 14, $P < 0.05$] post-paclitaxel treatment (**Figure 9**). Importantly, the *number* of entries into the light compartment was not significantly decreased at any time point for the paclitaxel-treated mice (**Table 1**), suggesting that the decrease in time spent in the light compartment is not due to motor deficits (**Supplementary Fig. 1B**).

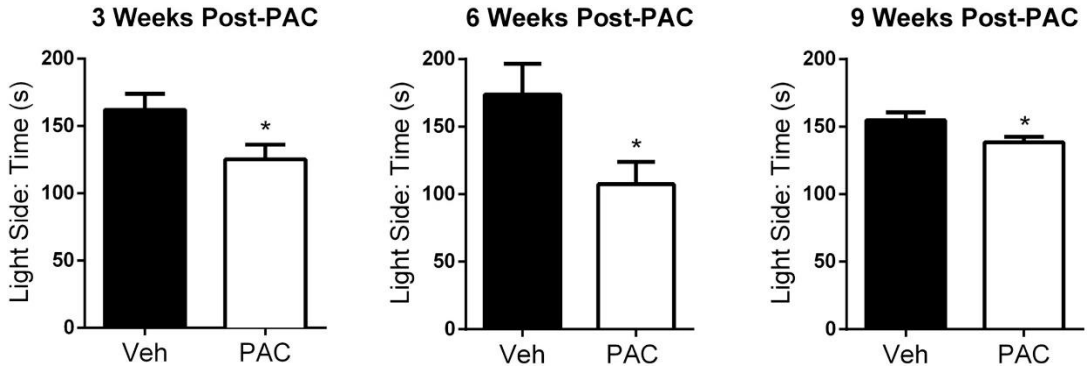

Figure 9. Paclitaxel induces anxiety-like behavior in the light/dark box test. Mice were free to explore both light and dark compartments for 5 min. The study was conducted with individual cohorts of mice (n = 8 per group) at 3, 6, and 9 weeks post-paclitaxel (8 mg/kg, i.p.) or vehicle injection; data expressed as mean ± SEM. *$P < 0.05$ vs vehicle. Post-PAC injection refers to the time following the first of four paclitaxel injections. Veh, vehicle; PAC, paclitaxel.

Light Side: Number of Entries

	3 Weeks Post-PAC	6 Weeks Post-PAC	9 Weeks Post-PAC
Vehicle	16 ± 1.7	15 ± 2.0	14 ± 1.7
Paclitaxel	14 ± 1.9	13 ± 1.9	12 ± 1.7

Table 1. Paclitaxel treatment does not interfere with entry into the light compartment of the light/dark box apparatus. Unpaired *t* tests revealed no significant differences between vehicle- and paclitaxel-treated mice at any time point. One experiment was conducted with individual cohorts of mice (n = 8 per group) at each time point. Post-PAC injection refers to the time following the first of four paclitaxel injections. Data are expressed as mean ± SEM.

The mice were then evaluated for depression-like behavior in FST, an experimental paradigm that assesses immobility when placed in a container of water. Within the same cohort of mice, paclitaxel treatment induced an emotional-like deficit during FST [$F_{treatment\ x\ time}$ (3,15) = 6.200, $P < 0.01$; **Figure 10**]. The time spent immobile during FST was significantly increased at 2 and 3 weeks post paclitaxel-injection ($P < 0.01$), an effect that dissipated by week 4 (**Figure 10**).

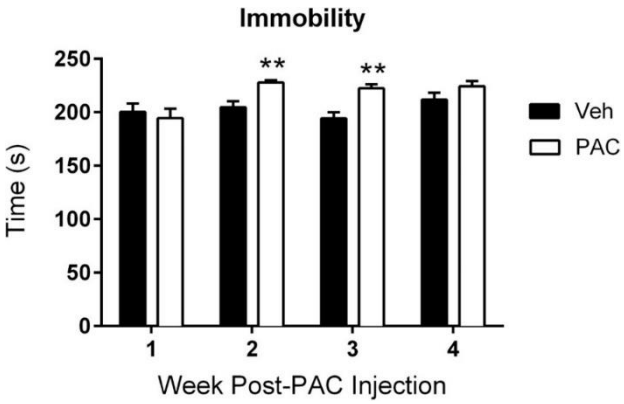

Figure 10. Paclitaxel induces depression-like behavior in the forced swim test. Time represents the number of seconds the mouse was immobile when placed in water; the cut-off time was 240 seconds. The same cohort of mice (n = 6 per group) was tested at weeks 1, 2, 3, and 4 post-paclitaxel (8 mg/kg, i.p.) or vehicle injection; data expressed as mean ± SEM. $^{**}P < 0.01$ vs vehicle. Post-PAC injection refers to the time following the first of four paclitaxel injections. Veh, vehicle; PAC, paclitaxel.

Lastly, anhedonia-like behavior was assessed using the sucrose preference test. The interaction between paclitaxel treatment and time was significant within the same cohort of mice [$F_{treatment\ x\ time}$ (8,112) = 9.424, $P < 0.0001$, **Figure 11**]. Paclitaxel produced a significant decrease in sucrose preference during ($P < 0.0001$) and shortly after ($P < 0.01$, $P < 0.05$) completion of the treatment regimen when compared to vehicle-treated mice (**Figure 11**). To ensure that the decrease in consumatory behavior was not due to a decrease in overall consumption, we assessed total fluid intake between vehicle- and paclitaxel-treated mice, which was found to not differ significantly between the two groups (**Supplementary Fig. 4**).

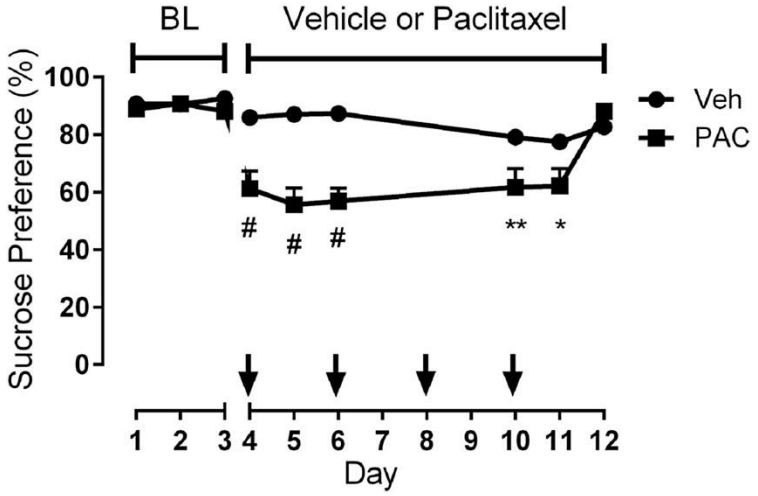

Figure 11. Paclitaxel induces anhedonia-like behavior in the sucrose preference test. Mice were provided with two sipper tubes, one containing normal drinking water and the other containing a 2% sucrose solution, for 24 h per day. Sucrose preference was determined as the percentage of 2% sucrose volume consumed over the total fluid intake volume. Arrows indicate the time of each paclitaxel (8 mg/kg, i.p.) or vehicle injection. The study was conducted with the same cohort of mice (n = 8 per group) during paclitaxel (8 mg/kg, i.p.) or vehicle injections; data expressed as mean ± SEM. *$P < 0.05$, **$P < 0.01$, $^{\#}P < 0.0001$ vs vehicle. BL, baseline; Veh, vehicle; PAC, paclitaxel.

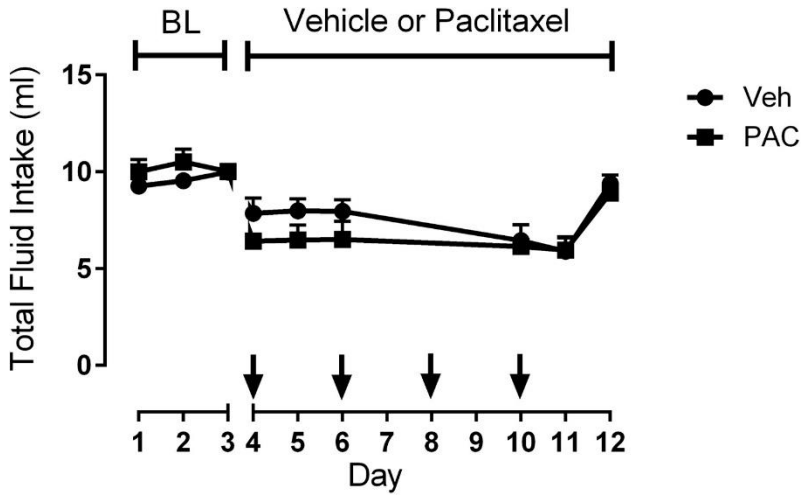

Supplementary Figure 4. Paclitaxel treatment does not interfere with total fluid intake. The total fluid intake is the sum of volumes of water and 2% sucrose consumed by each mouse. Arrows indicate the time of each paclitaxel (8 mg/kg, i.p.) or vehicle injection (n = 8 per group); data expressed as mean ± SEM. A two-way ANOVA was performed, followed by the Bonferroni post hoc test; no significant differences between vehicle- and paclitaxel-treated mice were found at any time point. BL, baseline; Veh, vehicle; PAC, paclitaxel.

D. Discussion

The results of the present study demonstrate that a clinically relevant dosing regimen of paclitaxel given systemically to male C57BL/6J mice causes the induction and long-term maintenance of mechanical and cold allodynia, as well as negative affective-related symptoms, including anxiety- and depression-like behaviors of shorter duration. These changes occurred without significant decreases in body weight or impairment of locomotion following paclitaxel treatment (**Supplementary Fig.1**), findings that are in accordance with other studies showing that various doses of paclitaxel do not alter body weight (Boehmerle *et al.*, 2014) or locomotor activity (Nieto *et al.*, 2008; Deng *et al.*, 2015).

This work also investigated the affective-related consequences of paclitaxel treatment. Using a paclitaxel regimen that caused a long-lasting allodynia (8 mg/kg, 1 cycle), we observed an increase in the latency to eat during the NSF assay and aversion to the light compartment of the LDB apparatus. These effects in two tests of anxiety suggest that, under the present experimental conditions, paclitaxel induces an anxiety-like state. We also found that paclitaxel-treated mice exhibit increased immobility time during FST and anhedonia-like behavior in the sucrose preference test. The observed decrease in sucrose preference could also indicate that an alteration in taste (dysgeusia), a phenomenon seen in some patients receiving paclitaxel (Turcott *et al.*, 2016), is occurring during paclitaxel treatment; yet, we cannot make that conclusion from a single oral consumption assay. The possible taste alteration may produce decreased appetite, but no significant changes in body weight were detected. Collectively, these results indicate that in addition to peripheral neuropathy signs, paclitaxel induces a deficit in the emotional-like state of the mice. Conversely, paclitaxel did not affect nesting behavior, an assay that has been shown to reflect pain-depressed behavior when lactic acid and complete Freund adjuvant (CFA) are used as noxious stimuli (Negus *et al.*, 2015). The lack of an effect in this assay is consistent with the hypothesis that the value of a habit-like survival task does not alter depending on the motivational state (Rock *et al.*, 2014). Thus, the necessity of establishing a nest for thermoregulation, fitness, and shelter may overcome the nociceptive and negative affective symptoms of paclitaxel.

To increase our understanding of paclitaxel-induced toxicity, the relationship between nociceptive and affective symptoms needs to be considered, as well as the temporal order in which these side effects develop. Studies have shown that the

pathology of a tumor itself can cause emotional disturbances in rodents (Pyter *et al.*, 2009), but our experiments in non-tumor-bearing mice reveal that paclitaxel alone is also capable of inducing anxiety- and depression-like behaviors. At 1-week post-paclitaxel injection, we observed the development of both mechanical and cold allodynia, as well as anhedonia-like behavior (**Table 2**). Anxiety- and depression-like behaviors arise in the subsequent weeks following paclitaxel treatment. The immediate appearance of nociceptive symptoms is consistent with paclitaxel acting directly on the peripheral nervous system, but there may be a separate central mechanism of the drug. While paclitaxel seems to accumulate in peripheral organs such as the peripheral nervous system, it has been detected in the brain of mice following tail vein injection, even at low concentrations (Kemper *et al.*, 2003; Gangloff *et al.*, 2005), suggesting that it crossed the blood brain barrier. Therefore, the presence of paclitaxel in the central nervous system and/or paclitaxel-induced peripheral neuropathy itself may be causing changes in affective behaviors through neuroinflammation mechanisms and/or an induction of central neurotoxicity. It is also possible that paclitaxel-induced sensitization of immune responses may have played a role in the development of peripheral neuropathy, and perhaps of affective-like behaviors. Indeed, hypersensitivity to stimuli, not only in neuropathic pain but also in inflammatory pain, can be explained by both peripheral and central sensitization of sensory nerve fibers (Fornasari, 2012). In regards to the neuroimmune interface, glial responses have also been shown to play a role in central and peripheral nervous system function during neuropathic pain (Scholz and Woolf, 2007).

		Weeks Post-PAC Injection					
Behavior	**Assay**	**1**	**2-3**	**4-5**	**6-7**	**8-9**	**10-11**
Nociceptive	Mechanical Allodynia	+	+	+	+	+	+
	Cold Allodynia	+	+	ND	ND	ND	ND
Natural	Nesting	-	-	ND	ND	-	-
Anxiety-like	NSF	ND	+	ND	ND	+	-
	LDB	ND	+	ND	+	+	ND
Depression-like	FST	-	+	-	ND	ND	ND
	Sucrose Preference	+	-	ND	ND	ND	ND

Table 2. Summary of onset and duration of nociceptive, natural, and affective behaviors. Post-PAC injection refers to the time following the first of four paclitaxel injections. NSF, novelty suppressed feeding; LDB, light/dark box; FST, forced swim test; (-), no phenotype; (+), nociceptive/affective behavior; ND, not determined.

The differences between the onset, duration, and resolution of these affective behaviors should also be considered. Although changes in nociceptive behavior, such as mechanical allodynia, occur immediately following paclitaxel administration, there appears to be a delay in the initiation of emotional-like deficits. Clinically, somatic and affective symptoms can occur simultaneously. Breast cancer patients often experience a cluster of symptoms including pain (77%), anxiety (21%), and depression (36%), indicating that they may share a common mechanism (So *et al.*, 2009). Those patients receiving chemotherapy experience the cluster symptoms to a greater degree and are at a higher risk for decreased quality of life.

The time-dependent development of both anxiety- and depression-like behaviors has also been observed in other mouse neuropathic pain models. La Porta *et al.*, (2016) reported ipsilateral mechanical and cold allodynia from day 3 to day 27 post-partial sciatic nerve ligation (PSNL) in Swiss albino male mice, with enhanced anxiety-like behavior in the elevated plus maze from 1 to 3 weeks post-PSNL and increased depressive-like behavior during FST, but only at 3 weeks post-PSNL. Also, a significant decrease in sucrose preference was observed from day 1 to day 20 post-PSNL. Although this study utilized a different model of neuropathic pain, alterations in nociceptive behaviors were also induced immediately and persisted for approximately four weeks. However, we found that anxiety-like behavior can be maintained for 9 weeks following nerve exposure to a noxious stimulus. Consistent findings were made in regards to depression-like behavior, in which increased immobility during FST did not appear until 2-3 weeks. We recognize that repeated testing of the same cohort during FST could be a limitation, however, vehicle-treated mice did not express adaptation to the assay. The development of anhedonia-like behavior was also similar, during which a decrease in sucrose preference was observed the day following PSNL or paclitaxel treatment, but the effect only persisted for 11 days post-paclitaxel injection, whereas PSNL induced this behavior until day 20.

Similarly, using sciatic nerve constriction (SNC) in male C57BL/6J mice, Yalcin *et al.*, (2011) reported that ipsilateral mechanical allodynia persisted for 90 days, and increased anxiety-like behavior in the light/dark box test was observed at 4, 7, and 8 weeks post-SNC, a time-dependent effect similar to that seen in the present study. Latency to first contact and bite the food pellet during the NSF assay was observed at 5 and 8 weeks post-SNC, an effect that appeared earlier in paclitaxel-induced neuropathic

pain. Increased immobility in neuropathic mice was observed at 8 and 9 weeks post-SNC during FST, whereas paclitaxel-induced neuropathic pain caused immobility at 2 and 3 weeks post-paclitaxel injection. The differences and similarities amongst these studies illustrate the importance of establishing a clinically relevant model specific to the type of neuropathic pain of interest in order to best determine the responsible mechanisms. Also, these data suggest that multiple pathways and/or brain regions are involved in the manifestation of affective-related behaviors. Yet it remains plausible that paclitaxel administration and models of nerve injury share common mechanisms for the induction of affective-related behaviors.

In conclusion, this work characterizes a preclinical mouse model of both the nociceptive and negative affective symptoms of paclitaxel treatment, which can be utilized to test the efficacy of potential therapeutics for the treatment of paclitaxel-induced side effects, as well as investigate mechanisms of action. In addition, this study allows for the separate investigation of chemotherapy-induced pain-related behaviors in a tumor-free environment, which cannot be ethically accomplished in a clinical setting.

Acknowledgements

This study was supported by NIH grant R01-CA206028 to MID and DAG, and partly supported by pilot funding from the VCU Massey Cancer Center supported, in part, with funding from NIH-NCI Cancer Center Support Grant P30 CA016059.

CHAPTER TWO

Nicotine Prevents and Reverses Paclitaxel-Induced Mechanical Allodynia in a Mouse Model of CIPN

S. Lauren Kyte[1], Wisam Toma[1], Deniz Bagdas, Julie A. Meade, Lesley D. Schurman, Aron H. Lichtman, Zhi-Jian Chen, Egidio Del Fabbro, Xianjun Fang, John W. Bigbee, M. Imad Damaj, and David A. Gewirtz

[1]These authors contributed equally to this work.

Departments of Pharmacology and Toxicology (S.L.K., W.T., D.B., J.A.M., L.D.S., A.H.L., M.I.D., D.A.G.), Neurology (Z.C.), Internal Medicine (E.D.), Biochemistry and Molecular Biology (X.F.), Anatomy and Neurobiology (J.W.B.), and Massey Cancer Center (D.A.G.), Virginia Commonwealth University, Richmond, Virginia; Experimental Animals Breeding and Research Center (D.B.), Uludag University, Bursa, Turkey

Disclosure #1: The work included in this chapter has been published in the Journal of Pharmacology and Experimental Therapeutics (364:110-119, January 2018).

Disclosure #2: The cancer studies in this work were conducted by S. Lauren Kyte. The behavioral and immunohistochemical experiments were performed in the laboratory of Dr. M. Imad Damaj, primarily by Dr. Wisam B. Toma.

A. Introduction

Chemotherapy continues to play a significant role in the treatment and survival of cancer patients. However, a number of cancer chemotherapeutic drugs can promote either transient or prolonged tissue and organ toxicities, including chemotherapy-induced peripheral neuropathy (CIPN). CIPN, a result of peripheral nerve fiber dysfunction or degeneration, is characterized by sensory symptoms, including numbness, tingling, burning, hyperalgesia, allodynia, and in some cases neuropathic pain. Approximately 68% of cancer patients experience CIPN within a month following the completion of their treatment, whereas 30% suffer from symptoms of CIPN for 6 months or longer after chemotherapy (Seretny *et al.*, 2014). When CIPN manifests during the administration of chemotherapy, it can become dose-limiting and/or delay treatment, thereby interfering with the full course of treatment that may be required for a positive clinical outcome (Hama and Takamatsu, 2016).

Cancer chemotherapeutic drugs and drug classes associated with peripheral neuropathy include the taxanes (paclitaxel), platinum-based compounds (cisplatin, oxaliplatin), vinca alkaloids (vincristine), and bortezomib. Paclitaxel, a taxane commonly used to treat breast, lung, and ovarian cancers, increases both progression-free and overall survival in cancer patients (Dranitsaris *et al.*, 2015). Unfortunately, paclitaxel has been found to cause CIPN both acutely and chronically in 59-78% and 30% of cancer patients, respectively (Beijers *et al.*, 2012).

There are currently no effective preventative or therapeutic treatments for CIPN. Opioids, anticonvulsants, antidepressants, anesthetics, and muscle relaxants either perform modestly in relieving CIPN pain, do not show consistent efficacy in the majority

of patients, and/or produce intolerable side effects (Hershman *et al.*, 2014; Kim *et al.*, 2015; Majithia *et al.*, 2016).

Nicotine and nicotine analogues have demonstrated potential utility as analgesic and/or antinociceptive drugs, as well as anti-inflammatory agents in both human and experimental pain studies (AlSharari *et al.*, 2013; Umana *et al.*, 2013; Flood and Damaj, 2014). For example, nicotine elicits analgesic effects in nonsmokers suffering from spinal cord injury in a randomized, placebo-controlled, crossover design experiment (Richardson *et al.*, 2012). Additionally, a recent preclinical study demonstrated that i.p. administration of nicotine at a dose of 1.5 mg/kg reverses allodynia induced by oxaliplatin, a chemotherapeutic agent used to induce peripheral neuropathy in rats (Di Cesare Mannelli *et al.*, 2013).

The studies described in this report characterize the antinociceptive and/or neuroprotective effects of nicotine in a CIPN mouse model while further evaluating the influence of nicotine on lung tumor cell proliferation and sensitivity to the antitumor properties of paclitaxel.

B. Materials and Methods

Animals. Adult male C57BL/6J mice (8 weeks at the beginning of experiments, 20-30 g) were purchased from The Jackson Laboratory (Bar Harbor, ME). Mice were housed in an AAALAC-accredited facility in groups of four; the mice in each cage were randomly allocated to different treatment groups. Food and water were available *ad libitum*. Experiments were performed during the light cycle (7:00 am to 7:00 pm) and were approved by the Institutional Animal Care and Use Committee of Virginia Commonwealth

University and followed the National Institutes of Health Guidelines for the Care and Use of Laboratory Animals. Animals were euthanized via CO_2 asphyxiation followed by cervical dislocation. Any subjects that showed behavioral disturbances unrelated to chemotherapy-induced pain were excluded from further behavioral testing.

Drugs. Paclitaxel was purchased from Tocris (1097, Bristol, United Kingdom) and dissolved in a mixture of 1:1:18 [1 volume ethanol/1 volume Emulphor-620 (Rhone-Poulenc, Inc., Princeton, NJ)/18 volumes distilled water]. Paclitaxel injections were administered intraperitoneally (i.p.) every other day for a total of four injections to induce neuropathy, as previously described by Toma *et al.*, (2017). (-)-Nicotine hydrogen tartrate salt and mecamylamine HCl were purchased from Sigma-Aldrich (St. Louis, MO, USA) and dissolved in 0.9% saline. For acute administration, nicotine was injected i.p. at doses of 0.3, 0.6, or 0.9 mg/kg (Di Cesare Mannelli *et al.*, 2013; Bagdas *et al.*, 2017). Nicotine at doses of 6, 12, or 24 mg/kg/day was also administered chronically via 7-day subcutaneous (s.c.) osmotic minipumps (Alzet, Model 1007D, Cupertino, CA), which were implanted 2 days prior to paclitaxel treatment (Alsharari *et al.*, 2015). Mecamylamine was administered at a dose of 2 mg/kg s.c. 15 minutes before administration of nicotine or saline (Bagdas *et al.*, 2014). Methyllycaconitine (MLA) was purchased from RBI (Natick, MA, USA) and administered at a dose of 10 mg/kg s.c. 10 minutes before administration of nicotine (Freitas *et al.*, 2013). All doses were chosen based on previous works that demonstrated which dose, time of exposure, and route of administration for each drug effectively acted upon the appropriate receptor and was not toxic to the animal. All i.p. or

s.c. injections were given in a volume of 1 ml/100 g body weight, whereas the osmotic minipumps released 0.5 µl/hour.

Immunohistochemistry and quantification of intra-epidermal nerve fibers. The hind paw epidermis was collected from the following groups of mice: vehicle-saline, vehicle-nicotine (24 mg/kg/day), paclitaxel (8 mg/kg)-saline, and paclitaxel (8 mg/kg)-nicotine (24 mg/kg/day). The staining procedure was performed as previously described (Toma *et al.*, 2017). Briefly, the glabrous skin of the hind paw was excised, placed in freshly prepared 4% paraformaldehyde in 0.1 M PBS (pH 7.4), and stored overnight at 4 °C in the same fixative. The samples were embedded in paraffin, sectioned at 25 µm, and stained with PGP9.5 (Fitzgerald - 70R-30722, MA, USA) and goat anti-rabbit IgG (H+L) secondary antibody conjugated with Alexa Fluor® 594 (Life Technologies - A11037, OR, USA). Sections were examined using a Zeiss Axio Imager A1 – Fluorescence microscope (Carl Zeiss, AG, Germany) in a blinded fashion under 63x magnification, but imaged under 40x magnification; the density of fibers is expressed as fibers/mm.

Mechanical allodynia evaluation (von Frey test). Mechanical allodynia thresholds were determined using von Frey filaments according to the method suggested by Chaplan *et al.*, (1994) and as described previously (Bagdas *et al.*, 2015). The mechanical threshold is expressed as log10 (10 £ force in [mg]). For the nicotine-mediated reversal of CIPN experiment, paclitaxel-treated mice were tested for mechanical allodynia following acute nicotine administration on days 7-14 following the initial paclitaxel injection. All behavioral testing on animals was performed in a blinded manner.

Minipump Implantation. The procedure was performed as previously described in AlSharari *et al.*, (2013) with minor modifications. Mice were anesthetized with 2.5% isoflurane/ 97.5% oxygen. The anesthetized mice were prepared by shaving of the back and swabbing with betadine, followed by 70% ethanol pads. Sharp, sterile scissors was used to make a 1 cm incision in the skin of the upper back/neck. The sterile, preloaded minipump (Alzet, Model 1007D, Cupertino, CA) with different doses of nicotine or saline was inserted with sterile forceps by a technician wearing sterile gloves. The wound was closed with sterile 9 mm stainless steel wound clips. The mice were allowed to recover on heated pads and were monitored before returning to their home cages.

Cell culture. All lung cancer cells were maintained in DMEM supplemented with 10% (v/v) fetal bovine serum (FBS, Serum Source International, FB22-500HI, NC, USA) and 1% (v/v) combination of 10,000 U/ml penicillin and 10,000 µg/ml streptomycin (Pen/Strep, ThermoFisher Scientific, 15140-122, Carlsbad, CA), unless stated otherwise. Cells were incubated at 37°C under a humidified, 5% CO_2 atmosphere. The H460 non-small cell lung cancer (NSCLC) cell line was generously provided by the laboratory of Dr. Richard Moran at Virginia Commonwealth University (VCU), the A549 NSCLC cell line was a gift from the laboratory of Dr. Charles Chalfant at VCU, and the Lewis lung carcinoma (LLC) cells were provided by Dr. Andrew Larner at VCU. In order to establish the T1 primary lung cancer cell line, tissues were obtained from adenocarcinoma tumors in accordance with the VCU IRB protocol. Tissues were minced well and washed multiple times by centrifugation in sterile PBS. Thereafter, the tissues were resuspended in DMEM. Tissue

homogenates were layered on collagen (Sigma-Aldrich, C3867, St. Louis, MO)-coated plates. Cell colonies started to appear after 2-3 weeks. Upon confluence, the cells were trypsinized and passaged. The ovarian cancer cell lines, SKOV-3/DDP and OVCAR-3, were generously provided by the laboratory of Dr. Xianjun Fang at VCU and were cultured in RPMI160 supplemented with 10% (v/v) FBS and 1% (v/v) Pen/Strep.

Paclitaxel was dissolved in DMSO, diluted with sterile PBS, and added to the medium in order to obtain the desired concentration. Staurosporine (Sigma-Aldrich, S6942, St. Louis, MO) was purchased as 1 mM in DMSO. Cells were not exposed to greater than 0.1% DMSO in any experiment. (-)-Nicotine hydrogen tartrate salt was dissolved in sterile PBS. All experiments involving these light-sensitive drugs were performed in the dark.

Assessment of cell viability. Cell viability was measured by either the 3-(4,5-dimethylthiazol-2-yl)-2,5-diphenyltetrazolium bromide (MTT)/3-(4,5-dimethylthiazol-2-yl)-5-(3-carboxymethoxyphenyl)-2-(4-sulfophenyl)-2H-tetrazolium (MTS) colorimetric assay or trypan blue exclusion. For the MTT/MTS assay, cells were seeded in 96-well plates and treated with various concentrations of nicotine for 24 hours, at which time the drug was removed and replaced with fresh medium. Depending on the replication rate of the cell line, the cells were allowed 24 or 48 hours to proliferate following drug exposure. For the serum deprivation study, cells were seeded in DMEM (10% FBS) for 24 hours, then the medium was removed and replaced with DMEM supplemented with various concentrations of FBS (0-10%) with or without nicotine (1 μM); cell viability was assessed at either 48 or 96 hours post-treatment without drug removal. At the time of testing, the

medium was removed, then the cells were washed with PBS and stained with thiazolyl blue tetrazolium bromide (MTT, 2 mg/ml; Sigma-Aldrich, M2128, St. Louis, MO) in PBS for 3 hours. The MTT solution was aspirated and replaced with DMSO. The color change was measured by a spectrophotometer (ELx800UV, BioTek, VT) at 490 nm. To avoid potentially aspirating cells, the CellTiter 96® Aqueous One Solution Cell Proliferation Assay (MTS; Promega, G358C, Madison, WI) was utilized for less adherent cell lines (A549, LLC, and T1); the use of MTS rather than MTT eliminates washing steps before and after staining.

For trypan blue exclusion, cells were incubated with trypsin (0.25% trypsin-EDTA) for 3 minutes, stained with trypan blue (Invitrogen, 15250, Carlsbad, CA), and the viable, unstained cells were counted using a hemocytometer with bright-field microscopy.

Assessment of colony formation. Cells were seeded at a low density in DMEM (10% FBS). After 24 hours, the paclitaxel and paclitaxel + nicotine samples were exposed to paclitaxel (50 nM) for 24 hours, after which the medium was replaced with fresh, drug-free medium. After 24 hours, the nicotine and paclitaxel + nicotine samples were exposed to nicotine (1 μM) for 24 hours, after which the medium was replaced with fresh, drug-free medium. Once the control colonies reached a size of 50 cells per colony (approximately 8-10 days after seeding), the samples were fixed with methanol, stained with crystal violet, and quantified (ColCount, Discovery Technologies International).

Assessment of apoptosis and DNA content. Flow cytometry analyses were performed using BD FACSCanto II (BD Biosciences, San Jose, CA) and BD FACSDiva software at the Virginia Commonwealth University Flow Cytometry Core facility. For all studies, 10,000 cells per replicate within the gated region were analyzed. When collecting samples, both adherent and floating cells were harvested with 0.1% trypsin-EDTA and neutralized with medium after 48 hours of drug exposure. For quantification of apoptosis, cells were centrifuged and washed with PBS, then resuspended in 100 µl of 1x binding buffer with 5 µl of Annexin V and 5 µl of propidium iodide (BD Biosciences, FITC Annexin V Apoptosis Detection Kit, 556547, San Jose, CA). The samples were then incubated at room temperature while protected from light for 15 minutes. The suspension solution was then brought up to 500 µl using the 1x binding buffer and analyzed by flow cytometry. For quantification of DNA content, the cells were resuspended in 500 µl of a propidium iodide (PI) solution (50 µg/ml PI, 4 mM sodium citrate, 0.2 mg/ml DNase-free RNase A, and 0.1% Triton-X 100) for 1 hour at room temperature, while being protected from light (Tate et al., 1983). Before flow cytometry analysis, NaCl was added to the cell suspensions to achieve a final concentration of 0.20 M.

Assessment of tumor growth *in vivo*. Male C57BL/6J adult mice were subcutaneously injected with 1.5 x 10^6 Lewis lung carcinoma (LLC) cells in both flanks. The LLC cells were collected via trypsinization, then neutralized with medium, centrifuged, and washed with PBS. Pellets of 1.5 x 10^6 LLC cells were then resuspended in 30 µl of 80% basement membrane extract (Trevigen, 3632-010-02, Gaithersburg, MD)/20% PBS. Mice were anesthetized with isoflurane via inhalation during tumor cell injection. Palpable tumors

formed at approximately 7 days post-tumor cell injection, and on day 11 tumor volumes (*l* x *w* x *h*) were sufficient to be assessed with calipers; subsequent tumor volume measurements were collected every other day. Subcutaneous osmotic minipumps (Alzet, Model 1007D, Cupertino, CA) were implanted as previously described at 13 days post-tumor cell injection to release 24 mg/kg nicotine daily for a total of 7 days. Body weight and tumor volume were observed until humane endpoints were reached, at which time mice were euthanized via CO_2 asphyxiation followed by cervical dislocation.

Statistical analyses. A power analysis calculation was performed with the Lamorte's Power Calculator (Boston University Research Compliance) to determine the sample size of animals for each group (Charan and Kantharia, 2013). For assessing nociceptive behavior and tumor volume, the calculations showed that an n of 5 was required to achieve a power of 90% with an alpha error of 0.05; we used 8 mice per group for the nociceptive assay and 5-6 mice per group for the *in vivo* cancer study. The data were analyzed with GraphPad Prism software, version 6 (GraphPad Software, Inc., La Jolla, CA) and SPSS, version 24, and are expressed as mean ± SEM. One- and two-way analysis of variance (ANOVA) tests were conducted and followed by the Bonferroni post hoc test, three-way mixed factor ANOVAs were performed and followed by the Sidak post hoc test, and linear mixed models were conducted to account for the loss of tumor-bearing mice (Little and Rubin, 1987); repeated measures were considered for all *in vivo* studies. Differences were determined to be significant at $P < 0.05$.

C. Results

Nicotine reverses and prevents paclitaxel-induced mechanical allodynia. Initial experiments were designed to determine whether acute administration of nicotine reverses paclitaxel-induced mechanical allodynia. **Figure 12A** demonstrates that nicotine reversed mechanical allodynia in paclitaxel-treated mice in a time- and dose-dependent manner [$F_{\text{time x dose}}$ (18, 126) = 17.10, $P < 0.0001$], with full reversal (mechanical threshold values restored to baseline levels) following administration of 0.9 mg/kg and partial reversal with 0.6 mg/kg. Nicotine did not alter mechanical thresholds in vehicle-treated mice [$F_{\text{time x dose}}$ (18, 126) = 0.6122, $P = 0.88$] (**Supplementary Fig. 5**).

Having demonstrated that nicotine reversed the allodynic effect of paclitaxel, the next series of experiments was designed to investigate whether nicotine also prevents the development of paclitaxel-induced nociceptive (allodynic) responses. Seven days of nicotine (24 mg/kg per day) administration prevented the development of mechanical allodynia throughout the entire duration of the experiment, up to 35 days post-paclitaxel injection [F (9, 252) = 6.703, $P < 0.001$] (**Figure 12B**). As shown in **Supplementary Figure 6,** 6 and 12 mg/kg per day nicotine did not prevent the development of paclitaxel-induced mechanical allodynia.

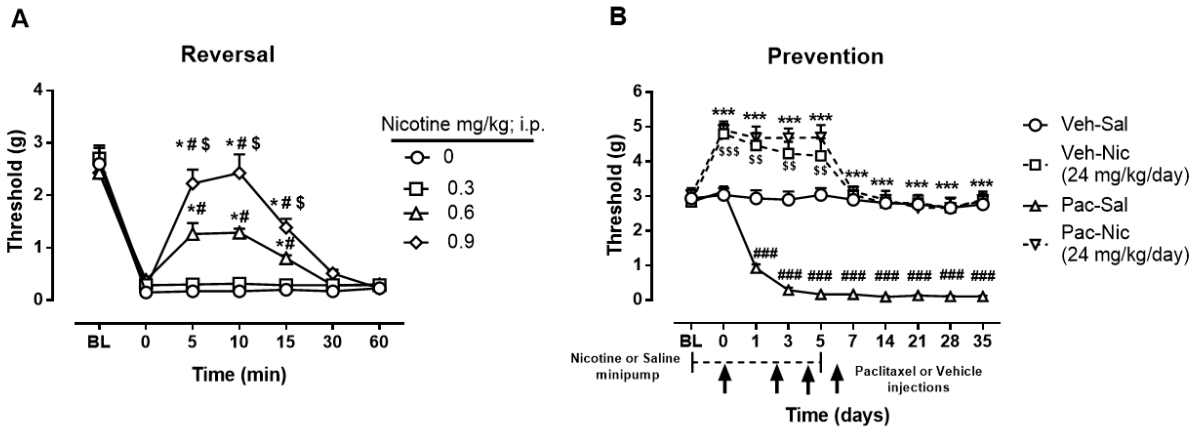

Figure 12. Antinociceptive and preventative effect of nicotine in a mouse model of paclitaxel-induced peripheral neuropathy. (A) Reversal of mechanical allodynia by acute administration of nicotine at doses of 0.3, 0.6, and 0.9 mg/kg i.p. in paclitaxel-treated mice at day 7-14 post-initial paclitaxel injection. $^{*}P < 0.0001$ vs Saline (0 mg/kg); $^{\#}P < 0.0001$ vs nicotine (0.3 mg/kg); $^{\$}P < 0.0001$ vs nicotine (0.6 mg/kg). (B) Prevention of mechanical allodynia by chronic administration of nicotine at a dose of 24 mg/kg per day. Arrows indicate vehicle/paclitaxel injections on days 0, 2, 4, and 6. Minipumps with nicotine were implanted s.c. in the mouse, starting 2 days before the vehicle/paclitaxel treatment cycle and ending on day 5. Baseline measurements were taken at BL before saline/nicotine minipump implantation and on day 0 before paclitaxel/vehicle administration. $^{***}P < 0.001$ Pac-Nic vs Pac-Sal; $^{\#\#\#}P < 0.001$ Pac-Sal vs Veh-Sal; $^{\$\$\$}P < 0.001$, $^{\$\$}P < 0.01$ Veh-Nic vs Veh-Sal. BL, baseline; Veh, vehicle; Sal, saline; Nic, nicotine; Pac, paclitaxel. n = 8 per group; data expressed as mean ± SEM. *Statistical analysis:* For mice treated with 24 mg/kg nicotine, a 2 x 2 x 10 Mixed Factor ANOVA of chemotherapy drug (paclitaxel or vehicle) in nicotine- or saline-treated mice by day showed a significant 3-way interaction [F (9, 252) = 7.851, $P < 0.001$]. A subsequent 2 x 10 Mixed Factor ANOVA of paclitaxel or vehicle treatment by day was calculated for each level of treatment (nicotine or saline). Saline-treated mice demonstrated a significant interaction of chemotherapy drug (paclitaxel or vehicle) by day [F (9, 252) = 15.054, $P < 0.001$], where a Sidak post hoc test revealed lower threshold responding in paclitaxel-treated mice compared to vehicle-treated mice on days 0 - 35 ($P < 0.001$). A separate 2 x 10 Mixed Factor ANOVA calculated where nicotine or saline treatment by day differed at each level of chemotherapy drug (paclitaxel or vehicle). Paclitaxel-treated mice demonstrated a significant interaction of drug pre-treatment (nicotine or saline) by day [F (9, 252) = 6.703, $P < 0.001$], where a Sidak post hoc test revealed higher threshold responding in nicotine-treated mice compared to saline-treated mice on days 0 - 35 ($P < 0.001$). Vehicle-treated mice also demonstrated a significant interaction of drug pre-treatment (nicotine or saline) by day [F (9, 252) = 37.064, $P < 0.001$], where a Sidak post hoc test revealed higher threshold responding in nicotine-treated mice compared to saline-treated mice, but only on days 0, 1, and 3 ($P < 0.001$).

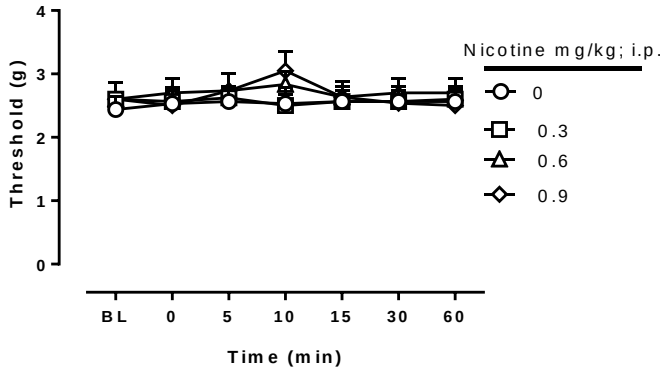

Supplementary Figure 5. Acute administration of nicotine at doses of 0.3, 0.6, and 0.9 mg/kg i.p. does not affect mechanical threshold in vehicle-treated mice. BL, baseline. n = 8 per group; data expressed as mean ± SEM.

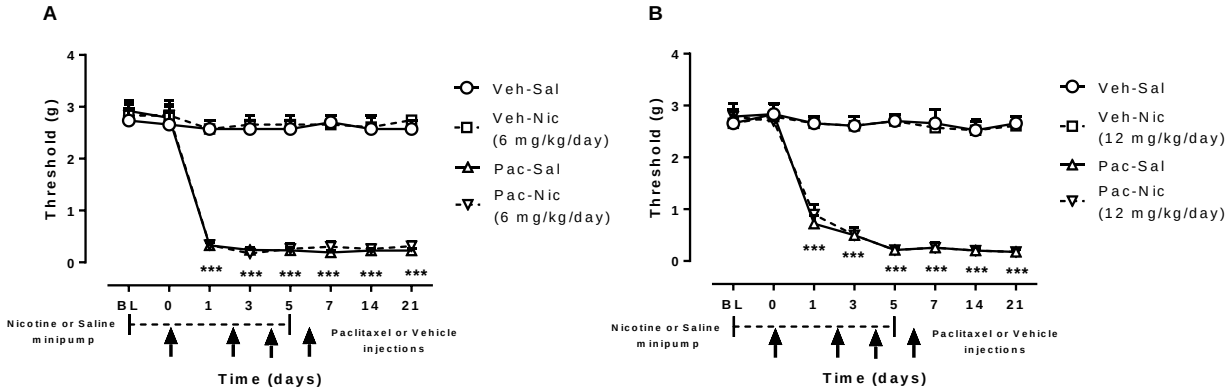

Supplementary Figure 6. Nicotine at doses of 6 and 12 mg/kg/day do not prevent paclitaxel-induced mechanical allodynia. Arrows indicate vehicle/paclitaxel injections on days 0, 2, 4, and 6. Minipumps with nicotine, 6 mg/kg/day (A) or 12 mg/kg/day (B), were implanted s.c. in the mouse, starting 2 days before the vehicle/paclitaxel treatment cycle and ending on day 5. Baseline measurements were taken at BL before saline/nicotine minipump implantation and on day 0 before paclitaxel/vehicle administration. ***$P < 0.001$ Pac-treated mice compared to Veh-treated mice. BL, baseline; Veh, vehicle; Sal, saline; Nic, nicotine; Pac, paclitaxel. n = 6 per group; data expressed as mean ± SEM. *Statistical analysis*: Comparisons were made between chemotherapy treatments (paclitaxel or vehicle) in nicotine- or saline-treated mice by day for both 6 and 12 mg/kg/day doses of nicotine in a 2 x 2 x 8 Mixed Factor ANOVA. The 6 mg/kg [F (7, 140) = 0.139, $P = 0.995$] and 12 mg/kg [F (7, 140) = 0.054, $P = 1.000$] nicotine 3-way interactions were not significant. However, both 6 mg/kg [F (7, 140) = 58.597, $P < 0.001$] and 12 mg/kg [F (7, 140) = 42.647, $P < 0.001$] nicotine produced a significant day by chemotherapy drug interaction, where paclitaxel-treated mice demonstrated lower threshold compared to vehicle-treated mice on days 1, 3, 5, 7, 14, and 21 when compared to both baseline and day 0 responding ($P < 0.001$) as evaluated by Sidak post hoc tests.

To examine the possibility that nicotinic acetylcholine receptors (nAChRs) mediate the antinociceptive effect of nicotine, mecamylamine, a nonselective nAChR antagonist, was administered prior to nicotine. Mecamylamine effectively blocked the antinociceptive effect of nicotine in paclitaxel-treated mice [$F_{\text{time x dose}}$ (6, 42) = 10.38, $P < 0.0001$] (**Figure 13A**). To begin determining which nAChR subtypes are involved in the reversal of paclitaxel-induced mechanical allodynia, we administered MLA, an α7 nAChR antagonist, before nicotine treatment, which effectively blocked the antinociceptive effect of nicotine in paclitaxel-treated mice [$F_{\text{time x dose}}$ (6, 42) = 15.58, $P < 0.0001$] (**Figure 13B**).

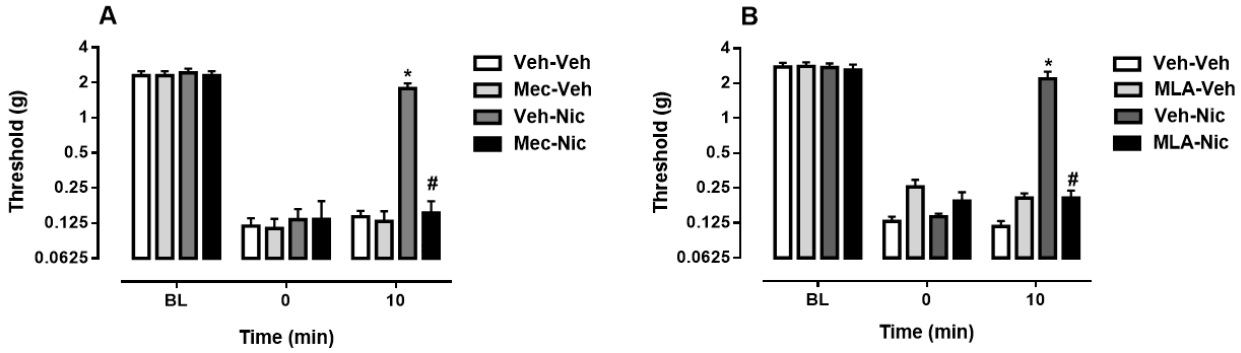

Figure 13. The antinociceptive effect of nicotine is mediated by nAChRs. (A) Mecamylamine, a non-selective nAChR antagonist, was injected at a dose of 2 mg/kg s.c. 15 minutes prior to nicotine to block the nicotine-mediated (0.9 mg/kg, i.p.) reversal of mechanical allodynia in paclitaxel-treated mice. (B) MLA, an α7 nAChR antagonist, was administered at a dose of 10 mg/kg s.c. 10 minutes before nicotine treatment (0.9 mg/kg, i.p.) in paclitaxel-treated mice. *$P < 0.0001$ Veh-Nic at 10 min vs 0 min; $^{\#}P < 0.0001$ Mec-Nic or MLA-Nic vs Veh-Nic at 10 min. Veh, vehicle; Nic, nicotine; Mec, mecamylamine. MLA, methyllycaconitine. n = 8 per group; data expressed as mean ± SEM.

Nicotine prevents paclitaxel-induced reduction of intra-epidermal nerve fibers. A decrease in the intra-epidermal nerve fiber (IENF) density in the paw epidermis is a common marker for evaluating CIPN in rodent models (Bennett *et al.*, 2011). To determine if nicotine also protects the IENFs from the toxic effect of paclitaxel, mice were treated with vehicle or paclitaxel (8 mg/kg, i.p.) and implanted with minipumps releasing saline or nicotine (24 mg/kg per day), and sacrificed 35 days following the first paclitaxel injection, when their hind paw epidermis was collected for immunohistochemical analysis. Quantification of IENFs revealed a significant overall interaction between paclitaxel and nicotine treatment [$F_{\text{paclitaxel x nicotine}}$ (1, 28) = 11.58, $P < 0.01$] (**Figure 14A**). As illustrated in **Figure 14B**, mice treated with paclitaxel-saline demonstrated a significant decrease in IENF density when compared with vehicle-saline-treated mice ($P < 0.0001$). In contrast, paclitaxel-nicotine-treated mice showed a significant increase in IENF density when compared to paclitaxel-saline-treated mice ($P < 0.01$). Paclitaxel-nicotine-treated mice did not show a change in the IENF density when compared to vehicle-nicotine-treated mice ($P = 0.54$), and vehicle-nicotine-treated mice did not exhibit an alteration in IENF density when compared to the vehicle-saline group ($P = 0.53$).

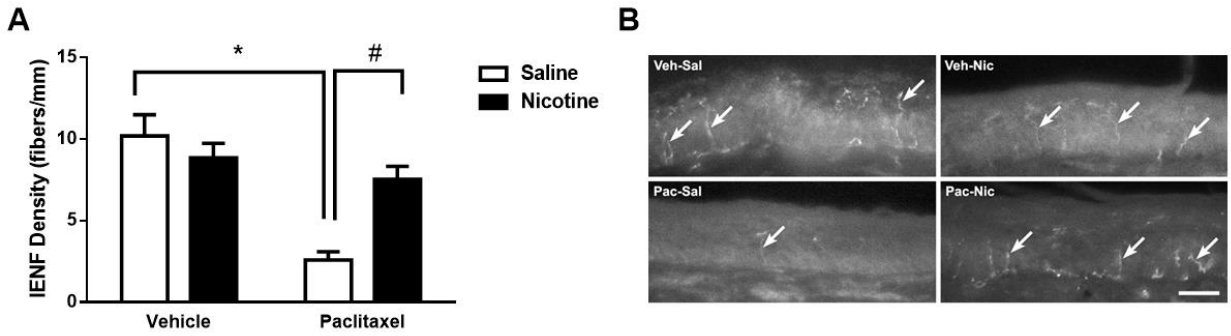

Figure 14. Paclitaxel induces a decrease in IENF density at 35 days post-paclitaxel injection, which is prevented by nicotine administration at a dose of 24 mg/kg per day, s.c. (A) Paclitaxel at a dose of 8 mg/kg i.p. significantly decreased IENF density compared to vehicle-saline and paclitaxel-nicotine groups. *P < 0.05 paclitaxel-saline vs vehicle-saline; $^{\#}P$ < 0.05 paclitaxel-nicotine vs paclitaxel-saline. (B) Immunostained sections of hind paw epidermis represent the reduction of IENF density by paclitaxel and protection by nicotine. Bar represents 20 microns in all images, which were captured under 40x magnification. IENF, intra-epidermal nerve fiber; Veh, vehicle; Sal, saline; Nic, nicotine; Pac, paclitaxel. n = 8 per group; data expressed as mean ± SEM.

Collectively, the behavioral and immunohistochemical studies presented in **Figures 12-14** indicate that nicotine reverses paclitaxel-induced mechanical allodynia, via the α7 nAChR, but also protects against paclitaxel-induced mechanical allodynia and IENF loss. However, multiple reports have argued that nicotine can stimulate tumor growth or interfere with cancer chemotherapeutic drug-induced apoptosis, which would severely limit the potential utility of nicotine in the clinic (Dasgupta *et al.*, 2006; Zhang *et al.*, 2009; Pillai *et al.*, 2011; Wu *et al.*, 2013; Liu *et al.*, 2015). As a review of the relevant literature revealed a number of inconsistencies (see *Discussion*), we re-evaluated the effect of nicotine on tumor cell proliferation and paclitaxel-induced apoptosis.

Nicotine fails to stimulate lung cancer cell proliferation or interfere with paclitaxel-induced cytotoxicity. Initial experiments were performed by utilizing the MTT/MTS colorimetric assay with both A549 and H460 cells, two commonly used experimental models of non-small cell lung cancer (NSCLC) that express multiple nAChRs (Tsurutani *et al.*, 2005; Dasgupta *et al.*, 2006; Yoo *et al.*, 2014). **Figure 15** indicates that 48 and 96-hour exposure to nicotine (1 μM) did not induce a significant increase in viable cell number when compared to untreated cells under both normal (10% FBS) and serum deprivation (0-5% FBS) conditions in A549 (**Figure 15A**) and H460 (**Figure 15B**) cells. The only observed effect was a significant increase in viable cell number under serum starvation (0% FBS) conditions in one cell line at a single time point (**Figure 15B**).

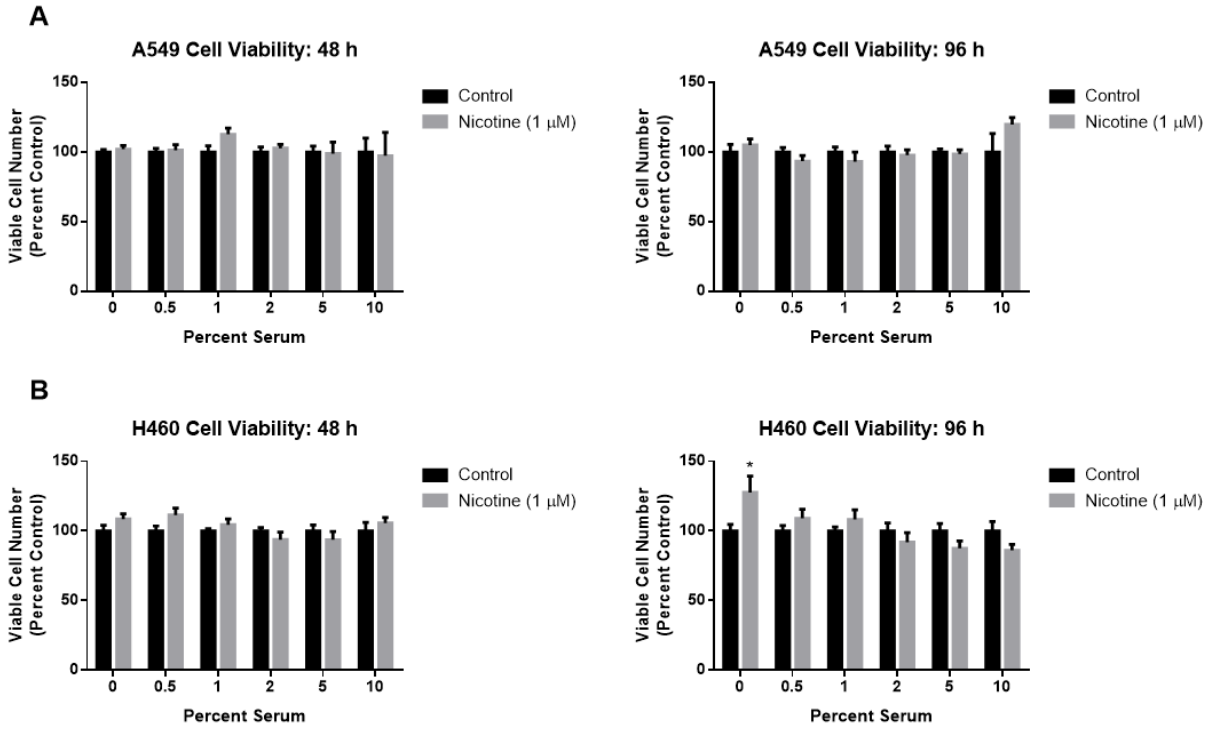

Figure 15. Nicotine fails to enhance NSCLC viable cell numbers under normal and serum-deprivation conditions. (A) A549 and (B) H460 cells were treated with nicotine (1 μM) for 48 or 96 hours in DMEM supplemented with various concentrations of FBS. Viability was determined with an MTT or MTS colorimetric assay. **P* < 0.05 vs control with 0% serum. Data are expressed as the mean + SEM of three independent experiments.

The influence of various concentrations of nicotine on tumor cell proliferation was further investigated under full serum (10% FBS) conditions that are the standard for cancer cell studies. Again, exposure to a range of nicotine concentrations (0.1-10 μM) for 24 hours under full serum conditions did not significantly increase the numbers of viable A549, H460, Lewis lung carcinoma (LLC), or T1 (primary lung cancer) cells (**Supplemental Fig. 7**).

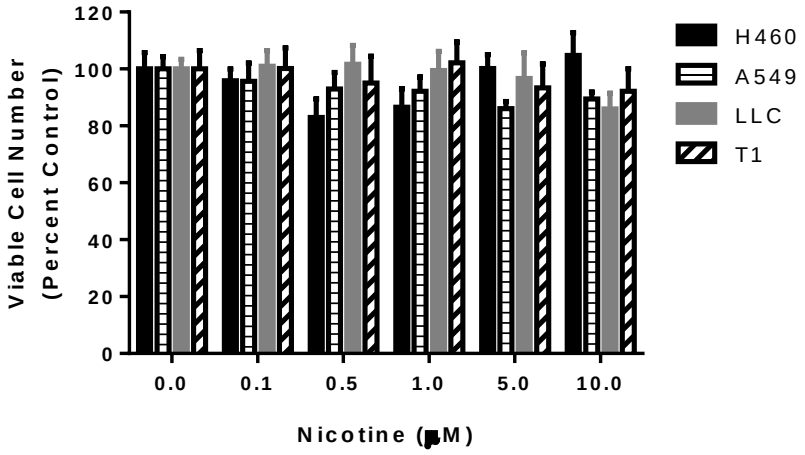

Supplementary Figure 7. Nicotine fails to enhance viable lung cancer cell number. NSCLC cells (A549, H460), Lewis lung carcinoma (LLC) cells, and human primary lung tumor cells (T1) were treated with nicotine for 24 h. Viability was determined with an MTT/MTS colorimetric assay. A one-way ANOVA followed by the Bonferroni post hoc test revealed no significant differences ($P > 0.05$) between control (0.0 μM) and any nicotine-treated cells within each cell line. Data are expressed as mean + SEM of two independent experiments.

Additional studies were designed to more closely mimic the potential use of nicotine after chemotherapy treatment in the clinic. NSCLC cells were first exposed to paclitaxel (50 nM) for 24 hours, followed by a 24-hour drug-free period and subsequent treatment with nicotine (1 μM) for 24 hours. Paclitaxel significantly decreased the number of A549 and H460 colonies, and the impact of paclitaxel was not altered by nicotine; nicotine alone did not stimulate colony formation (**Figure 16**).

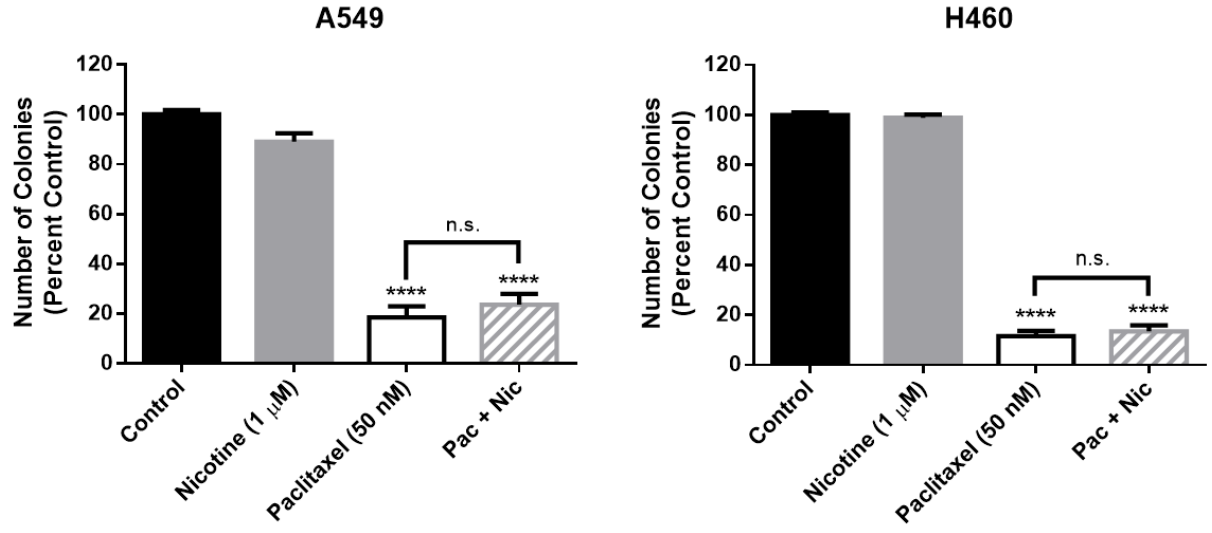

Figure 16. Nicotine fails to stimulate NSCLC colony formation alone or following paclitaxel treatment. For the single drug treatment conditions, A549 (left) and H460 cells (right) were exposed to nicotine (1 μM) or paclitaxel (50 nM) for 24 h. For the combination treatment, cells were first exposed to paclitaxel for 24 h, followed by a 24 h drug-free period, then treatment with nicotine for 24 h. Colony number was determined by crystal violet staining. ****$P < 0.0001$ vs control; n.s., not significant. Data are expressed as the mean + SEM of three independent experiments.

In previous work (Jones *et al.*, 2005; Roberson *et al.*, 2005; Efimova *et al.*, 2010; Emery *et al.*, 2014; Webster *et al.*, 2015; Alotaibi *et al.*, 2016), we and others have reported that growth arrest induced by cancer therapy is transient and that tumor cells recover proliferative capacity within 7-10 days post-treatment. To determine whether prior exposure to nicotine stimulates proliferation and/or promotes early tumor cell recovery from paclitaxel-induced growth arrest, NSCLC cell proliferation was monitored for a period of 7 days after treatment with nicotine (1 μM, 48 hours), paclitaxel (50 nM, 24 hours), or a combination of the two drugs, which consisted of a 24-hour nicotine pretreatment period preceding 24-hour cotreatment. Nicotine did not stimulate the proliferation of either the A549 or H460 cells throughout the duration of the assay and even induced a slight but significant decrease in H460 cell number on Day 5 (**Figure 17**). Most importantly, nicotine did not interfere with the paclitaxel-induced decrease in viable cell number at any time point (**Figure 17**). Furthermore, nicotine did not promote an early proliferative recovery in either cell line (**insets of Figure 17; Supplementary Fig. 8 in Appendix 1A**).

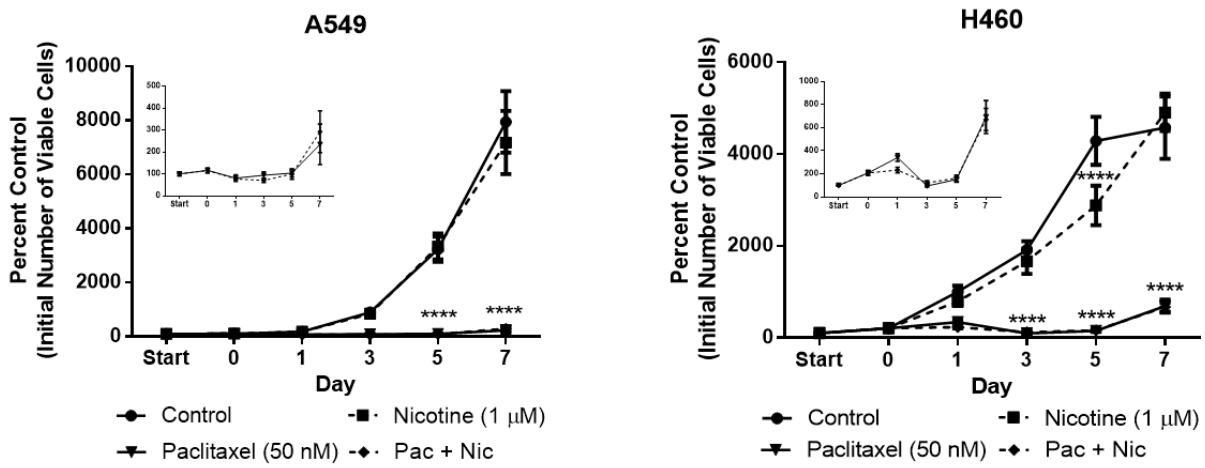

Figure 17. Nicotine fails to stimulate NSCLC cell proliferation alone or interfere with paclitaxel-induced growth inhibition of NSCLC cells. The "start" time point represents the initial number of A549 cells (left) or H460 cells (right) after seeding. A 24-hour nicotine pretreatment period occurred from Start to Day 0 for the Nicotine and Pac + Nic conditions, then all subsequent treatments lasted 24 hours; no drugs were present after Day 1. The number of cells was determined via trypan blue exclusion. ****P < 0.0001 vs control. Data are expressed as the mean ± SEM of three independent experiments.

Although we failed to detect any interference with the anti-tumor activity of paclitaxel in two different assays, other studies have argued that nicotine suppresses paclitaxel-induced apoptosis (Tsurutani *et al.*, 2005; Dasgupta *et al.*, 2006). Consequently, additional experiments were performed to evaluate the effects of nicotine on paclitaxel-induced apoptosis. Paclitaxel (100 nM) induced significant apoptosis in both the A549 and H460 cells after 48 hours of treatment (**Figure 18A**). Most importantly, nicotine (1 μM) did not interfere with the promotion of paclitaxel-induced apoptosis in either NSCLC cell line following cotreatment (**Figure 18A; Supplementary Fig. 9 in Appendix 1B**); staurosporine (2 μM), a nonselective protein kinase inhibitor, induced significant apoptosis and was used as a positive control. Similarly, cell cycle analysis revealed that paclitaxel (100 nM) induces significant sub-G1 fragmented DNA content, an

indicator of late-stage cell death, in both A549 and H460 cells, and that nicotine does not attenuate this effect (**Figure 18B; Supplementary Fig. 10 in Appendix 1C**).

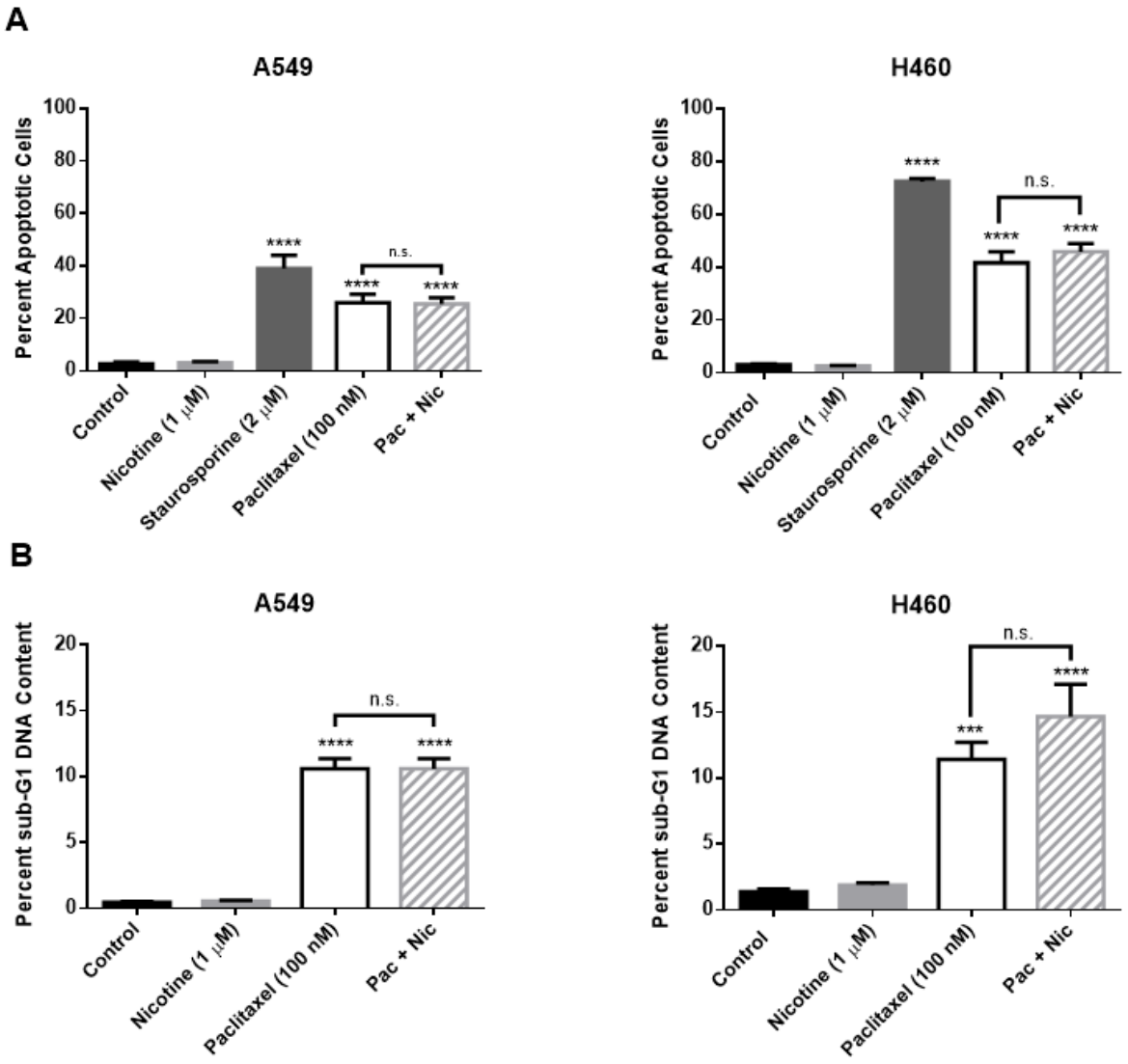

Figure 18. Nicotine fails to interfere with paclitaxel-induced apoptosis (A) and sub-G1 DNA content (B) of NSCLC cells. A549 and H460 cells were treated with nicotine (1 μM), staurosporine (2 μM), paclitaxel (100 nM), or the combination of paclitaxel and nicotine for 48 h. Quantification of apoptotic cells and sub-G1 DNA content was determined by the Annexin V/PI assay and propidium iodide staining, respectively, followed by flow cytometry analysis. ***P < 0.001, ****P < 0.0001 vs control; n.s., not significant. Data are expressed as mean + SEM of three (A) or two (B) independent experiments.

To ensure that our observations applied to other cancer types commonly treated with paclitaxel, we also evaluated the effects of nicotine on cancer cell proliferation in two human ovarian cancer cell lines. As was the case with the lung cancer cells, nicotine did not stimulate ovarian cancer cell proliferation in SKOV-3/DDP and OVCAR-3 cells (**Supplementary Fig. 11**).

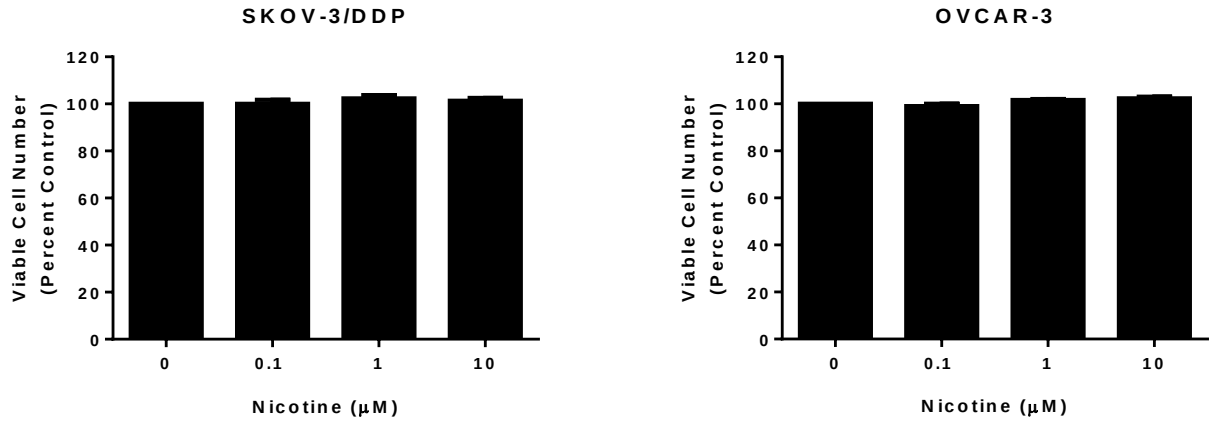

Supplementary Figure 11. Nicotine fails to stimulate ovarian cancer cell proliferation. SKOV-3/DDP and OVCAR-3 cells were treated with nicotine for 48 h, then counted via trypan blue exclusion. A one-way ANOVA followed by the Bonferroni post-hoc test revealed no significant differences ($p > 0.05$) between any concentration of nicotine vs. control (0 μM) in each cell line. Data are expressed as mean + SEM of one representative study of two independent experiments.

To investigate whether the *in vitro* findings are indicative of tumor cell responses *in vivo*, immunocompetent C57BL/6J mice were injected s.c. with LLC cells in the flank, a commonly used syngeneic model of lung cancer (Kellar *et al.*, 2015). Once the tumors formed, the mice were treated with nicotine at a dose of 24 mg/kg per day for 7 days via a s.c. osmotic minipump to mimic the nicotine treatment regimen administered in the peripheral neuropathy studies. In accordance with the *in vitro* findings, chronic administration of nicotine failed to enhance LLC tumor growth (**Figure 19**). We were unable to investigate if nicotine would interfere with the antitumor effect of paclitaxel in this model since the LLC cells were found to be resistant to paclitaxel (**Supplementary Fig. 12 in Appendix 2A**). These tumor-bearing mice also posed a challenge for assessing mechanical allodynia because the vehicle-treated mice exhibited a similar decrease in mechanical threshold as the paclitaxel-treated mice (**Supplementary Fig. 13 in Appendix 2B**).

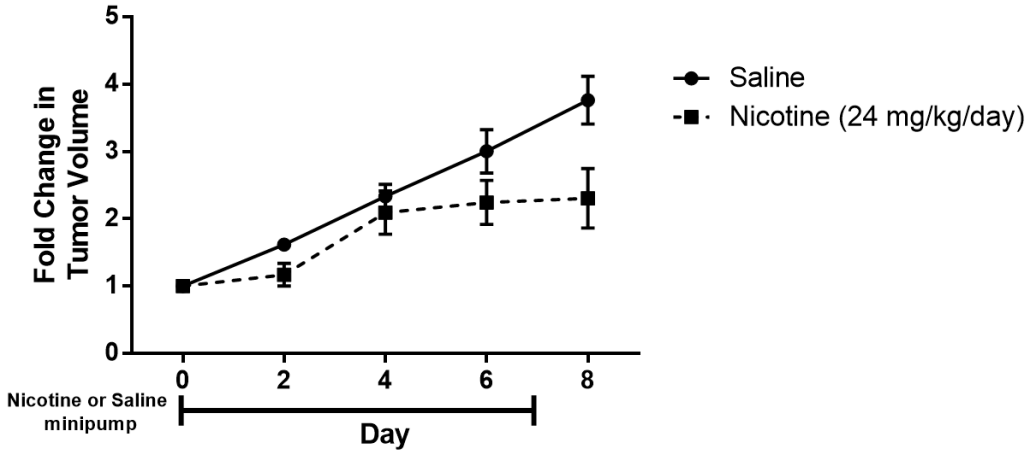

Figure 19. Nicotine fails to enhance LLC tumor growth *in vivo*. C57BL/6J mice were injected s.c. with 1.5 x 10^6 LLC cells in both flanks. Once tumors formed, subcutaneous osmotic minipumps were implanted on day 0 to release 24 mg/kg nicotine daily for a total of 7 days. The left and right flank tumor volumes (*l* x *w* x *h*) were compared to the respective baseline tumor volumes to calculate fold change (A); the fold change values were averaged for each mouse. A linear mixed model analysis revealed a significant effect of time [F (4, 39) = 25.747, P < 0.001] and treatment [F (1, 39) = 15.683, P < 0.001], but no interaction between time and treatment [F (4, 39) = 2.560, P = 0.054]. n = 5-6 per group; data are expressed as mean + SEM.

D. Discussion

Effects of nicotine on chemotherapy-induced peripheral neuropathy. To the best of our knowledge, this is the first study to report that nicotine reverses paclitaxel-induced mechanical allodynia, as well as prevents paclitaxel-induced peripheral neuropathy when administered prior to and during paclitaxel treatment in the mouse. Our work also indicates that nAChRs mediate the antinociceptive effects of nicotine based on interference by mecamylamine, a nonselective nAChR antagonist, and MLA, an α7 nAChR antagonist. Our studies further demonstrate that chronic nicotine infusion prevents the loss of IENFs in the epidermis of the hind paw after paclitaxel treatment. Taken together, these findings suggest that nicotine could have potential utility for the prevention and/or treatment of CIPN.

Mice treated with 8 mg/kg of paclitaxel developed significant mechanical allodynia, which is consistent with our recent report (Toma *et al.*, 2017) and previous studies (Deng *et al.*, 2015; Neelakantan *et al.*, 2016; Slivicki *et al.*, 2016). Acute administration of nicotine reverses the mechanical allodynia induced by paclitaxel, which is consistent with studies by Di Cesare Mannelli *et al.*, (2013) in a rat model of oxaliplatin-induced peripheral neuropathy. As nicotine has a very short half-life of approximately 15 minutes in mice (Damaj *et al.*, 2007), it was also administered chronically via 7-day osmotic minipumps to achieve and maintain steady-state levels. We have previously reported that s.c. minipump administration of 12 and 25 mg/kg per day nicotine leads to plasma nicotine concentrations of approximately 56 and 97 ng/ml, or 0.121 and 0.210 μM, respectively (AlSharari *et al.*, 2013; Alsharari *et al.*, 2015). Chronic administration of nicotine (24 mg/kg per day prior to and during paclitaxel injections significantly prevents both the development of mechanical allodynia and the reduction of IENFs induced by paclitaxel, as previously described by our group (Toma *et al.*, 2017); others have also shown protection from paclitaxel-induced IENF loss with pifithrin-μ (Krukowski *et al.*, 2015).

The antinociceptive and antiallodynic properties of nicotine have been demonstrated in numerous animal and human studies (Flood and Damaj, 2014), including neuropathic pain in humans (Rowbotham *et al.*, 2009; Richardson *et al.*, 2012). Randomized, double-blind, placebo-controlled trials have reported that intranasal or transdermal administration of nicotine preoperatively or postoperatively results in significantly decreased pain scores and lower morphine consumption, respectively (Flood and Daniel, 2004; Habib *et al.*, 2008; Yagoubian *et al.*, 2011). Similarly, laboratory animal studies have revealed that nicotine acts as an antinociceptive drug in a variety of acute

and chronic pain models in rodents (AlSharari *et al.*, 2012; Alsharari *et al.*, 2015). More specifically, the α7 nAChR subtype has been reported to mediate the antinociceptive effects of nicotine in a mouse model of postoperative pain (Rowley *et al.*, 2008).

Others have also investigated targeting nAChRs for the treatment of CIPN. For example, a recent study (Romero *et al.*, 2017) indicated that pharmacological and genetic blockade of the α9α10 nAChR subtype prevents the development of neuropathic pain induced by oxaliplatin in mice, suggesting that nAChRs play a significant role in the development and, potentially, the treatment of CIPN. Furthermore, nicotine reduces the ratio of pro-inflammatory monocytes compared to anti-inflammatory monocytes in murine bone marrow via the α7 nAChR subtype, thus significantly decreasing the level of pro-inflammatory cytokines, including tumor necrosis factor-α and interleukin-1β, and enhancing the release of anti-inflammatory cytokines, such as interleukin-12 (St-Pierre *et al.*, 2016). Moreover, nicotine exhibits a neuroprotective effect in animal models of neurodegenerative diseases, such as Alzheimer's disease, an action that is predominantly mediated through the α7 nAChR subtype (Ferrea and Winterer, 2009). Overall, it appears that the α7 nAChR may be one of the predominant nAChR subtypes involved in the neuroprotective actions of nicotine.

Although the current work clearly demonstrates the potential for nicotine to both prevent and reverse paclitaxel-induced peripheral neuropathy, there is an extensive body of literature suggesting that nicotine may stimulate tumor growth and/or interfere with the effectiveness of chemotherapy. This untoward effect is thought to occur via the binding of nicotine to an nAChR on the plasma membrane of the tumor cell, thereby promoting proliferative and antiapoptotic signaling via the extracellular signal-regulated kinase and

phosphoinositide 3-kinase/Akt (protein kinase B) pathways, respectively (Grando, 2014; Schaal and Chellappan, 2014). However, the only experimental condition under which we identified an effect of nicotine was on tumor cell proliferation in serum-free media, in which cells are deprived of nutrients, cytokines, and other growth factors, which is a nonphysiological environment. Under standard cell growth conditions, nicotine did not enhance viability, colony formation, or proliferation of a number of experimental tumor cell lines or interfere with apoptosis induced by paclitaxel.

It is somewhat difficult to make direct comparisons between our studies and those in the literature focusing on human NSCLC cell lines because the concentrations of paclitaxel and nicotine vary widely in these experiments, with paclitaxel concentrations ranging between 0.1 and 20 μM, and nicotine concentrations ranging from 0.1 to 10 μM. The human steady-state plasma concentration of paclitaxel falls between 5 and 200 nM, whereas the nicotine concentration in cigarette smokers ranges from 20 to 60 ng/ml, or 0.1 to 0.4 μM (Blagosklonny and Fojo, 1999; Benowitz *et al.*, 2009). In addition to the lack of consistency in the concentrations of paclitaxel and nicotine, the duration of drug exposure (18 hours to 7 days) and serum concentration (0-10%) also cover a wide range. In our work, we used 1 μM nicotine for 24-96 hours, a treatment regimen that involves both acute and chronic exposure to a nicotine concentration that is slightly higher than peak human plasma levels to use a clinically relevant dose of nicotine. Similarly, we used paclitaxel concentrations of 50 and 100 nM because the former is appropriate for experiments involving low cell numbers, such as the clonogenic assay, and the latter induces substantial apoptosis; yet, most importantly, both concentrations are within the range of human plasma levels.

Given the various experimental conditions, it is perhaps not surprising that the reported effects of nicotine vary widely as well. For example, some studies have shown increases of 23-200% in NSCLC cell proliferation (Zhang *et al.*, 2009; Pillai *et al.*, 2011; Wu *et al.*, 2013; Liu *et al.*, 2015), whereas others demonstrate modest increases of 7-18% (Chen *et al.*, 2002; Jarzynka *et al.*, 2006; Puliyappadamba *et al.*, 2010) and in one case decreases of 40-72% (Gao *et al.*, 2016). Nicotine has been reported to reduce paclitaxel-induced apoptosis by a significant 50% (Dasgupta *et al.*, 2006) or only by a modest 8% (Tsurutani *et al.*, 2005). These studies utilized sub-G1 DNA content, the terminal deoxynucleotidyl transferase-mediated digoxigenin-deoxyuridine nick-end labeling assay, and poly-ADP ribose polymerase cleavage to assess the impact of nicotine on paclitaxel-induced apoptosis, whereas we included quantification of early and late apoptotic populations with the Annexin V/PI assay. In part, this may provide a rationale for the inconsistencies in outcomes since sub-G1 DNA content alone does not distinguish between apoptotic and necrotic cell death (Mattes, 2007). The observation of substantially more apoptosis than sub-G1 DNA content after 48 hours of paclitaxel treatment likely reflects the possibility that early apoptotic cells had not yet become fragmented.

With regard to *in vivo* studies, while nicotine exposure has been reported to significantly increase lung tumor incidence, volume, weight, and Ki-67+ populations (Heeschen *et al.*, 2001; Jarzynka *et al.*, 2006; Improgo *et al.*, 2013; Iskandar *et al.*, 2013; Liu *et al.*, 2015), other reports have shown that chronic nicotine treatment does not significantly stimulate lung tumor growth in mice (Maier *et al.*, 2011; Murphy *et al.*, 2011; Warren *et al.*, 2012). Similarly, we found that chronic nicotine administration did not

enhance LLC tumor growth in immunocompetent mice, suggesting that nicotine may be a potential therapy for CIPN prior to or after chemotherapy with the aim of preventing and reversing peripheral neuropathy, respectively.

In summary, our results provide a proof of concept that nicotine is efficacious in preventing and reversing CIPN, actions that may enhance the quality of life of cancer patients and survivors. In addition, our findings suggest that nicotine does not significantly promote tumor cell proliferation or interfere with chemotherapy in lung cancer cell lines. In this context, we are encouraged by the report that nicotine replacement therapy is not a significant predictor of cancer in humans (Murray *et al.*, 2009).

Acknowledgements

The research was supported by the National Institutes of Health (NIH) [Grant 1R01-CA-206028-01] (to M.I.D. and D.A.G.), [Grant T32-DA-007027-41] (to S.L.K.), [Grant 1F31-NS-095628-01A1] (to L.D.S.) and, in part, by a Massey Cancer Center Pilot Project Grant (to D.A.G. and M.I.D.). Microscopy was performed at the VCU Microscopy Facility, and flow cytometry analysis was conducted at the VCU Massey Cancer Center Flow Cytometry Shared Resource, which were supported, in part, with funding by NIH-National Cancer Institute Cancer Center Support Grant P30-CA-016059. The content is solely the responsibility of the authors and does not necessarily represent the official views of the NIH.

CHAPTER THREE

The Influence of Nicotine on Lung Tumor Growth and Cancer Chemotherapy

S. Lauren Kyte and David A. Gewirtz

Department of Pharmacology & Toxicology (S.L.K., D.A.G.) and Massey Cancer Center (D.A.G.), Virginia Commonwealth University, Richmond, VA

Disclosure #1: The work included in this chapter has been published in the Journal of Pharmacology and Experimental Therapeutics (366: 303-313, August 2018).

Disclosure #2: Figures 20-23 were not included in the publication.

A. Introduction

Nicotine action in the nervous system and in tumor cells. Nicotine is an agonist of the nicotinic acetylcholine receptors (nAChRs), which are pentameric ligand-gated ion channels located on the membranes of various cells in the nervous and immune systems, as well as in lung tumor cells. These receptors can be homomeric, with five subunits of the same type (α7, α9), or heteromeric, with a combination of both α and β subunits (including α1-7, α9-10, and β1-4). Binding of an agonist such as nicotine to a nAChR induces a conformational change that allows for the influx of sodium and calcium ions. In neurons, this ion flux results in depolarization of the cell and initiation of an action potential. In tumor cells, both calcium-dependent and calcium-independent downstream signaling pathways of nAChRs appear to be activated; stimulation of these signaling pathways has been reported to contribute to proliferative and anti-apoptotic actions of nicotine [see reviews by (Egleton *et al.*, 2008; Improgo *et al.*, 2011; Schaal and Chellappan, 2014; Czyzykowski *et al.*, 2016)].

Antinociceptive and analgesic actions of nicotine. Both human and animal studies have demonstrated that nicotine possesses analgesic and antinociceptive properties, respectively. For example, randomized placebo-controlled clinical trials have revealed that nicotine can reduce post-operative pain scores in non-smokers, as well as decrease morphine consumption (Flood and Daniel, 2004; Habib *et al.*, 2008). In rats, Di Cesare Mannelli *et al.*, (2013) demonstrated that acute administration of nicotine can reverse trauma-induced neuropathic pain as well as oxaliplatin-induced cold and mechanical allodynia, both of which are characteristic of chemotherapy-induced peripheral

neuropathy (CIPN). Our laboratory, in collaboration with the Damaj group, has also shown that nicotine can both prevent and reverse paclitaxel-induced mechanical allodynia in mice following chronic and acute administration, respectively (Kyte *et al.*, 2018). These two reports are, to our knowledge, currently the only publications investigating the use of nicotine in CIPN animal models, indicating that there is a need to explore the anti-allodynic property of nicotine with other classes of cancer chemotherapy drugs that cause CIPN, such as the vinca alkaloids and bortezomib.

The potential utility of nicotine for mitigation of chemotherapy-induced peripheral neuropathy. Further investigation of the promising actions of nicotine in suppressing the development of and/or reversing the symptoms of CIPN could be compromised by the extensive body of literature, largely focused on lung cancer, that suggests nicotine can either promote tumor growth and/or reduce the antitumor effects of cancer chemotherapy. If these properties of nicotine translate to the clinic, then its use may be limited to patients who have previously undergone cancer therapy and are currently considered to be disease-free, since CIPN symptoms can persist for over 6 months after cancer chemotherapy administration has been completed (Seretny *et al.*, 2014). Therefore, even patients with cancer in complete remission may still be experiencing neuropathic pain and could benefit from nicotine treatment. If, however, nicotine could also be administered in combination with chemotherapy to *prevent* the development of CIPN in cancer patients, this would potentially provide an even greater patient benefit.

In our recent publication establishing the antinociceptive actions of nicotine in a mouse model of paclitaxel-induced peripheral neuropathy (Kyte *et al.*, 2018), we also reported that nicotine does not stimulate proliferation of non-small cell lung cancer (NSCLC) or ovarian cancer cells *in vitro*, or enhance NSCLC tumor growth *in vivo*. This work also demonstrated that nicotine fails to interfere with the antiproliferative and cytotoxic actions of paclitaxel in NSCLC cells in culture. These observations are in conflict with a large body of evidence that argues against the use of nicotine within the framework of tumor growth or the utilization of cancer chemotherapy [see reviews by (Catassi *et al.*, 2008; Grando, 2014)]. More specifically, nicotine has been shown to be capable of promoting tumor cell proliferation, invasion and metastasis, angiogenesis, and resistance to apoptotic cell death via various signaling pathways. In order to evaluate the potential utilization of nicotine for the alleviation of CIPN symptoms in cancer patients and/or cancer survivors, an analysis of the previous literature regarding nicotine's effects on lung cancer progression both alone and in combination with antitumor drugs has been performed. Our laboratory has also conducted additional experiments with nicotine *in vitro* and *in vivo* to investigate nicotine-mediated downstream signaling in lung cancer cell lines and the influence of chronic nicotine administration in tumor-bearing mice in an attempt to shed light on the remaining questions in the literature.

B. Materials and Methods

Animals. Adult male NOD *scid* gamma (NSG) mice (8 weeks at the beginning of experiments, 20-30 g) were either received as a gift from Dr. J. Chuck Harrell at Virginia Commonwealth University or purchased from the Cancer Mouse Models Core at VCU

Massey Cancer Center (Richmond, VA). Mice were housed in an AAALAC-accredited facility in groups of five; the mice in each cage were randomly allocated to different treatment groups. Food and water were available *ad libitum*. Experiments were performed during the light cycle (7:00 am to 7:00 pm) and were approved by the Institutional Animal Care and Use Committee of Virginia Commonwealth University and followed the National Institutes of Health Guidelines for the Care and Use of Laboratory Animals. Mice were euthanized via CO_2 asphyxiation followed by cervical dislocation.

Drugs. Paclitaxel was purchased from the VCU Health Pharmacy (NDC# 0703-4768-01, TEVA Pharmaceuticals, North Wales, PA) and diluted in a mixture of 1:1:18 [1 volume ethanol/1 volume Emulphor-620 (Rhone-Poulenc, Inc., Princeton, NJ)/18 volumes distilled water]. Paclitaxel injections of 10 mg/kg were administered intraperitoneally (i.p.) every day for a total of four injections; the injection site was swabbed with 70% ethanol prior to injection. (-)-Nicotine hydrogen tartrate salt was purchased from Sigma-Aldrich (St. Louis, MO, USA) and dissolved in PBS. Nicotine was administered chronically at a dose of 24 mg/kg per day via 7- or 28-day subcutaneous (s.c.) osmotic minipumps (Alzet, Model 1007D or 2004, Cupertino, CA), which were implanted 2 or 25 days prior to paclitaxel treatment, respectively. These paclitaxel and nicotine regimens were chosen based on previous unpublished and published studies that demonstrated which dose, duration of exposure, and route of administration for each drug effectively arrested tumor growth or prevented paclitaxel-induced peripheral neuropathy, respectively, but were not toxic to the animal (**Supplementary Fig. 14 in Appendix 2C**; Kyte *et al.*, 2018). All i.p.

or s.c. injections were given in a volume of 1 ml/100 g body weight, whereas the osmotic minipumps released 0.5 or 0.28 µl/hour.

Minipump Implantation. The procedure was performed as previously described in AlSharari *et al.*, (2013) with minor modifications. Mice were anesthetized with 3% isoflurane/97% oxygen. The anesthetized mice were prepared by shaving the back and swabbing the area with povidone-iodine, followed by 70% ethanol. Sharp, sterile scissors were used to make a 1 cm incision in the skin of the upper back/neck. The sterile, preloaded minipump (Alzet, Model 1007D or 2004, Cupertino, CA) containing nicotine or PBS was inserted with sterile forceps by a technician wearing sterile gloves. The wound was closed with sterile 9 mm stainless steel wound clips. Immediately after wound closure, the mice received a subcutaneous injection of 0.5 mg/kg Meloxicam SR (ZooPharm, Wildlife Pharmaceuticals, Windsor, CO) anterior to the shoulder. The mice were allowed to recover on heated pads and were monitored before returning to their home cages.

Assessment of tumor growth *in vivo*. Male adult NSG mice were subcutaneously injected with 1.0×10^6 or 1.5×10^6 A549 NSCLC cells in both flanks. The A549 cells were collected via trypsinization, then neutralized with medium, centrifuged, and washed with PBS. Pellets of 1.0×10^6 or 1.5×10^6 A549 cells were then resuspended in 30 µl of 80% basement membrane extract (Trevigen, 3632-010-02, Gaithersburg, MD)/20% PBS. Mice were anesthetized with isoflurane (2% isoflurane/98% oxygen) via inhalation during tumor cell inoculation; the injection site was swabbed with 70% ethanol prior to injection.

Palpable tumors formed at approximately 20 days post-tumor cell inoculation, after which tumor volumes (*l* x *w* x *h*) were assessed with calipers every 2 to 3 days. Subcutaneous osmotic minipumps (Alzet, Model 1007D or 2004, Cupertino, CA) were implanted as previously described at 3-weeks or 1-day post-tumor cell inoculation to release 24 mg/kg nicotine daily for a total of 7 or 28 days, respectively. Body weight and tumor volume were observed until humane endpoints were reached (tumor volume exceeds 1 cm^3), at which time mice were euthanized via CO_2 asphyxiation followed by cervical dislocation. Tumors were then extracted and preserved in 10% formalin.

Immunohistochemistry. Formalin-fixed tumors were embedded in paraffin and sectioned (5 μm thickness) for immunostaining of cleaved PARP. Tissue sections were deparaffinized, rehydrated, and quenched of endogenous peroxidase activity. After blocking with 1.5% goat serum for 1 hour, the tissues were incubated with the primary antibody (PARP cleavage site 214/215, Invitrogen, 1:100 dilution) for 1 hour at room temperature in a humidified chamber. The tissues were then incubated with a biotinylated secondary antibody (peroxidase anti-rabbit IgG, Vector Laboratories, 1:200 dilution) for an hour at room temperature in a humidified chamber. Immunostaining was completed with a Vectastain Avidin-Biotin Complex (ABC) kit (Vector Laboratories, Burlingame, CA) and the Pierce 3,3'-diaminobenzidine (DAB) horseradish peroxidase (HRP) substrate kit (Thermo Scientific, Rockford, IL) according to the manufacturer's recommendation. The tissues were subsequently stained with hematoxylin and eosin (Vector Laboratories, Burlingame, CA) and mounted. Images were taken with an inverted microscope (Olympus, Tokyo, Japan) under bright field at 20x magnification.

Cell culture. A549 and H460 NSCLC cells were maintained in DMEM supplemented with 10% (v/v) fetal bovine serum (FBS, Serum Source International, FB22-500HI, NC, USA) and 1% (v/v) combination of 10,000 U/ml penicillin and 10,000 µg/ml streptomycin (Pen/Strep, ThermoFisher Scientific, 15140-122, Carlsbad, CA). Cells were incubated at 37°C under a humidified, 5% CO_2 atmosphere. The A549 and H460 cell lines were generously provided by the laboratories of Dr. Charles Chalfant and Dr. Richard Moran at VCU, respectively.

Paclitaxel was dissolved in DMSO, diluted with sterile PBS, and added to the medium in order to obtain the desired concentration. Cells were not exposed to greater than 0.1% DMSO in any experiment. (-)-Nicotine hydrogen tartrate salt was dissolved in sterile PBS. All experiments involving these light-sensitive drugs were performed in the dark. For the radiation conditions, cells were irradiated at a dose of 8 Gray (Gy) with a ^{137}Cs irradiator.

Western blot analysis. Western blots were performed as previously described (Sharma et al., 2014), with minor modifications. After the indicated treatments, cells were trypsinized, collected, and lysed in CHAPS buffer containing protease and phosphatase inhibitors (Thermo Scientific, Waltham, MA) containing protease and phosphatase inhibitors. Protein concentrations were determined by the Bradford assay (Bio-Rad Laboratories, Hercules, CA). Total protein was then diluted in sodium dodecyl sulfate polyacrylamide gel electrophoresis (SDS-PAGE) sample buffer and boiled for 5 min. Protein samples were subjected to SDS-PAGE, transferred to polyvinylidene difluoride

membrane, and blocked in 5% milk in PBS-tween for 1 hour. Membranes were incubated with primary antibodies (1:1000 dilution) overnight: p-Akt (Cell Signaling Technology), Akt (Cell Signaling Technology), Rb (Transduction Laboratories), p53 (BD Biosciences), p21 (BD Biosciences), GAPDH (Cell Signaling Technology), followed by incubation with a secondary antibody (1:200 dilution) of either horseradish peroxidase-conjugated goat anti-rabbit IgG antibody (Cell Signaling Technology) or goat anti-mouse IgG antibody (Cell Signaling Technology) for 1 hour. Membranes were then washed with PBS-tween and developed using Pierce enhanced chemiluminescence reagents (Thermo Scientific, 32132, Rockford, IL).

Statistical analyses. A power analysis calculation was performed with the Lamorte's Power Calculator (Boston University Research Compliance) to determine the sample size of animals for each group (Charan and Kantharia, 2013). For assessing tumor volume, the calculations showed that an n of 9 was required to achieve a power of 90% with an alpha error of 0.05. Therefore, we began each study with 10 mice per group; some mice were euthanized prior to the final time point of the experiment due to tumor burden. The data were analyzed with GraphPad Prism software, version 6 (GraphPad Software, Inc., La Jolla, CA) and SPSS, version 24, and are expressed as mean ± SEM. Student's t-tests were performed to analyze tumor weight and linear mixed models were utilized to account for the loss of tumor-bearing mice when analyzing tumor volume over time (Little and Rubin, 1987); repeated measures were considered. Differences were determined to be significant at $P < 0.05$.

C. Studies in Cell Culture

Nicotine alone. Approximately half of the publications relating to nicotine and lung cancer *in vitro* have reported significant increases in various assays assessing lung cancer cell progression (**Tables 4 and 5**); the lung cancer type for each cell line used in these studies is indicated in **Table 3**. However, the experimental systems used are not uniform. Almost half of the *in vitro* experiments were conducted under conditions of serum deprivation or serum starvation with the purpose of eliminating exogenous growth factors and/or inducing quiescence to synchronize the cell cycle. This approach creates an environment where enhanced proliferation induced by nicotine is likely to be more pronounced (Rosner *et al.*, 2013); however, the physiological relevance may be limited. The majority of serum starvation/deprivation studies show an increase in lung tumor cell viability (viable cell number), proliferation, growth, invasion, and/or migration following nicotine exposure over a wide range of nicotine concentrations (10 nM – 500 μM; **Table 5**). In contrast, a number of studies reported no effects of nicotine (1 pM – 100 μM for 48-72 hours) on lung cancer cell viability, growth, or proliferation even under the relatively non-physiological condition of serum deprivation (Heeschen *et al.*, 2001; Jarzynka *et al.*, 2006; Mucchietto *et al.*, 2017). In our own studies, nicotine exposure (1 μM for 24 hours) under either serum deprivation or serum starvation conditions had essentially no influence on NSCLC cell viability (Kyte *et al.*, 2018).

If the administration of nicotine via nicotine patches or gum could prove to have utility for the prevention or treatment of CIPN, then it is necessary to evaluate the previous literature within the framework of plasma nicotine concentrations in patients using nicotine replacement therapy (NRT). Nicotine patches (21 mg) deliver peak plasma

concentrations of 18-23 ng/ml or 111-142 nM nicotine within 8 hours of use, after which the levels gradually decline until the patch is removed at 24 hours post-application (Fant *et al.*, 2000); 2-4 mg nicotine gum provides maximum nicotine concentrations of 6-17 ng/ml or 37-105 nM after 30 minutes of chewing (Benowitz *et al.*, 1987). Although e-cigarettes are unlikely to be considered for therapeutic use, these devices can generate circulating nicotine concentrations of 7-25 ng/ml or 43-154 nM (Wagener *et al.*, 2017). These values suggest that concentrations of nicotine in cell culture studies between 35 nM and 200 nM would encompass the range of plasma nicotine levels that would be achieved in patients using NRT. However, the majority of studies have tested nicotine concentrations from 100 nM to 1 μM, a range that is comparable to or slightly higher than the plasma nicotine levels of 20-60 ng/ml or 100-400 nM observed after tobacco cigarette smoking (Benowitz *et al.*, 2009). Overall, the studies shown in **Table 4** demonstrate the capacity of nicotine to increase lung cancer cell viability, growth, proliferation, invasion, migration, and/or angiogenesis following 30-minute to 2-week exposure to 0.1-1 μM nicotine. However, only half of these publications demonstrate *significant* increases in characteristics of tumor growth, ranging from a 20% to a 750% increase, while half of the studies do not demonstrate significant enhancement. When considering nicotine levels achieved during NRT use (35 – 200 nM), only a third of the studies report significant increases in lung cancer cell viability, proliferation, migration, and/or invasion, with approximately half of these experiments having been performed under conditions of serum deprivation or serum starvation (**Tables 4 and 5**). When excluding studies performed under serum deprivation/starvation conditions and limiting our analysis to the lower, therapeutically relevant concentrations of nicotine, it may be surmised that the

effects of nicotine on lung tumor progression with nicotine patch or gum use *are likely to be negligible*.

On the other hand, approximately 40% of publications testing 0.1 to 1 μM nicotine *under full serum conditions* report no effects or modest, *non-significant* effects of nicotine on tumor cell viability, growth, and/or proliferation following 12 hours to 2 weeks of nicotine exposure (**Table 4**). In addition, studies using nicotine concentrations between 100 nM to 1 μM for 24-72 hours under full serum conditions (Zeng *et al.*, 2012; Gao *et al.*, 2016) have reported that nicotine *decreases* lung tumor cell viability and growth; these reports also showed decreases in lung cancer cell viability with 2.5 to 15 μM nicotine. However, the impact of nicotine at higher non-physiological and non-pharmacological concentrations is likely the result of off-target effects and general toxicity; ultrastructural analysis of A549 NSCLC cells treated with 10 μM nicotine revealed shrunken nuclei, an increase in both nucleoli and lysosomes, swollen mitochondria, and changes in endoplasmic reticulum morphology after 24 hours (Gao *et al.*, 2016).

Species	Lung Cancer Type	Lung Cancer Cell Lines
Human	Non-small cell lung cancer (NSCLC)	A549, H23, H157, H358, H460, H1299, H1703, H1975, H5800, PC9, 11-18
	Small cell lung cancer (SCLC)	DMS-53, H446, N417, N592
	Adenocarcinoma	HCC827, T1 (primary), 201T (primary)
	Bronchoalveolar carcinoma	H1650
	Papillary adenocarcinoma	H441
	Squamous cell carcinoma	SW900
Mouse	Lewis lung carcinoma	LLC
	Adenocarcinoma	LKR, Line1

Table 3. Lung cancer cell lines grouped by species and lung cancer type. The cell lines indicated as “primary” were derived from human lung cancer tissue samples, not purchased commercially.

Lung Cancer Cell Line	[Nicotine]	Duration of Treatment	Serum Conc.	Cellular Response (Assay)	Result (Relative to Control)	Reference
14 SCLC and NSCLC lines	0.1 – 1 μM	5 d	10%	Viability (MTT)	No effect	(Maneckjee and Minna, 1990)
H460, H157	0.1 – 1 μM	7 d	10%	Viability (MTT)	No effect	(Chen *et al.*, 2002)
201T	1 μM	48 h	10%	Viability (MTS)	No effect	(Carlisle *et al.*, 2007)
H460	0.1, 1 μM	5 d	10%	Viability (Cell Titer-Glo)	20, 25% increase*	(Zheng *et al.*, 2007)
A549	1 μM	24 h	10%	Viability (MTT)	20% increase*	(Zhang *et al.*, 2009)
				Growth ([^{3}H]-thymidine)	50% increase*	
A549, H1299	0.1, 1 μM	72 h	Not indicated	Viability (MTT)	H1299: 20, 5% increase† A549: 10, 15% increase†	(Puliyappadamba *et al.*, 2010)
		72 h		Growth ([^{3}H]-thymidine)	H1299:15, 5% increase† A549: 20, 10% increase†	
		previously treated for 72 h, then seeded		Proliferation (Colony formation)	A549: 175% increase (1 μM) †	
H441, H1299	1 μM	30 min or 7 d$^\#$	10%	Viability (MTT)	100, 75% increase (30 min)*, 375, 250% increase (7 d)*	(Al-Wadei *et al.*, 2012)
H446	0.1 – 1 μM	12-72 h	10%	Viability (MTT)	8, 5% increase at 12 h (0.1, 0.25 μM)†, no effect at 24-48 h, 8% decrease at 72 h (0.5, 1 μM) †	(Zeng *et al.*, 2012)
A549	1 μM	3-5 d	10%	Viability (MTT)	40-80% increase*	(Wu *et al.*, 2013)
		24 h		Invasion (Boyden)	60% increase*	
A549	0.1, 1 μM	24 h	10%	Viability (MTS)	40, 55% decrease*	(Gao *et al.*, 2016)
LKR, H5800	1 μM	2 w^	10%	Proliferation (Colony formation)	13, 24% increase†	(Nishioka *et al.*, 2010)
SW900	1 μM	24 h	Not Indicated	Proliferation (Cell counting)	275% increase*	(Chernyavsky *et al.*, 2015)
A549	1 μM	24 h	10%	Invasion (Transwell)	7% increase	(Sun and Ma, 2015)
		8 or 24 h		Migration (Wound-healing)	10% increase (8 h), 28% increase (24 h)*	
A549, H460, LLC, T1	0.1-1 μM	24 h	10%	Viability (MTS, MTT)	No effect	(Kyte *et al.*, 2018)
A549, H460	1 μM	48-96 h		Viability (MTS, MTT)	No effect	
	1 μM	48 h		Proliferation (Cell counting)	No effect	

	1 μM	24 h		Proliferation (Colony formation)	No effect	
A549	0.5, 1 μM	16 h	10%	Angiogenesis (HIF-1α)	350, 750% increase*	(Zhang *et al.*, 2007)
				Angiogenesis (VEGF)	14% increase (0.5 μM), 43% increase (1 μM)*	
A549, H1299, H1975	0.1, 1 μM	24 h	10%	Viability (MTT)	A549: 39, 52% increase* H1299: 13% increase (0.1 μM), 20% increase (1 μM)* H1975: 30% increase (0.1 μM), 52% increase (1 μM)*	(Ma *et al.*, 2014)
A549	0.1-1 μM	16 h		Angiogenesis (HIF-1α)	20-40% increase (0.1, 0.5 μM), 100% increase (1 μM)*	
A549	0.1-1 μM	16 h		Angiogenesis (VEGF)	75, 125% increase (0.1, 0.5 μM), 175% increase (1 μM)*	

Table 4. *In vitro* effects of nicotine on lung cancer. Abbreviations: d, days; HIF-1α, hypoxia-inducible factor 1-alpha; h, hours; LLC, Lewis lung carcinoma; min, minutes; MTS, (3-(4,5-dimethylthiazol-2-yl)-5-(3-carboxymethoxyphenyl)-2-(4-sulfophenyl)-2H-tetrazolium); MTT, 3-(4,5-dimethylthiazol-2-yl)-2,5-diphenyltetrazolium bromide; NSCLC, non-small cell lung cancer; SCLC, small cell lung cancer; T1, primary human lung carcinoma; VEGF, vascular endothelial growth factor; w, weeks. [#]nicotine was replaced every 24 hours, ^nicotine was replenished every 4 days, *statistically significant, [†]statistical significance not indicated.

Lung Cancer Cell Line	[Nicotine]	Duration of Treatment	Serum Concentration	Cellular Response (Assay)	Result (Relative to Control)	Reference
H460, H157	0.01 – 1 mM	7 d	10%	Viability (MTT)	H460: 5% increase (10, 100 μM), 5% decrease (1 mM) H157: 5% decrease (10 μM), 5% increase (0.1-1 mM)	(Chen *et al.*, 2002)
201T	10 μM	48 h	10%	Viability (MTS)	No effect	(Carlisle *et al.*, 2007)
H460	10 nM, 0.01-1 mM	5 d	10%	Viability (Cell Titer-Glo)	12.5-50% increase (10 nM, 10-100 μM)*, no effect (1 mM)	(Zheng *et al.*, 2007)
A549, H1299	1 nM – 10 mM	72 h	Not indicated	Viability (MTT)	A549: 5-18% increase (1 nM – 10 μM), no effect (100 μM), 5-40% decrease (1-10 mM)† H1299: 10-30% increase (1-100 nM), no effect (1-100 μM), 40-80% decrease (1-10 mM)†	(Puliyappadamba *et al.*, 2010)
H446	2.5-15 μM	12-72 h	10%	Viability (MTT)	0-85% decrease†	(Zeng *et al.*, 2012)
A549	0.01, 10 μM	24 h	10%	Viability (MTS)	No effect (0.01 μM), 75% decrease (10 μM)*	(Gao *et al.*, 2016)
A549, H1975	10 nM – 100 μM	48 h	0% for 72 h, then treated	Viability (MTS)	A549:12.5% increase (50 nM – 100 μM)*, H1975: no effect	(Mucchietto *et al.*, 2017)
				Proliferation (Cell counting)	A549: 33-66% increase*, H1975: no effect	
A549	0.5 - 10 μM	72 h	0%	Growth (BrdU)	0-9% increase	(Jarzynka *et al.*, 2006)
Line1	1 μM	18 h	0% for 72 h, then treated	Growth (BrdU)	180% increase†	(Davis *et al.*, 2009)
LKR	1 μM	24 h	0.2% for 24 h, then treated	Growth ([^{3}H]-thymidine)	200% increase†	(Nishioka *et al.*, 2010)
A549, H1299	1 nM – 100 μM	24 h	Not indicated	Growth ([^{3}H]-thymidine)	5-20% increase (1 nM – 1 μM)†, 5-20% decrease (10-100 μM)†	(Puliyappadamba *et al.*, 2010)
A549	1 μM	18 h	0% for 36 h, then treated	Growth (BrdU)	150% increase*	(Dasgupta *et al.*, 2011)
A549, H1650	1 μM	18 h	0% for 24 h, then treated	Growth (BrdU)	175-180% increase†	(Pillai *et al.*, 2011)
		24 h		Invasion (Boyden)	90-100% increase†	
A549, H1650	1 μM	18 h	0% for 24 h, then treated	Growth (BrdU)	75, 100% increase†	(Nair *et al.*, 2014)
		24 h		Invasion (Boyden)	75, 150% increase†	
LLC	1 pM – 100 μM	Not indicated	0.1%	Proliferation (Cell counting)	No effect	(Heeschen *et al.*, 2001)
H157, H1703	100 nM	3 d#	0.1%	Proliferation (Cell counting)	50-95% increase*	(Tsurutani *et al.*, 2005)
H1299	10 nM	previously treated for 72 h, then seeded	Not indicated	Proliferation (Colony formation)	150% increase†	(Puliyappadamba *et al.*, 2010)
A549	0.01-10 μM	18 h	0% (before and during treatment)	Invasion (Boyden)	10% decrease (10 nM), 50-160% increase (0.1-1 μM), 90% increase (10 μM) †	(Dasgupta *et al.*, 2009)
		24 h	0% (during treatment)	Migration (Wound-healing)	10-100% increase (0.01-1 μM), 25% increase (10 μM) †	
N417	500 μM		10%	Proliferation	130% increase*	

		previously treated for 7 d, then seeded		(Colony formation)		(Martínez-García *et al.*, 2010)
			0.5%	Migration (Transwell)	55% increase*	
A549, H1299	0.1-1 μM	36 h	0% for 24 h, treated, then seeded	Proliferation (Cell counting)	50-200% increase*	(Liu *et al.*, 2015)
				Migration (Wound healing)	30% increase*	
				Invasion (Transwell)	20% increase*	
A549, H1650, H1975, H23, H358	1 μM	24 h	0% for 36 h, then treated	Invasion (Boyden)	120-430% increase*	(Pillai *et al.*, 2015)
A549, H1299	1 μM, 10 nM	48 h	0% for 12 h, then treated	Viability (CCK-8)	25, 40% increase*	(Gong *et al.*, 2014)
		48 h		Invasion (Transwell)	75% increase*	
		48 h, 72 h		Migration (Wound-healing)	25, 30% increase*	
A549, H460, LLC, T1	5, 10 μM	24 h	10%	Viability (MTS, MTT)	No effect	(Kyte *et al.*, 2018)
A549, H460	1 μM	48-96 h	0-5%	Viability (MTS, MTT)	A549: No effect, H460: 25% increase w/ 0% serum at 96 h*	
A549	5 μM	48 h	10%	Invasion (QCM^{TM})	950% increase*	(Zhang *et al.*, 2007)
	5, 10 μM	16 h		Angiogenesis (HIF-1α)	1000, 1100% increase*	
	5, 10 μM	16 h		Angiogenesis (VEGF)	130, 170% increase*	
A549, H1299, H1975	10, 50 μM	24 h	10%	Viability (MTT)	A549: 40% increase (10 μM)*, no effect (50 μM) H1299: 13, 14% increase H1975: 65% increase (10 μM)*, 40% increase (50 μM)	(Ma *et al.*, 2014)
A549	5 μM	16 h		Angiogenesis (HIF-1α)	25% increase	
A549	5 μM	16 h		Angiogenesis (VEGF)	150% increase	
A549	5 μM	36 h	10%	Invasion (Transwell)	230% increase*	(Shi *et al.*, 2015)
		16 h		Angiogenesis (VEGF protein, mRNA)	25% increase*, 700% increase*	
		16 h		Angiogenesis (HIF-1α mRNA)	100% increase*	

Table 5. *In vitro* effects of nicotine on lung cancer under non-physiological conditions and/or with non-pharmacological concentrations of nicotine. Abbreviations: BrdU, bromodeoxyuridine; CCK-8, cell counting kit-8; d, days; HIF-1α, hypoxia-inducible factor 1-alpha; h, hours; LLC, Lewis lung carcinoma; min, minutes; MTS, (3-(4,5-dimethylthiazol-2-yl)-5-(3-carboxymethoxyphenyl)-2-(4-sulfophenyl)-2H-tetrazolium); MTT, 3-(4,5-dimethylthiazol-2-yl)-2,5-diphenyltetrazolium bromide; T1, primary human lung carcinoma; VEGF, vascular endothelial growth factor; w, weeks. #nicotine was replaced every 24 hours, *statistically significant, †statistical significance not indicated.

Nicotine in combination with cancer chemotherapy. Nearly three quarters of cell culture studies assessing the influence of nicotine on sensitivity to chemotherapy in lung cancer cells show significant interference with chemotherapy (**Tables 6 and 7**). A nicotine-induced resistance to chemotherapy (average of 50% decrease in apoptosis with 1 μM nicotine) has been observed with Annexin V-Propidium Iodide staining, caspase activity, and DNA fragmentation assays (ELISA and cell cycle analysis for Sub-G1 population), as well as standard viability assays (**Table 6**). Lung cancer cells exposed to both cancer chemotherapy and nicotine over the range of 0.1 – 1 μM have been shown to exhibit increased viability and decreased apoptosis, though statistical significance was only reported for about two-thirds of these studies. In contrast, our findings that nicotine (1 μM for 24-48 hours with 10% serum) does not attenuate paclitaxel-induced growth arrest or apoptosis (Kyte *et al.*, 2018) are consistent with studies by other laboratories that have shown a lack of significant effects of nicotine (0.1-1 μM for 1 hour to 1 week with 10% serum) on cisplatin-induced DNA fragmentation (apoptosis) and decreased viability, or on gefitinib-induced decreases in lung cancer cell viability (Carlisle *et al.*, 2007; Nishioka *et al.*, 2010; Zeng *et al.*, 2012; Togashi *et al.*, 2015). Nevertheless, it is apparent that anti-apoptotic and pro-survival effects can occur as the concentration of nicotine increases (**Table 7**). Surprisingly, only one study has been conducted with nicotine in the NRT range, in this case 100 nM nicotine, in combination with chemotherapy (Zeng *et al.*, 2012). This report demonstrated that 100 nM nicotine induces only a modest increase in viability in the presence of 10 μM cisplatin and has *no effect* on cisplatin-induced apoptosis.

Lung Cancer Cell Line	[Nicotine]	Chemotherapy	Duration of Treatment	Serum Conc.	Cellular Response (Assay)	Result (Relative to Chemotherapy Alone)	Reference
A549	1 μM	Cisplatin 40 μM	24 h	10%	Apoptosis (Annexin V)	30% decrease†	(Jin *et al.*, 2004)
A549, H157	1 μM	Cisplatin 40 μM	6-48 h	10%	Apoptosis (Annexin V)	0-40% decrease†	(Xin and Deng, 2005)
			24 h			40% decrease†	
LKR	1 μM	Cisplatin 5 μM	Nicotine for 1 h, then cisplatin for 24 h	10%	Apoptosis (Sub-G1)	20% decrease†	(Nishioka *et al.*, 2010)
			Nicotine for 1 w, then cisplatin for 24 h			5% decrease†	
H446	0.1-1 μM	Cisplatin 10 μM	12-72 h	10%	Viability (MTT)	13-20% increase†	(Zeng *et al.*, 2012)
			36 h		Apoptosis (AV/PI)	No effect (0.1-0.5 μM), 15% decrease (1 μM)*	
H5800, LKR	0.5 μM	Cisplatin 0.6 μM	Nicotine for 24 h, then co-treatment for 48 h	10%	Apoptosis (Annexin V)	60% decrease*	(Nishioka *et al.*, 2014)
A549	1 μM	Cisplatin 20 μM	Nicotine for 24 h, then cisplatin for 24 h	10%	Apoptosis (AV/PI)	40% decrease*	(Liu *et al.*, 2015)
A549	1 μM	Cisplatin 35 μM	Nicotine for 24 h, then co-treatment for 24 h	10%	Viability (MTT)	25% increase*	(Zhang *et al.*, 2009)
		Etoposide 20 μM				35% increase*	
		Cisplatin 35 μM			Apoptosis (DNA fragmentation ELISA)	35% decrease*	
		Etoposide 20 μM				20% decrease*	
H1299	1 μM	Cisplatin 40 μM	96 h	10%	Apoptosis (Annexin V)	40% decrease*	(Zhao *et al.*, 2009)
		Etoposide 40 μM				30% decrease*	
A549	1 μM	Doxorubicin 10 μM	Nicotine for 1 h, then co-treatment for 48 h	10%	Viability (XTT)	25% increase*	(Nakada *et al.*, 2012)
					Apoptosis (Caspase-Glo 3/7)	300% decrease*	
PC9, HCC827	1 μM	Erlotinib 1 nM-5 μM	72 h	10%	Viability (MTS)	IC_{50} 31 nM → 43 nM (PC9)*, IC_{50} 46 nM → 140 nM	(H Li *et al.*, 2015)
201T	1 μM	Gefitinib 35 μM	48 h	10%	Viability (MTS)	30% increase	(Carlisle *et al.*, 2007)
PC9, 11-18	1 μM	Gefitinib 5 nM-50 μM	72 h	10%	Viability (MTT)	IC_{50} 24 nM → 22 nM, 0.35 μM → 0.33 μM	(Togashi *et al.*, 2015)
			Nicotine for 3 m, then co-treatment for 72 h			IC_{50} 24 nM → 76 nM*, 0.35 μM → 1.09 μM*	
A549, H460	1 μM	Paclitaxel 50 nM	Paclitaxel for 24 h, 24 h drug-free, nicotine for 24 h	10%	Proliferation (Colony formation)	No effect	(Kyte *et al.*, 2018)
		Paclitaxel 50 nM	Nicotine for 24 h, then 24 h cotreatment		Proliferation (Cell counting)	No effect	

		Paclitaxel 100 nM	48 h		Apoptosis (AV/PI)	No effect	
		Paclitaxel 100 nM	48 h		Apoptosis (Sub-G1)	No effect	

Table 6. *In vitro* effects of nicotine in combination with chemotherapy on lung cancer. Abbreviations: AV/PI, annexin V/propidium iodide; ELISA, enzyme-linked immunosorbent assay; h, hours; MTS, (3-(4,5-dimethylthiazol-2-yl)-5-(3-carboxymethoxyphenyl)-2-(4-sulfophenyl)-2H-tetrazolium); MTT, 3-(4,5-dimethylthiazol-2-yl)-2,5-diphenyltetrazolium bromide; XTT, 2,3-Bis(2-methoxy-4-nitro-5-sulfophenyl)-2*H*-tetrazolium-5-carboxanilide inner salt**.** *statistically significant, †statistical significance not indicated.

Lung Cancer Cell Line	[Nicotine]	Chemotherapy	Duration of Treatment	Serum Concentration	Cellular Response (Assay)	Result (Relative to Chemotherapy Alone)	Reference
A549	1 μM	Cisplatin 20 μM	24 h	0% for 36 h, then treated	Apoptosis (TUNEL)	40% decrease*	(Dasgupta *et al.*, 2011)
H446	2.5-15 μM	Cisplatin 10 μM	12-72 h	10%	Viability (MTT)	10-20% increase (2.5 μM), 0-50% decrease (5-15 μM)†	(Zeng *et al.*, 2012)
			36 h		Apoptosis (AV/PI)	25-50% decrease*	
A549, H1299, H23	1 μM	Cisplatin 20 μM	36 h	0%	Apoptosis (TUNEL)	20-40% decrease†	(Dasgupta *et al.*, 2006)
		Gemcitabine 20 μM				20-25% decrease†	
		Paclitaxel 20 μM				25-50% decrease†	
N417	previous nicotine exposure (500 μM for 7 d)	Cisplatin (5-100 μM)	48 h	10%	Viability (MTT)	50% increase*	(Martínez-García *et al.*, 2010)
		Etoposide (5-100 μM)				50% increase*	
		Mitomycin (5-50 μM)				IC_{50} 10 μM → 20 μM*	
		Paclitaxel (5-100 μM)				IC_{50} 35 μM → 70 μM*	
201T	10 μM	Gefitinib 35 μM	48 h	10%	Viability (MTS)	47% increase (10 μM)*	(Carlisle *et al.*, 2007)
A549	1 μM	Gemcitabine 10 μM	36 h	0% for 24 h, then treated	Apoptosis (TUNEL)	20% decrease*	(Guo *et al.*, 2013)
H157, H1703	10 μM	Paclitaxel 100 nM	48 h	0.1%	Apoptosis (Sub-G1)	8% decrease*	(Tsurutani *et al.*, 2005)
		Etoposide 100 μM				15% decrease*	

Table 7. *In vitro* effects of nicotine in combination with chemotherapy on lung cancer under non-physiological conditions and/or with non-pharmacological concentrations of nicotine. Abbreviations: AV/PI, annexin V/propidium iodide; d, days; h, hours; MTS, (3-(4,5-dimethylthiazol-2-yl)-5-(3-carboxymethoxyphenyl)-2-(4-sulfophenyl)-2H-tetrazolium); MTT, 3-(4,5-dimethylthiazol-2-yl)-2,5-diphenyltetrazolium bromide; TUNEL, terminal deoxynucleotidyl transferase (TdT) dUTP nick-end labeling**.** *statistically significant, †statistical significance not indicated.

D. Studies in Tumor-Bearing Animals

As with the cell culture work, studies regarding the effects of nicotine on lung tumor growth and sensitivity to cancer chemotherapy drugs in tumor-bearing animals vary greatly in their design, given the use of both human and murine lung tumor xenografts, carcinogen-induced tumor development, and oncogene-induced spontaneous tumor formation. Excluding studies of nicotine-exposed lung cancer cell xenografts, where the cells were treated with nicotine *ex vivo* before implantation, approximately two-thirds of the publications show that chronic nicotine administration can significantly increase lung tumor incidence/recurrence, size, weight, and/or metastasis, as well as Ki-67 and angiogenic factor expression *in vivo* (**Table 8**). One study included the use of 14 mg NicoDerm® CQ® patches that were cut to represent 0.45 mg or 25 mg/kg nicotine (Davis *et al.*, 2009). These transdermal patches were applied to the lower dorsal region of female immunocompetent tumor-bearing mice daily for 2 weeks during tumor growth. Cotinine, a predominant metabolite of nicotine, was quantified in the urine of these mice (5000 ng/ml) and was shown to be comparable with urine cotinine concentrations in human smokers (1500-8000 ng/ml). Although this animal model well represents cancer patients receiving NRT, the dose of nicotine appears to be higher than what would be expected clinically since non-pregnant women receiving nicotine via a 22 mg patch have been reported to produce 2240 ng cotinine in their urine (Ogburn *et al.*, 1999). In addition, the remaining third of the literature has shown that chronic nicotine administration *does not* enhance lung tumor incidence, multiplicity, volume, and/or growth (Ki-67+ population) in mice (Pratesi *et al.*, 1996; Maier *et al.*, 2011; Murphy *et al.*, 2011), as also reported in our own studies (Kyte *et al.*, 2018; **Figures 19 and 20**).

Surprisingly, few studies involving systemic co-administration of nicotine and cancer chemotherapy have been conducted *in vivo*. Li *et al.*, (2015) observed significant increases in PC9 human lung adenocarcinoma tumor volume in BALB/c nude mice following administration of erlotinib (100 mg/kg, p.o.) for 10 days in combination with 100 µg/ml nicotine in the drinking water or given intravenously (0.6 mg/kg, 5x/week) when compared to erlotinib alone. In contrast, immune-deficient NSG mice inoculated with A549 human NSCLC cells displayed no significant interference with paclitaxel-induced decreases in tumor volume and weight when nicotine was administered at a dose of 24 mg/kg per day for 2 days prior to paclitaxel and for an additional 5 days during the chemotherapy (**Figures 20A and B**). The tumors of both the paclitaxel + PBS- and paclitaxel + nicotine-treated mice were significantly smaller in both volume and weight when compared to vehicle + PBS-treated mice. The tumors extracted from these mice underwent immunohistochemical staining for qualitative analysis of cleaved PARP, a protein that normally participates in DNA repair, but is rendered inactive upon cleavage by caspases during apoptosis (Los *et al.*, 2002). Similar to the tumor growth outcomes, tumors from both paclitaxel + PBS- and paclitaxel + nicotine-treated mice exhibited positive staining for cleaved PARP, whereas vehicle + PBS- and vehicle + nicotine-treated mice possessed tumors with relatively less cleaved PARP staining (**Figure 20C**). Likewise, in the absence of chemotherapy, there was no enhancement in tumor growth in vehicle + nicotine-treated mice when compared to vehicle + PBS-treated mice.

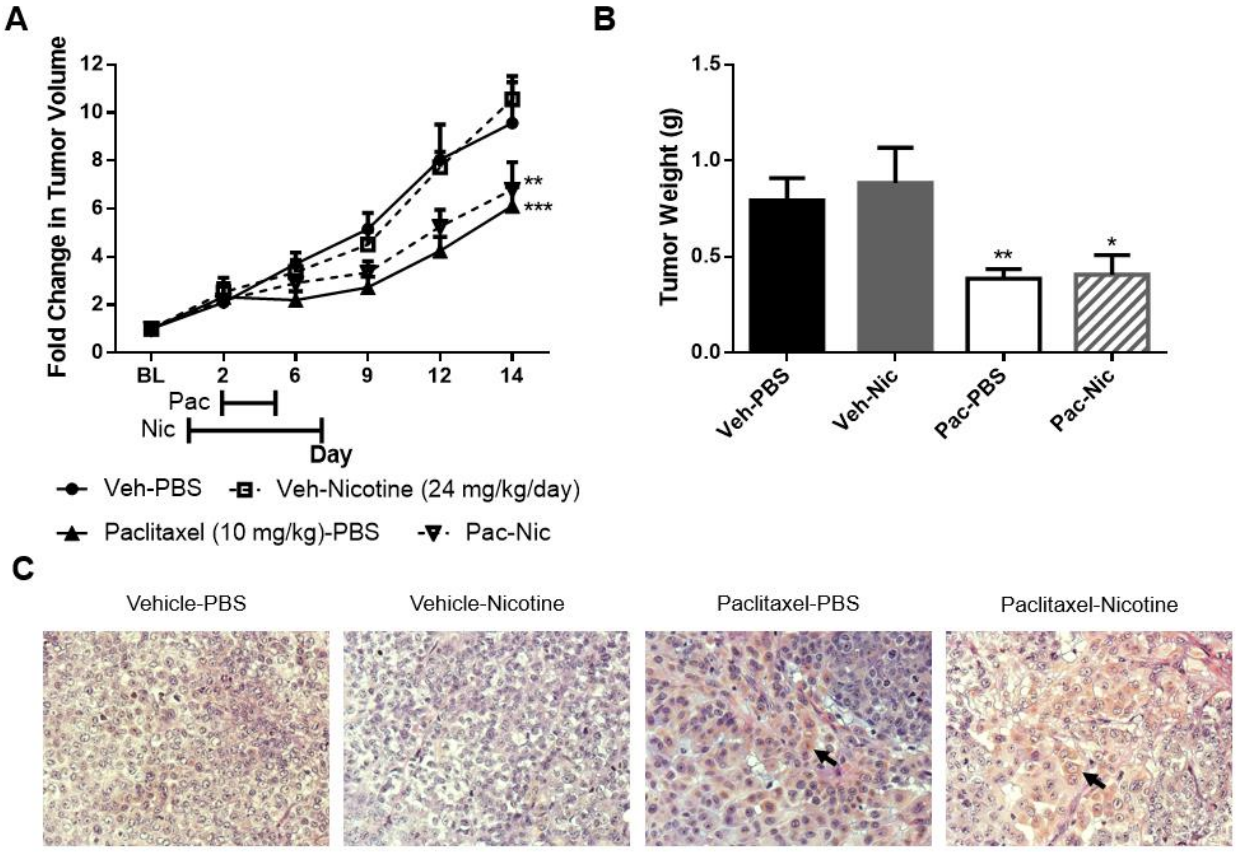

Figure 20. Nicotine fails to enhance A549 NSCLC tumor growth or interfere with the antitumor property of paclitaxel *in vivo*. NSG mice were injected s.c. with 1.5 x 10^6 A549 cells in both flanks. Once tumors formed, subcutaneous osmotic minipumps were implanted on day 0 to release PBS or 24 mg/kg nicotine daily for a total of 7 days. Paclitaxel treatment consisted of 10 mg/kg i.p. injections daily for 4 days, starting on day 2. A) The left and right flank tumor volumes (*l* x *w* x *h*) were determined with calipers and compared to the respective baseline tumor volumes to calculate fold change; the fold change values were averaged for each mouse. A two-way linear mixed model analysis revealed a significant interaction between time and treatment [F (15, 168) = 2.094, P = 0.012] and was followed by a Bonferroni post hoc test. **P = 0.01, ***P < 0.001 vs Veh-PBS. n = 7-9 mice per group; one outlier in the Pac-Nic group on day 14 was removed according to Chauvenet's criterion. Data are expressed as mean + SEM. B) Mice were euthanized on day 14, after which tumors were extracted and weighed; tumor weights were averaged for each mouse. *P < 0.05, **P < 0.01 vs Veh-PBS. n = 6-7 mice per group. Data are expressed as mean + SEM. C) Immunohistochemical staining for cleaved PARP, an apoptosis marker, was performed on paraffin-embedded tumor sections; brown color (arrow) indicates positive staining. Tissues were also stained with hematoxylin and eosin to better observe cell morphology. Images were taken with an Olympus microscope at 20x magnification. Representative images of 4 tumors per group are shown. Veh, vehicle; Nic, nicotine; Pac, paclitaxel.

As it is common for lung cancer patients to be former and/or current smokers, we tested whether chronic lung cancer cell exposure to nicotine would influence both tumor formation and tumor growth in the mouse. Based on our previous unpublished studies, A549 cells were injected into the flanks of mice as follows: 1.5 x 10^6 A549 cells, a cell density known to consistently induce tumor formation within three weeks, and 1.0 x 10^6 A549 cells, a cell density that produces relatively delayed tumor formation and growth. Although drug treatment following tumor cell inoculation does not represent nicotine exposure during carcinogenesis, observing the effect of nicotine on the rate of tumor establishment in the mouse could be indicative of its role in tumor promotion. Our results demonstrate that systemic nicotine administration at a dose of 24 mg/kg per day for 28 days does not promote accelerated tumor formation or enhanced tumor growth in mice. This chronic nicotine regimen did not increase tumor volume or tumor weight when administered alone or in combination with paclitaxel (**Figure 21**). In fact, the chronic nicotine treatment caused a significant decrease in tumor volume and tumor weight in paclitaxel + nicotine-treated mice compared to paclitaxel-treated mice.

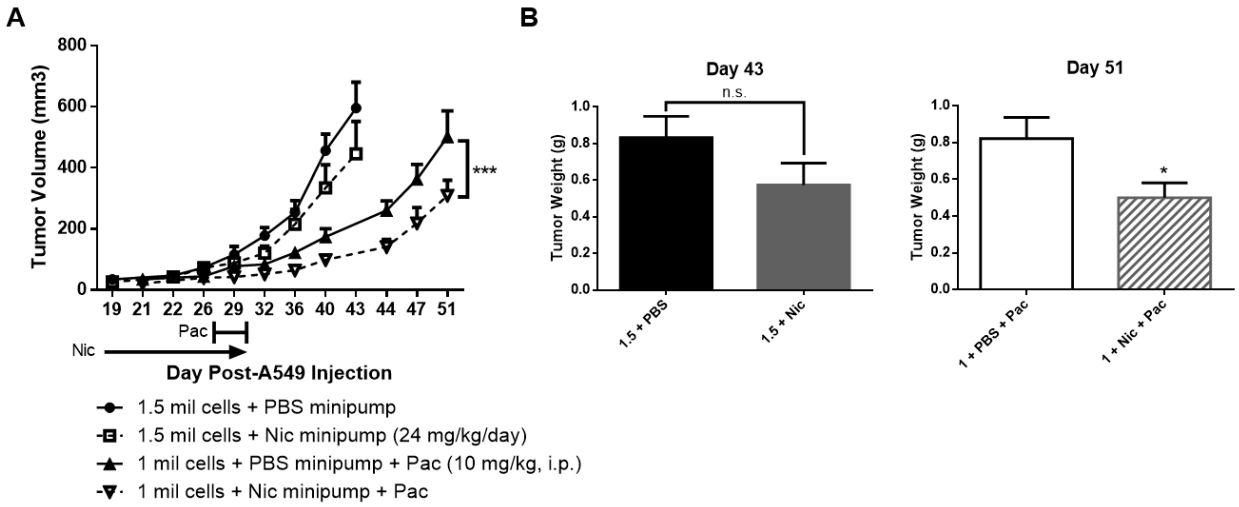

Figure 21. Chronic nicotine fails to enhance A549 NSCLC tumor growth or interfere with the antitumor property of paclitaxel *in vivo*. NSG mice were injected s.c. with 1.5 x 10^6 or 1 x 10^6 A549 cells in both flanks on day 0. On day 1 or 2, mice were implanted with subcutaneous osmotic minipumps to release PBS or 24 mg/kg nicotine daily for a total of 28 days. Paclitaxel treatment consisted of 10 mg/kg i.p. injections daily for 4 days, starting on day 27. A) The left and right flank tumor volumes (*l* x *w* x *h*) were determined with calipers and averaged for each mouse. The data were analyzed with a two-way linear mixed model analysis, revealing no significant interaction between time and treatment [F (7, 131) = 0.780, P = 0.605] for the mice receiving 1.5 x 10^6 cells/flank. The mice that received 1 x 10^6 cells/flank exhibited a significant interaction between treatment and time [F (8, 159) = 2.184, P = 0.031] and a Bonferroni post hoc analysis revealed a significant difference between PBS + Pac and Nic + Pac (P < 0.001). n = 9-10 mice per group. Data are expressed as mean + SEM. B) Mice were euthanized on either day 43 or 51, after which tumors were extracted and weighed; tumor weights were averaged for each mouse. *P < 0.05 vs PBS + Pac. n = 8-9 mice per group. Data are expressed as mean + SEM. n.s, not significant; Nic, nicotine; Pac, paclitaxel.

A possible explanation for the incongruent outcomes in the literature regarding the role of nicotine in cancer relates to differences in the route and duration of nicotine administration. Studies have been reported where nicotine was administered via subcutaneous, intraperitoneal, and intravenous injections, as well as subcutaneous minipump infusions, intake via drinking water, and transdermal absorption via nicotine patches, with all lasting anywhere from 6 days to 46 weeks. While osmotic minipumps allow for steady-state plasma levels of nicotine similar to those achieved in humans either between cigarettes or during NRT (Matta *et al.*, 2007), only a few publications utilized this

technology; another group used a transdermal patch, which releases nicotine in a similar manner as the subcutaneous pump (Davis *et al.*, 2009). Approximately half of the studies were performed with nicotine being ingested via the drinking water, which achieves a similar effect as the minipump, with relatively stable plasma concentrations of nicotine when compared to intermittent injections (Rowell *et al.*, 1983).

The route of administration could play a role in how the nAChRs are responding to nicotine over time. For example, chronic exposure of nAChRs to nicotine via a subcutaneous minipump or via drinking water could cause prolonged desensitization of nAChRs, which has been shown to occur in neuroblastoma cells chronically treated with nicotine (Sokolova *et al.*, 2005). On the other hand, Sokolova *et al.*, (2005) also showed that acute exposure to nicotine could produce nAChR activation, followed by rapid desensitization and/or reduced responsiveness. After washout and repeat exposure to nicotine, the nAChRs recover sensitivity to nicotine; this response could be occurring during intermittent injections of nicotine. Therefore, it is possible that the duration of tumor exposure to nicotine, which can be influenced by the route of administration, could be contributing to the induction or inhibition of nAChR-mediated signaling.

However, unless the plasma concentration of nicotine is monitored over time, it is difficult to determine how much nicotine the mice are receiving systemically. AlSharari *et al.*, (2013) determined the plasma concentration of nicotine following various dosing regimens in C57BL/6J mice: 0.5-2 mg/kg s.c. twice daily for 10 days (51-163 ng/ml or 314-1,005 nM), 2.5-25 mg/kg/day s.c. via 14-day minipump (13-97 ng/ml or 80-598 nM), and 25-100 µg/ml p.o. for 10 days (18-27.5 ng/ml or 111-170 nM). Although direct comparisons cannot be made between animals and humans, this study demonstrates

that the nicotine concentrations being achieved via subcutaneous or oral administration in mice, the predominant animal model for cancer and CIPN studies, are similar to that of circulating nicotine levels in humans using NRT and are expected to be predictive of patient response.

Lung Cancer Model	Mouse Strain	Nicotine Dose, Route of Administration	Duration of Treatment	Tumor Measurement	Result (Relative to Control)	Reference
N592	Nude	20 or 200 µg/day, s.c. (osmotic minipump)	14 d	Volume	No effect	(Pratesi *et al.*, 1996)
N417 (nicotine-treated, 500 µM for 7 d)	Nude	-	-	Volume	100% increase*	(Martínez-García *et al.*, 2010)
				Growth (Ki-67+)	30% increase	
DMS-53	Nude	24 mg/kg/day, s.c. (osmotic minipump)	1 m	Volume	250% increase*	(Improgo *et al.*, 2013)
				Weight	380% increase*	
A549	Nude, ovariectomized	200 µg/ml in drinking water	38 d	Volume	20% increase	(Jarzynka *et al.*, 2006)
				Growth (Ki-67+)	300% increase*	
				Microvascular density	80% increase	
H460	Foxn1^{nu}	60 µg, s.c., every other day	6 or 28 d	Volume	No effect	(Warren *et al.*, 2012)
				Angiogenesis (HIF-1α)	75% increase (acute), 1300% increase (chronic)*	
A549	SCID-Beige	i.p., every other day (dose not indicated)	7 w	Size (Luminescence)	120% increase*	(Pillai *et al.*, 2015)
				Lung Metastasis	75% increase†	
A549	Nude BALB/c	1 µM in drinking water	20 d	Volume	88% increase†	(Liu *et al.*, 2015)
				Weight	185% increase*	
A549 (nicotine-treated, 5 µM)	Nude BALB/c	-	-	Angiogenesis (Hemoglobin)	170% increase*	(Shi *et al.*, 2015)
PC9	BALB/cAJc1-nu/nu	0.6 mg/kg, i.v., 5x/week or 100 µg/ml in drinking water, then combination with erlotinib (100 mg/kg, p.o.)	Nicotine for 18 d	Volume	24% and 39% increase for i.v. and p.o., respectively*	(H Li *et al.*, 2015)
			Nicotine + Erlotinib for 10 d		200% and 300% increase for i.v. Nic + ER and p.o. Nic + ER, respectively, compared to ER alone*	
Line1	BALB/c	1 mg/kg, i.p., 3x/week	2 w	Volume	225% increase*	(Davis *et al.*, 2009)
				Tumor Recurrence	200% increase*	
				Lung Metastasis	700% increase*	
		25 mg/kg/day via transdermal patch		Volume	65% increase*	
				Lung Metastasis	230% increase*	
LLC	C57BL/6J	100 µg/ml in drinking water	16 d	Volume	100% increase*	(Heeschen *et al.*, 2001)
LLC	C57BL/6	100 µg/ml in drinking water	14 d	Volume	75% increase*	(Nakada *et al.*, 2012)

LLC	C57BL/6J	24 mg/kg/day, s.c. (osmotic minipump)	7 d	Volume	No effect	(Kyte *et al.*, 2018)
NNK, i.p.	A/J	1 mg/kg, i.p., 3x/week	4 w	Area	135% increase†	(Davis *et al.*, 2009)
				Lung Metastasis	60% increase*	
NNK, i.p.	Ab6F1 (A/J x C57BL/6J)	100 µg/ml in drinking water	12 w	Multiplicity	No effect	(Maier *et al.*, 2011)
				Volume	No effect	
				Incidence	35% increase	
				Growth (Ki-67+)	No effect	
NNK, i.p.	A/J	200 µg/ml in drinking water	2, 44, or 46 w	Volume	No effect	(Murphy *et al.*, 2011)
				Multiplicity	No effect	
				Incidence	No effect	
NNK, i.p.	A/J	1 mg/kg, i.p., 3x per week	10 w	Incidence	125% increase*	(Iskandar *et al.*, 2013)
				Volume	80% increase*	
Spontaneous tumor	$Kras^{LA2/+}$ C57BL/6J	100 µg/ml in drinking water	6 w	Multiplicity	No effect	(Maier *et al.*, 2011)
				Growth (Ki-67+)	No effect	

Table 8. *In vivo* effects of nicotine on lung cancer. Abbreviations: d, days; HIF-1α, hypoxia-inducible factor 1-alpha; i.p., intraperitoneal; i.v., intravenous; LLC, Lewis lung carcinoma; m, months; NNK, nicotine-derived nitrosamine ketone; p.o., oral; s.c., subcutaneous; w, weeks. *statistically significant, †statistical significance not indicated.

E. The Complexity of the Problem

It is challenging to determine which specific experimental factors and/or properties of nicotine are responsible for the contradictory observations in the literature. One possibility worthy of consideration involves the initial transient response to nicotine, including the phosphorylation of Akt, a key player in proliferative and anti-apoptotic pathways. Jin *et al.*, (2004) demonstrated a peak of Akt phosphorylation at 30-60 minutes post-nicotine (1 µM) treatment in A549 NSCLC cells that returns to baseline levels at 120 minutes, which we have also observed under similar conditions (**Figure 22A**). Depending on the time of observation post-nicotine treatment, it is possible that activation of the PI3K/Akt pathway is contributing to a temporary enhancement of proliferation, which dissipates even in the presence of nicotine (**Figure 22B**). In addition, chronic nicotine treatment may be inducing prolonged alterations in nAChR expression. For example, exposure to 100 nM to 10 µM nicotine for 96 hours leads to a significant upregulation of

α7 nAChR expression in H520 small cell lung cancer cells (Brown *et al.*, 2013). Yet it appears that this increased receptor expression does not persist in the absence of nicotine. Studies in human bronchial epithelial cells revealed that 100 nM nicotine significantly increases the expression of genes that encode nAChR subunits, including *CHRNA1*, *CHRNA5*, and *CHRNA7* within 72 hours but, following removal of nicotine, the expression levels return to baseline at 144 hours (Lam *et al.*, 2007). This observation raises the question of how quickly we might expect to observe similar changes in nAChR expression in the lung tumors of cancer patients, as well as how the initial nAChR expression profile differs from patient to patient and possibly determines nicotine's predominant effect.

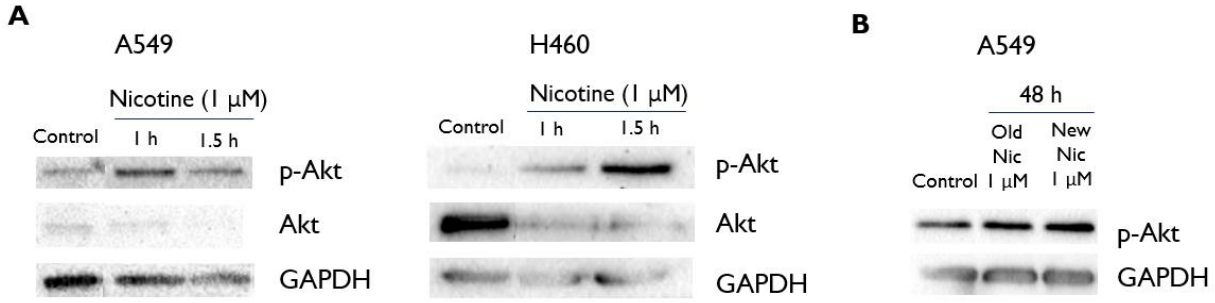

Figure 22. Nicotine induces phosphorylation of Akt at 1 to 1.5 hours post-treatment in NSCLC cell lines. A) A549 and H460 cells were either untreated (control) or exposed to 1 μM nicotine for either 1 or 1.5 hours, at which time cells were collected and lysed for protein isolation. Western blots were run to determine the expression of phosphorylated and total Akt protein. GAPDH was used as a loading control. B) A549 cells were either untreated (control) or treated with frozen (old) or freshly prepared (new) 1 μM nicotine for 48 hours, after which cells were collected and lysed for protein isolation. A western blot was run to determine the expression of phosphorylated Akt. GAPDH was used as a loading control.

There is also evidence that nicotine can induce both p53 and p21 tumor suppressor proteins, which could be responsible for the lack of enhanced proliferation reported by some research groups. It has previously been shown that nicotine can induce p53 and p21 at concentrations ranging from 1 nM to 1 μM in A549 NSCLC cells (Puliyappadamba *et al.*, 2010). Both of these proteins are induced when the cell is undergoing stress, including the presence of reactive oxygen species, which has been observed in HT-29 colon cancer cells following treatment with 100 nM nicotine (Pelissier-Rota *et al.*, 2015). The cellular response to stress involves upregulation of p21, which inhibits the cyclins that normally allow for retinoblastoma protein (Rb) phosphorylation and subsequent E2F transcription factor-mediated initiation of DNA synthesis and progression through the cell cycle (Giacinti and Giordano, 2006). Conversely, it has been observed that nicotine can activate E2F via the nAChR-β-arrestin-Src-Raf-Rb pathway [see review by (Schaal and Chellappan, 2014)]. In preliminary studies, we have observed that 24-hour exposure to nicotine (1 μM) does not alter p53 expression but reduces both p21 and Rb levels when compared to untreated cells, indicating that enhanced DNA synthesis may be occurring (**Figure 23**). However, as with Akt phosphorylation, this response may be time-dependent and transient. If the p21-mediated anti-proliferative pathway is being stimulated by nicotine shortly after application, then any proliferative signaling induced downstream of the nAChRs could be offset, resulting in little or no stimulation of tumor cell growth.

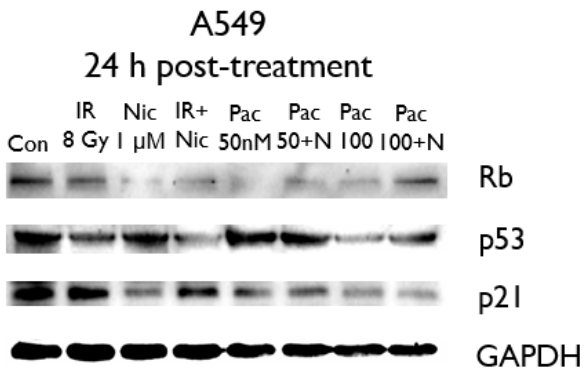

Figure 23. Nicotine reduces p21 expression in A549 NSCLC cells at 24 hours post-treatment. A549 cells were either untreated (control), irradiated (8 Gy), irradiated and treated with nicotine (1 μM), or exposed to nicotine (1 μM), paclitaxel (50-100 nM), or the combination for 24 hours, at which time cells were collected and lysed for protein isolation. A western blot was run to determine the expression of Rb, p53, and p21. GAPDH was used as a loading control. Con, control; IR, radiation; Nic/N, nicotine; Pac, paclitaxel.

Another possibility is that the nicotine-mediated activation of the pro-survival and anti-apoptotic nAChR downstream signaling is counterbalanced by inhibition of this same signaling downstream of the α9 nAChR. It has been known for decades that nicotine can act as an antagonist at the α9 nAChR, as shown by Elgoyhen *et al.*, (1994), where α9 nAChR-expressing Xenopus oocytes were exposed to increasing concentrations of nicotine in the presence of acetylcholine (ACh), which led to a dose-dependent decrease in ACh-evoked currents. It has also been shown in MDA-MB 231 metastatic breast cancer cells that CRISPR-Cas9 knockout of α9 nAChR expression leads to a significant decrease in both migration and invasion of these cells (Huang *et al.*, 2017). Therefore, the nAChR subtype expression profile in different lung cancer cell lines may play a role in the varying outcomes following nicotine exposure.

F. Conclusions

Although the findings pertaining to the effects of nicotine alone on lung tumor cells in culture are somewhat inconclusive, the evidence supporting nicotine-induced chemoresistance *in vitro* is relatively strong. However, additional studies with nicotine in

the low nanomolar range in combination with cancer chemotherapy would provide much-needed clarity. Furthermore, there is a deficiency of data relating to the interaction of nicotine with cancer chemotherapeutic agents *in vivo*. Despite our observations that nicotine does not interfere with the antitumor properties of paclitaxel in tumor-bearing mice, our analysis of the literature suggests that nicotine could be tested safely in patients exhibiting CIPN who have *completed* chemotherapy and are cancer-free by using FDA-approved commercially available nicotine patches or gum, thereby eliminating the concern for tumor growth promotion or interference with the effectiveness of chemotherapy. Finally, it should be noted that human studies have reported nicotine replacement therapy as *not being a significant predictor of cancer* (Murray *et al.*, 2009).

CHAPTER FOUR

The Effect of α7 nAChR Agonists R-47 and PNU-282987 on Lung Cancer

Disclosure #1: The behavioral data discussed in this chapter were generated in the laboratory of Dr. M. Imad Damaj, primarily by Dr. Wisam B. Toma.

A. Introduction

Previous work in the Damaj laboratory has shown that nicotine fails to reverse paclitaxel-induced mechanical allodynia in the presence of MLA, an α7 nAChR antagonist, suggesting that the α7 nAChR is involved in this antinociceptive property of nicotine (**Figure 13B**). In order to target this nAChR subtype, R-47, an α7 nAChR silent agonist, was tested in our mouse model of paclitaxel-induced neuropathy, which was established and described by Toma *et al.*, (2017). Briefly, C57BL/6J male mice received intraperitoneal injections of 8 mg/kg paclitaxel every other day for a total of 4 injections. At 7-14 days post-initial paclitaxel injection, R-47 (1-10 mg/kg, p.o.) dose-dependently reversed paclitaxel-induced mechanical allodynia with peak mechanical threshold increases at 180 minutes post-administration and full reversal with the 10 mg/kg dose; mechanical threshold values returned to baseline at 480 minutes post-administration (data not shown). With regard to prevention of CIPN, 10 mg/kg of R-47 was administered orally twice daily for 10 days, starting 72 hours prior to paclitaxel treatment. Mice that received both paclitaxel and R-47 exhibited a significantly greater mechanical threshold

than the paclitaxel-treated mice, with values that were equal to those of vehicle-treated mice for up to 35 days; R-47 alone did not have an effect on mechanical threshold in vehicle-treated mice (data not shown). In accordance with the behavioral observations, the 10-day R-47 treatment also prevented the loss of intra-epidermal nerve fibers in the hind paws of paclitaxel-treated mice (data not shown). These results suggest that R-47 pretreatment and coadministration with paclitaxel prevents the development of CIPN in mice.

R-47 is a silent agonist with high affinity for the α7 nAChR subtype (Clark *et al.*, 2014). The drug binds to a unique site that overlaps with the orthosteric binding site, in this case located on the extracellular surface between two subunits of the nAChR (Papke *et al.*, 2017). When a full agonist such as nicotine binds to the receptor, the ion channel opens to allow for an inward current. However, binding of a silent agonist results in rapid closure of the ion channel and the formation of a non-conducting state, resulting in desensitization of the receptor (Van Maanen *et al.*, 2015). It is thought that the silent agonist can cause an initial conformational change of the α7 nAChR to induce downstream signaling pathways via JAK-2 autophosphorylation and subsequent JAK-2-mediated phosphorylation of STAT and PI3K, as observed with other α7 nAChR agonists (Shaw *et al.*, 2002; Marrero *et al.*, 2011); yet, the full mechanism of action of R-47 is currently unknown.

As opposed to nicotine, a silent agonist specific for the α7 nAChR subtype may be a better alternative for treating CIPN for a myriad of reasons. First, although nicotine gum and transdermal patches are FDA-approved and commercially available, there is concern for its abuse liability, especially if nicotine must be chronically administered to alleviate

the neuropathic pain of cancer patients. We predict that this would not be the case in the preventive application of nicotine, since our animal model of CIPN indicates that short-term administration of nicotine prior to and during chemotherapy would prevent the development of CIPN (**Figure 12B**). In contrast, R-47 binds with high affinity to the α7 nAChR (K_i = 6.9 nM) rather than the α4β2 nAChR (K_i ≥ 100,000 nM) (Van Maanen *et al.*, 2015), which is the predominant nAChR subtype involved in the addictive property of nicotine (Rollema *et al.*, 2007). In addition, R-47 binds primarily in the periphery, with brain-to-plasma ratios ≤ 0.06 at 5-30 minutes after intravenous administration in mice (Clark *et al.*, 2014). These characteristics of R-47 suggest that the drug could be administered chronically to relieve CIPN symptoms, with little to no risk of addiction. This prediction is supported by observations in the conditioned place preference test, where R-47 was found to significantly increase preference score in paclitaxel-treated mice, but not in vehicle-treated mice (data not shown). Lastly, the specificity of R-47 decreases the possibility of minor adverse events, as reported with nicotine patch use, which can induce nausea and respiratory symptoms (Greenland *et al.*, 1998). However, further testing of R-47 is required to ensure its safe use in the clinic.

B. Materials and Methods

Animals. Adult male NOD *scid* gamma (NSG) mice (8 weeks at the beginning of experiments, 20-30 g) were received as a gift from Dr. J. Chuck Harrell at Virginia Commonwealth University. Mice were housed in an AAALAC-accredited facility in groups of five; the mice in each cage were randomly allocated to different treatment groups. Food and water were available *ad libitum*. Experiments were performed during the light cycle

(7:00 am to 7:00 pm) and were approved by the Institutional Animal Care and Use Committee of Virginia Commonwealth University and followed the National Institutes of Health Guidelines for the Care and Use of Laboratory Animals. Mice were euthanized via CO_2 asphyxiation followed by cervical dislocation.

Drugs. Paclitaxel was purchased from the VCU Health Pharmacy (NDC# 0703-4768-01, TEVA Pharmaceuticals, North Wales, PA) and diluted in a mixture of 1:1:18 [1 volume ethanol/1 volume Emulphor-620 (Rhone-Poulenc, Inc., Princeton, NJ)/18 volumes distilled water]. Paclitaxel injections of 10 mg/kg were administered intraperitoneally (i.p.) every day for a total of four injections; the injection site was swabbed with 70% ethanol prior to injection. R-47, also known as PMP-072, was provided by the laboratory of Ganeshsingh Thakur at Northeastern University and dissolved in distilled water. R-47 was administered chronically at a dose of 10 mg/kg twice daily (one dose in the morning and one dose in the afternoon) via oral gavage for three days, then once daily in the morning followed by a 3-hour rest before a paclitaxel/vehicle injection for 4 days. These paclitaxel and R-47 regimens were chosen based on previous unpublished studies that demonstrated which dose, duration of exposure, and route of administration for each drug effectively arrested tumor growth or prevented paclitaxel-induced peripheral neuropathy, respectively, but were not toxic to the animal (**Supplementary Fig. 14 in Appendix 2C**; data not shown). Because our laboratories had not previously used the oral gavage method to deliver drugs in NSG mice, unexpected weight loss was observed (**Supplementary Fig. 15 in Appendix 2D**), which led to administration of R-47 once a day during paclitaxel treatment as opposed to twice daily, as was used in the behavioral

studies. All i.p. injections and oral gavages were given in a volume of 1 ml/100 g body weight.

Cell culture. A549 and H460 NSCLC cells were maintained in DMEM supplemented with 10% (v/v) fetal bovine serum (FBS, Serum Source International, FB22-500HI, NC, USA) and 1% (v/v) combination of 10,000 U/ml penicillin and 10,000 µg/ml streptomycin (Pen/Strep, ThermoFisher Scientific, 15140-122, Carlsbad, CA), unless stated otherwise. Cells were incubated at 37°C under a humidified, 5% CO_2 atmosphere. The A549 and H460 cell lines were generously provided by the laboratories of Dr. Charles Chalfant and Dr. Richard Moran at VCU, respectively.

Paclitaxel was dissolved in DMSO, diluted with sterile PBS, and added to the medium in order to obtain the desired concentration. Cells were not exposed to greater than 0.1% DMSO in any experiment. R-47 and PNU-282987 (RTI International, Durham, NC) were dissolved in sterile PBS. All experiments involving these light-sensitive drugs were performed in the dark.

Assessment of cell viability. Cell viability was measured by either the 3-(4,5-dimethylthiazol-2-yl)-2,5-diphenyltetrazolium bromide (MTT)/3-(4,5-dimethylthiazol-2-yl)-5-(3-carboxymethoxyphenyl)-2-(4-sulfophenyl)-2H-tetrazolium (MTS) colorimetric assay or trypan blue exclusion. For the dose-response MTT/MTS assay, cells were seeded in 96-well plates and treated with various concentrations of R-47 or PNU-282987 for 24 hours, at which time the drug was removed and replaced with fresh medium, then the

cells were allowed 48-72 hours to proliferate following drug exposure. For the serum deprivation study, cells were seeded in DMEM (10% FBS) for 24 hours, then the medium was removed and replaced with DMEM supplemented with various concentrations of FBS (0-10%) with or without R-47 (1 μM); cell viability was assessed at 48 hours post-treatment without drug removal. On the day of testing, the medium was removed and cells were washed with PBS and stained with thiazolyl blue tetrazolium bromide (MTT, 2 mg/ml; Sigma-Aldrich, M2128, St. Louis, MO) in PBS for 3 hours. The MTT solution was then aspirated and replaced with DMSO. The color change was measured by a spectrophotometer (ELx800UV, BioTek, VT) at 490 nm. To avoid potentially aspirating cells, the CellTiter 96® Aqueous One Solution Cell Proliferation Assay (MTS; Promega, G358C, Madison, WI) was utilized for the less adherent A549 cell line; the use of MTS rather than MTT eliminates washing steps before and after staining.

For trypan blue exclusion, cells were incubated with trypsin (0.25% trypsin-EDTA) for 3 minutes, stained with trypan blue (Invitrogen, 15250, Carlsbad, CA), and the viable, unstained cells were counted using a hemocytometer with bright-field microscopy.

Assessment of colony formation. Cells were seeded at a low density in DMEM (10% FBS). After 24 hours, the paclitaxel and paclitaxel + R-47 samples were exposed to paclitaxel (50 nM) for 24 hours, after which the medium was replaced with fresh, drug-free medium. After 24 hours, the R-47 and paclitaxel + R-47 samples were exposed to R-47 (1 μM) for 24 hours, after which the medium was replaced with fresh, drug-free medium. For the dose-response studies, cells were treated with various concentrations

of R-47 or PNU-282987 for 72 hours, then the medium was replaced with fresh, drug-free medium. Once the control colonies reached a size of 50 cells per colony (approximately 8-10 days after seeding), the samples were fixed with methanol, stained with crystal violet, and quantified (ColCount, Discovery Technologies International).

Assessment of apoptosis and DNA content. Flow cytometry analyses were performed using BD FACSCanto II (BD Biosciences, San Jose, CA) and BD FACSDiva software at the Virginia Commonwealth University Flow Cytometry Core facility. For all studies, 10,000 cells per replicate within the gated region were analyzed. When collecting samples, both adherent and floating cells were harvested with 0.1% trypsin-EDTA and neutralized with medium after 48 hours of drug exposure. For quantification of apoptosis, cells were centrifuged and washed with PBS, then resuspended in 100 µl of 1x binding buffer with 5 µl of Annexin V and 5 µl of propidium iodide (BD Biosciences, FITC Annexin V Apoptosis Detection Kit, 556547, San Jose, CA). The samples were then incubated at room temperature while protected from light for 15 minutes. The suspension solution was then brought up to 500 µl using the 1x binding buffer and analyzed by flow cytometry. For quantification of DNA content, the cells were resuspended in 500 µl of a propidium iodide (PI) solution (50 µg/ml PI, 4 mM sodium citrate, 0.2 mg/ml DNase-free RNase A, and 0.1% Triton-X 100) for 1 hour at room temperature, while being protected from light (Tate et al., 1983). Before flow cytometry analysis, NaCl was added to the cell suspensions to achieve a final concentration of 0.20 M.

Assessment of tumor growth *in vivo*. Male adult NSG mice were subcutaneously injected with 1.5 x 10^6 A549 NSCLC cells in both flanks. The A549 cells were collected via trypsinization, then neutralized with medium, centrifuged, and washed with PBS. Pellets of 1.5 x 10^6 A549 cells were then resuspended in 30 µl of 80% basement membrane extract (Trevigen, 3632-010-02, Gaithersburg, MD)/20% PBS. Mice were anesthetized with isoflurane (2% isoflurane/98% oxygen) via inhalation during tumor cell inoculation; the injection site was swabbed with 70% ethanol prior to injection. Palpable tumors formed at approximately 20 days post-tumor cell inoculation, after which tumor volumes (*l* x *w* x *h*) were assessed with calipers every 2 to 3 days. Body weight and tumor volume were observed until humane endpoints were reached (tumor volume exceeds 1 cm^3), at which time mice were euthanized via CO_2 asphyxiation followed by cervical dislocation. Tumors were then extracted and preserved in 10% formalin.

Immunohistochemistry. Formalin-fixed tumors were embedded in paraffin and sectioned (5 µm thickness) for immunostaining of cleaved PARP. Tissue sections were deparaffinized, rehydrated, and quenched of endogenous peroxidase activity. After blocking with 1.5% goat serum for 1 hour, the tissues were incubated with the primary antibody (PARP cleavage site 214/215, Invitrogen, 1:100 dilution) for 1 hour at room temperature in a humidified chamber. The tissues were then incubated with a biotinylated secondary antibody (peroxidase anti-rabbit IgG, Vector Laboratories, 1:200 dilution) for an hour at room temperature in a humidified chamber. Immunostaining was completed with a Vectastain Avidin-Biotin Complex (ABC) kit (Vector Laboratories, Burlingame, CA) and the Pierce 3,3'-diaminobenzidine (DAB) horseradish peroxidase (HRP) substrate kit

(Thermo Scientific, Rockford, IL) according to the manufacturer's recommendation. The tissues were subsequently stained with hematoxylin and eosin (Vector Laboratories, Burlingame, CA) and mounted. Images were taken with an inverted microscope (Olympus, Tokyo, Japan) under bright field at 20x magnification.

Statistical analyses. A power analysis calculation was performed with the Lamorte's Power Calculator (Boston University Research Compliance) to determine the sample size of animals for each group (Charan and Kantharia, 2013). For assessing tumor volume, the calculations showed that an n of 9 was required to achieve a power of 90% with an alpha error of 0.05. Therefore, we began each study with 9 mice per group; one mouse died shortly after a paclitaxel injection on the second day of the chemotherapy regimen. The data were analyzed with GraphPad Prism software, version 6 (GraphPad Software, Inc., La Jolla, CA) and are expressed as mean ± SEM. One- and two-way analysis of variance (ANOVA) tests were conducted and followed by the Bonferroni post hoc test; student's t-tests were performed to analyze tumor weight. Differences were determined to be significant at $P < 0.05$.

C. Results

A dose-response MTT/MTS cell viability assay was initially performed with R-47 to determine if concentrations above the drug's IC_{50} value of 19 nM (determined by a rat PC12 fluorescently labeled α-bungarotoxin binding assay) would affect viable non-small cell lung cancer (NSCLC) number (Clark *et al.*, 2014); the concentration of R-47 to elicit a half maximal response is considered to be an IC_{50} because a silent agonist possesses

a reduced efficacy when compared to a full agonist, such as acetylcholine, and can prevent that full agonist from binding due to their overlapping binding sites (Papke *et al.*, 2017). The MTT/MTS assay revealed that R-47 (0.1-10 μM) does not significantly increase A549 and H460 NSCLC viable cell number 72 hours following 24-hour exposure (**Figure 24**). In the subsequent experiments, 1 μM R-47 was further tested with the assumption that plasma concentrations orders of magnitude higher than the IC_{50} may be required to produce antinociceptive and neuroprotective effects in the clinic since R-47 has not yet been tested in humans. Similar to the observations made with nicotine, 1 μM R-47 did not affect viable cell number under serum starvation and deprivation (0-5% FBS) conditions, which are typically used to synchronize the cell cycle and observe homogenous growth (**Figure 25**). As for the effect of R-47 over time, treatment with 1 μM R-47 under full serum for 48 hours did not cause an increase in A549 or H460 viable cell number according to trypan blue exclusion for up to 7 days post-treatment when compared to untreated cells (**Figure 26**).

If R-47 is to be administered in conjunction with chemotherapy, it must also be tested whether R-47 will influence the antitumor activity of paclitaxel. When observing viable cell number over time, R-47 (1 μM) pretreatment and subsequent co-treatment with paclitaxel (50 nM) did not interfere with the significant reduction in viable A549 or H460 cell number induced by paclitaxel alone (**Figure 26**). This effect of paclitaxel is due in part by growth arrest in the G2/M phase of the cell cycle (Jordan *et al.*, 1996). Similar to the growth profile observed in **Figure 26**, the NSCLC cells co-treated with paclitaxel and R-47 exhibit a significant increase in G2/M-arrested cells as seen with paclitaxel alone when

compared to control; also, all cell cycle phase populations for the paclitaxel and paclitaxel + R-47 groups are not significantly different from one another (**Figure 27**).

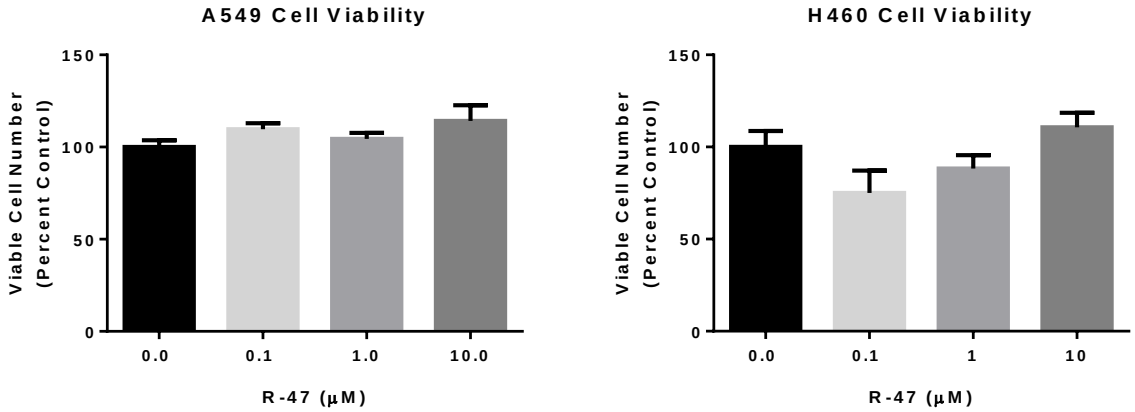

Figure 24. R-47 fails to significantly increase A549 and H460 NSCLC viable cell number. A549 (left) and H460 (right) cells were treated with various concentrations of R-47 for 24 hours, then allowed to grow for 72 hours before viability was assessed with the MTT or MTS assay. Data are expressed as the mean + SEM of three independent experiments.

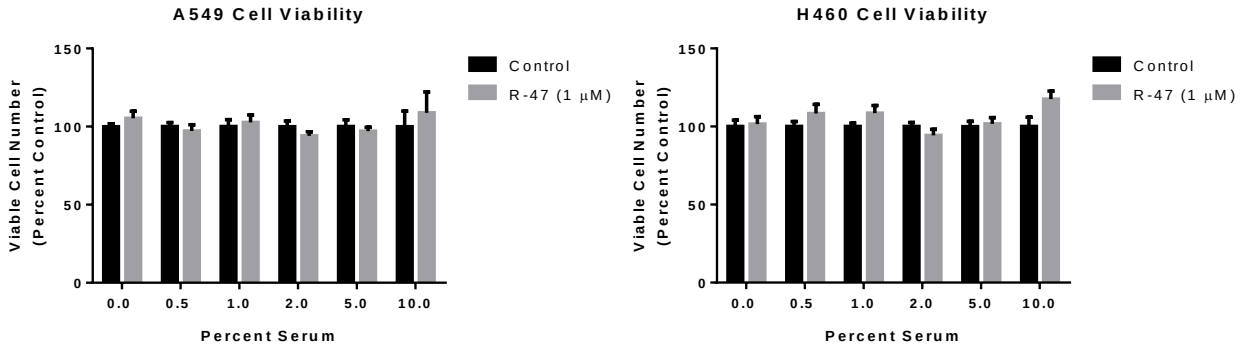

Figure 25. R-47 does not increase NSCLC viable cell numbers under serum starvation or deprivation. A549 (left) and H460 (right) cells were treated with R-47 (1 µM) for 48 hours in DMEM supplemented with various concentrations of FBS. Viability was determined with an MTT or MTS colorimetric assay. Data are expressed as the mean + SEM of three independent experiments.

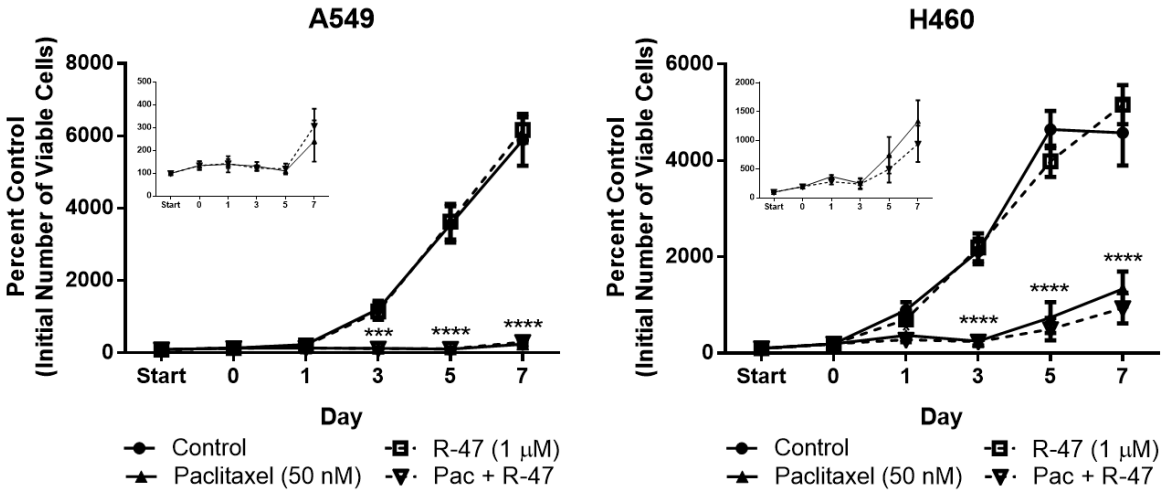

Figure 26. R-47 fails to stimulate NSCLC cell proliferation alone or interfere with paclitaxel-induced growth inhibition of NSCLC cells. The "start" time point represents the initial number of A549 cells (left) or H460 cells (right) after seeding. A 24-hour R-47 pretreatment period occurred from Start to Day 0 for the R-47 and Pac + R-47 conditions, then all subsequent treatments lasted 24 hours; no drugs were present after Day 1. The number of viable cells was determined via trypan blue exclusion. ***P < 0.001, ****P < 0.0001 vs control. Data are expressed as the mean ± SEM of three independent experiments.

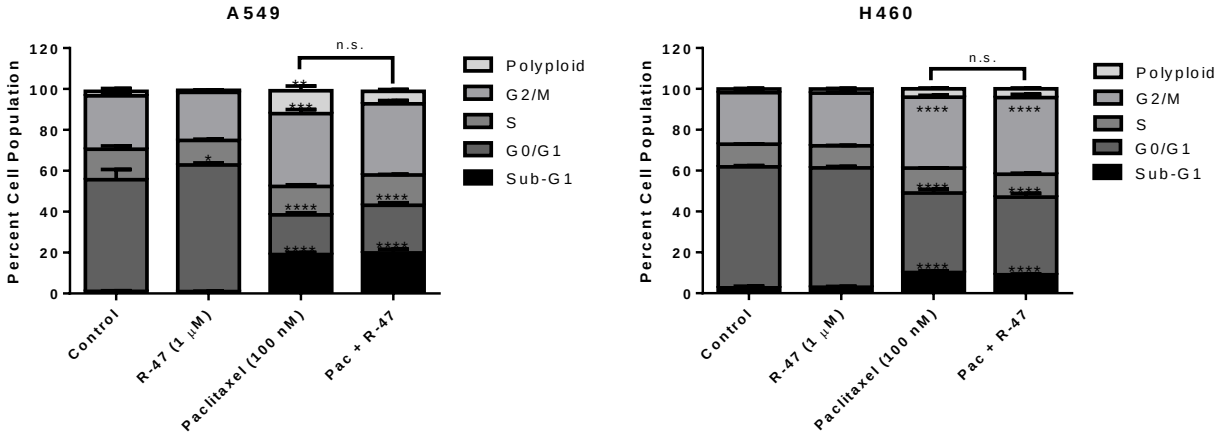

Figure 27. R-47 does not interfere with paclitaxel-induced G2/M arrest of NSCLC cells. A549 (left) or H460 (right) cells were treated with R-47, paclitaxel, or the combination for 48 hours. Cell cycle analysis was determined by propidium iodide staining and subsequent flow cytometry analysis. *P < 0.05, **P < 0.01, ***P < 0.001, ****P < 0.0001 vs control. Data are expressed as the mean ± SEM of three independent experiments. n.s., not significant.

Similar to the MTT/MTS viability assay, 24-hour treatment with 1 μM R-47 did not significantly increase the number of A549 or H460 colonies when compared to control (**Figure 28**). In order to consider the use of R-47 after cancer chemotherapy has been completed, A549 and H460 cells were also exposed to paclitaxel (50 nM) for 24 hours, followed by a 24-hour drug-free period, and subsequent exposure to R-47 (1 μM) for 24 hours. This post-paclitaxel treatment with R-47 did not increase NSCLC colony number when compared to paclitaxel alone (**Figure 28B**).

The predominant antitumor mechanism of paclitaxel is to induce growth arrest and subsequent programmed cell death, also known as apoptosis (Jordan *et al.*, 1996). Therefore, A549 and H460 cells were co-treated with paclitaxel (100 nM) and R-47 (1 μM) for 48 hours, after which Annexin V/Propidium Iodide (AV/PI) staining was used to label and quantify the early and late apoptotic populations (AV+/PI- and AV+/PI+, respectively) via flow cytometry. R-47 did not induce apoptosis alone, nor did it significantly decrease paclitaxel-induced apoptosis (**Figure 29A**). PI staining was also performed to label the DNA of A549 and H460 cells after 48-hour treatment with R-47, paclitaxel, or paclitaxel + R-47. Flow cytometry analysis allowed for the quantification of fragmented DNA within the sub-G1 phase of the cell cycle, which is a result of late-stage apoptosis. As expected, paclitaxel significantly increased sub-G1 DNA content when compared to untreated cells, and this effect was not attenuated by the R-47 + paclitaxel combination treatment (**Figure 28B**). These results suggest that the antitumor activity of paclitaxel is not affected by R-47 (1 μM).

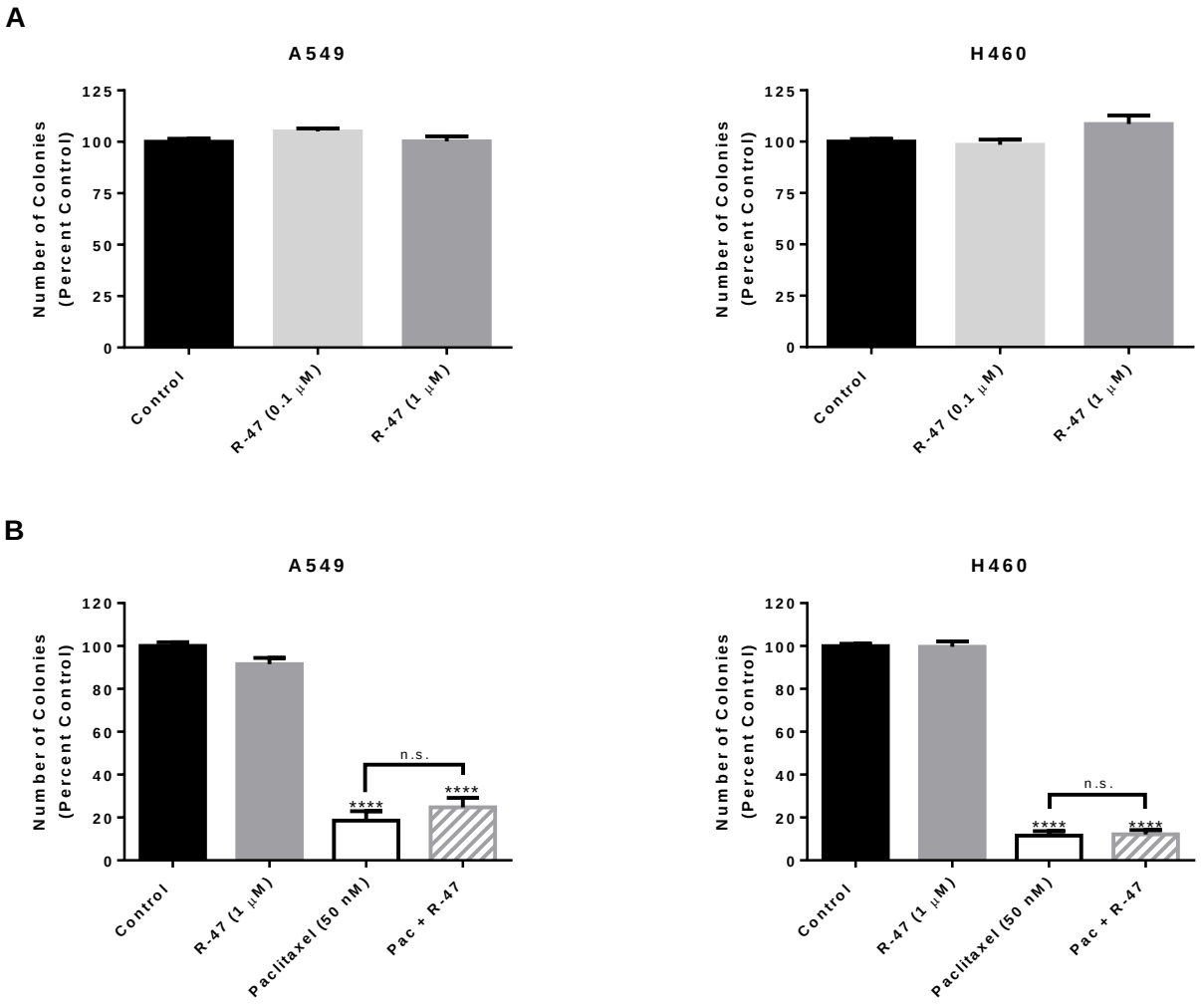

Figure 28. R-47 fails to stimulate NSCLC colony formation alone or following paclitaxel treatment. A) A549 (left) and H460 (right) cells were treated with various concentrations of R-47 for 72 hr. B) For the single drug treatment conditions, A549 (left) and H460 (right) cells were exposed to R-47 (1 μM) or paclitaxel (50 nM) for 24 hr. For the combination treatment, cells were first exposed to paclitaxel for 24 hr, followed by a 24-hr drug-free period, then treatment with R-47 for 24 hr. Colony number was determined by crystal violet staining. One-way ANOVAs were performed, followed by the Bonferroni post hoc test. ****$P < 0.0001$ vs control; n.s., not significant. Data are expressed as the mean + SEM of three independent experiments. Pac, paclitaxel.

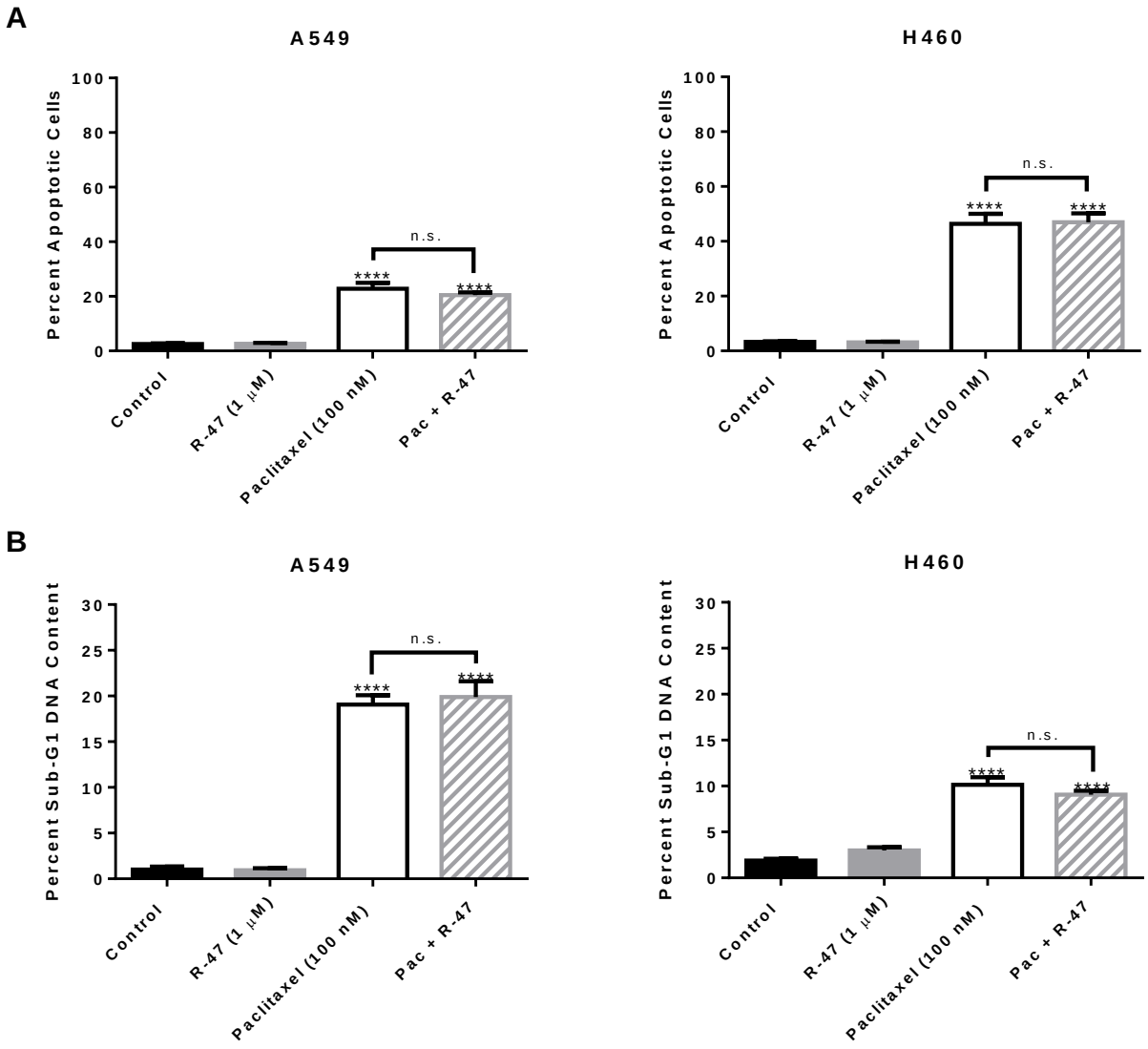

Figure 29. R-47 fails to interfere with paclitaxel-induced apoptosis (A) and sub-G1 DNA content (B) of NSCLC cells. A549 and H460 cells were treated with R-47 (1 μM), paclitaxel (100 nM), or the combination of paclitaxel and R-47 for 48 h. Quantification of apoptotic cells and sub-G1 DNA content was determined by the Annexin V/PI assay and propidium iodide staining, respectively, followed by flow cytometry analysis. ****$P < 0.0001$ vs control; n.s., not significant. Data are expressed as mean + SEM of three independent experiments.

In order to test whether these *in vitro* findings translate to an animal cancer model, A549 NSCLC cells were subcutaneously injected into the flanks of male, immunodeficient NSG mice. Once the tumors were established, mice were given R-47 (10 mg/kg, p.o.) twice daily for 3 days, then once daily in combination with paclitaxel (10 mg/kg, i.p.) for 4

days. Tumor volume was determined over time with calipers and tumors were weighed following extraction 17 days after treatment began. The paclitaxel regimen significantly decreased tumor volume when compared to vehicle-treated mice (**Figure 30A**). Most importantly, R-47 did not increase tumor volume either alone or in combination with paclitaxel when compared to vehicle- and paclitaxel-treated mice, respectively. The tumor weights followed the same trend, with R-47 having no significant effect alone or when administered with paclitaxel (**Figure 30B**). The extracted tumors were qualitatively assessed for cleaved PARP, a DNA-repair protein inactivated by caspases during apoptosis (Los *et al.*, 2002). Tumors from both paclitaxel + water- and paclitaxel + R-47-treated mice demonstrated positive staining for cleaved PARP, whereas the tumors of vehicle + water- and vehicle + R-47-treated mice presented relatively less cleaved PARP (**Figure 30C**). The *in vivo* data suggest that R-47 will most likely not affect lung tumor growth when administered prior to and during cancer chemotherapy for the purposes of preventing chemotherapy-induced peripheral neuropathy.

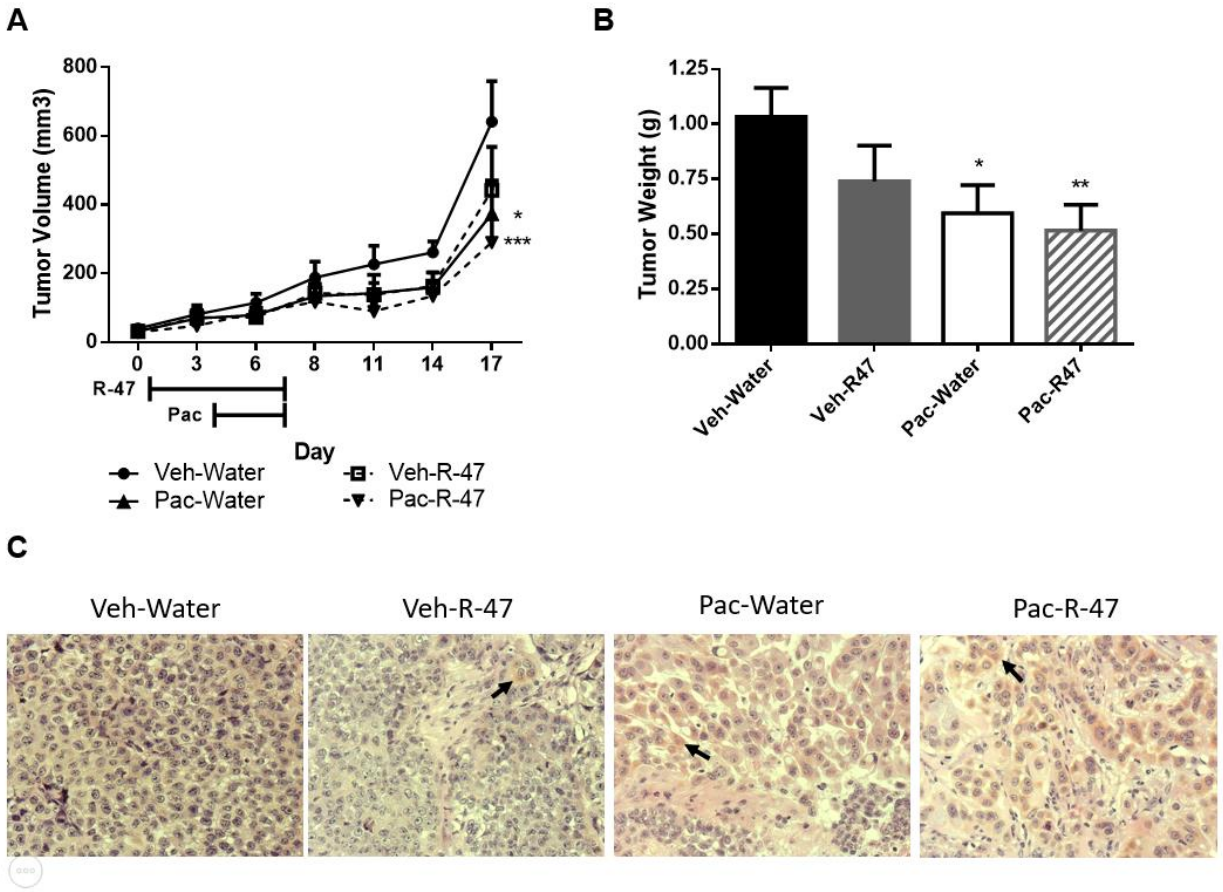

Figure 30. R-47 does not enhance A549 NSCLC tumor growth alone or in combination with paclitaxel in NSG mice. Mice were subcutaneously injected with 1.5 x 10^6 cells in each flank. Once tumors became palpable, mice were given R-47 (10 mg/kg, p.o.) twice daily for 3 days starting on day 1, then once daily in combination with paclitaxel (10 mg/kg, i.p.) for 4 days starting on day 4. A) The left and right flank tumor volumes (*l* x *w* x *h*) were determined with calipers and values were averaged for each mouse. A linear mixed model analysis followed by a Bonferroni post hoc test revealed significant differences. **P* < 0.05, ****P* < 0.001 vs Veh-Water. n = 8-9 mice per group. Data are expressed as mean + SEM. B) Mice were euthanized on day 17, after which tumors were extracted and weighed; tumor weights were averaged for each mouse. Student's t-tests were performed. **P* < 0.05, ***P* < 0.01 vs Veh-Water. n = 8-9 mice per group. Data are expressed as mean + SEM. C) Immunohistochemical staining for cleaved PARP, an apoptosis marker, was performed on paraffin-embedded tumor sections; brown color (arrow) indicates positive staining. Tissues were also stained with hematoxylin and eosin to better observe cell morphology. Images were taken with an Olympus microscope at 20x magnification. Representative images of 4 tumors per group are shown. Veh, vehicle; Pac, paclitaxel.

Since the α7 nAChR is thought to be the main subtype involved in nicotine-mediated effects in lung cancer (Paleari *et al.*, 2008; Improgo *et al.*, 2011), we also tested a selective α7 nAChR full agonist, PNU-282987, as a positive control for α7 nAChR activation (Bodnar *et al.*, 2005). An initial dose-response viability assay revealed that 24-hour treatment with PNU-282987 increases H460 cell viability; yet, this effect was not statistically significant (**Figure 31**). However, PNU-282987 significantly increased both A549 and H460 colony formation following a 72-hour treatment period, indicating that longer exposure to the drug can promote NSCLC cell growth (**Figure 32**). Similar to the viability assay, there was no significant enhancement in viable A549 cell number with 48-hour treatment of PNU-282987 alone, but co-treatment with paclitaxel did result in accelerated proliferative recovery, whereas paclitaxel alone maintained growth arrest for 7 days (**Figure 33**). This observation was supported by cell cycle analysis, which showed that PNU-282987 decreases the G2/M-arrested population of paclitaxel-treated A549 cells, yet this effect was not robust; the paclitaxel and paclitaxel + PNU-282987 groups are not significantly different from one another (**Figure 34**). Although PNU-282987 appears to interfere with growth inhibition, it does not attenuate paclitaxel-induced apoptosis or DNA fragmentation (**Figure 35**). Overall, the α7 nAChR full agonist PNU-282987 can enhance lung cancer cell growth and reduce the effectiveness of paclitaxel, indicating that complete activation of the α7 nAChR may produce pro-tumor effects, as indicated by the literature.

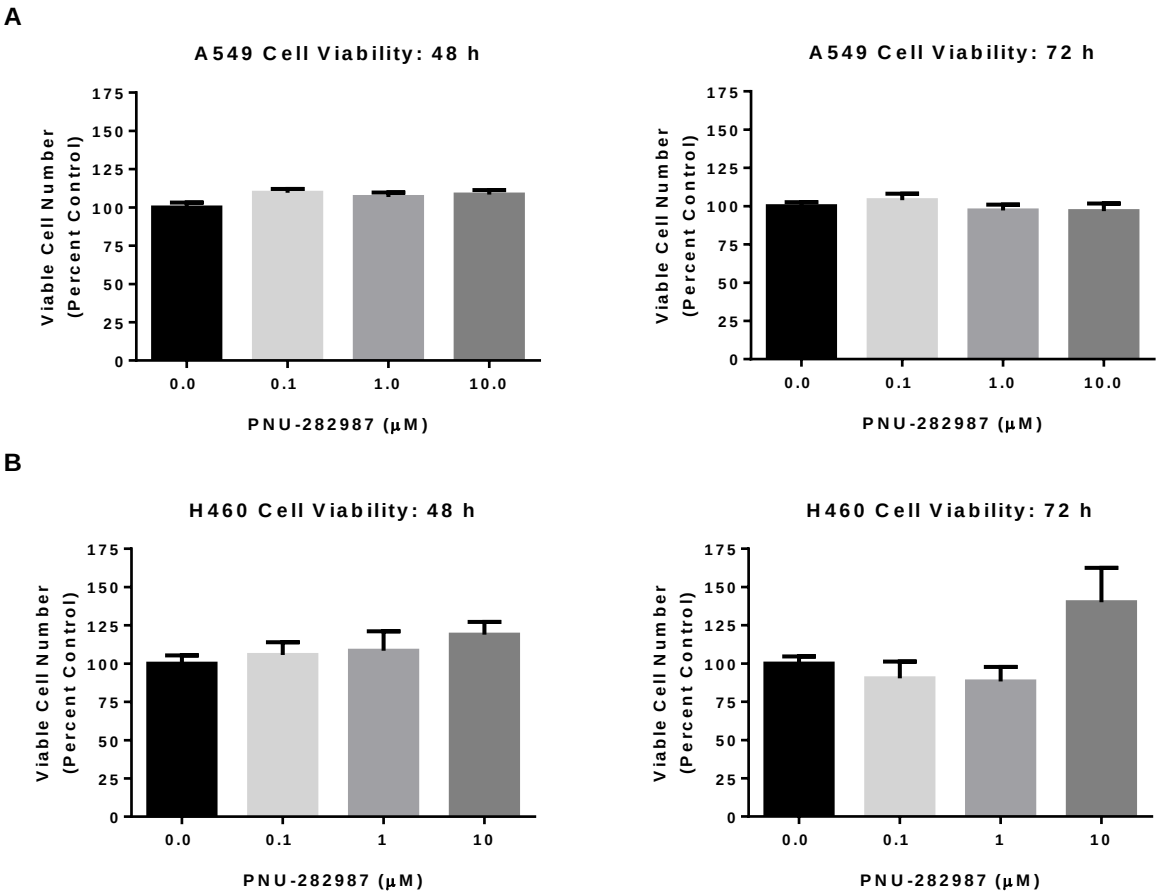

Figure 31. PNU-282987 fails to significantly increase A549 and H460 NSCLC viable cell number. A549 (A) and H460 (B) cells were treated with various concentrations of PNU-282987 for 24 hours, then allowed to grow for 48 or 72 hours before viability was assessed with the MTT or MTS assay. Data are expressed as the mean + SEM of three independent experiments.

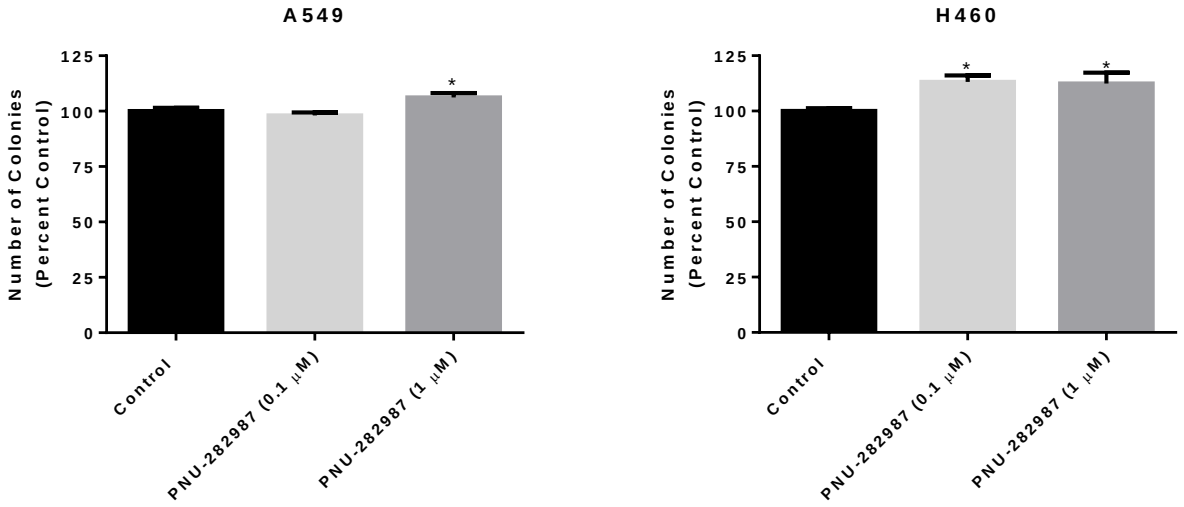

Figure 32. PNU-282987 can increase NSCLC colony formation. A549 (left) and H460 (right) cells were exposed to PNU-282987 (0.1 or 1 μM) for 72 hr. Colony number was determined by crystal violet staining. **P* < 0.05 vs control; n.s., not significant. Data are expressed as the mean + SEM of three independent experiments.

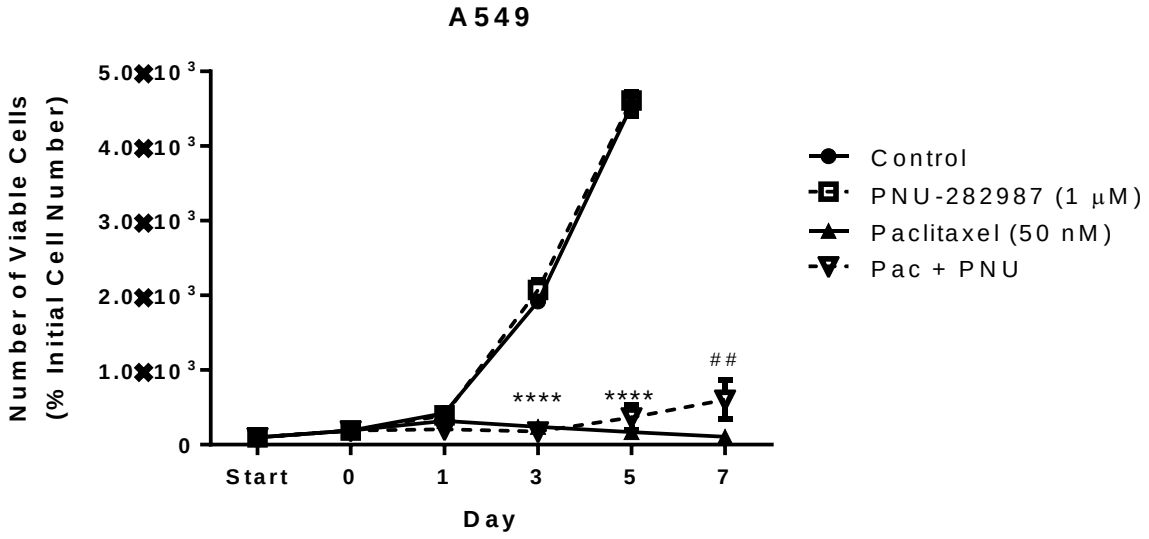

Figure 33. PNU-282987 fails to stimulate A549 NSCLC cell proliferation alone or interfere with paclitaxel-induced growth inhibition of A549 cells. The "start" time point represents the initial number of A549 cells after seeding. A 24-hour PNU-282987 pretreatment period occurred from Start to Day 0 for the PNU-282987 and Pac + PNU-282987 conditions, then all subsequent treatments lasted 24 hours; no drugs were present after Day 1. The number of viable cells was determined via trypan blue exclusion. *****P* < 0.0001 vs control, $^{\#\#}P$ < 0.01 vs paclitaxel. Data are expressed as the mean ± SEM of two independent experiments.

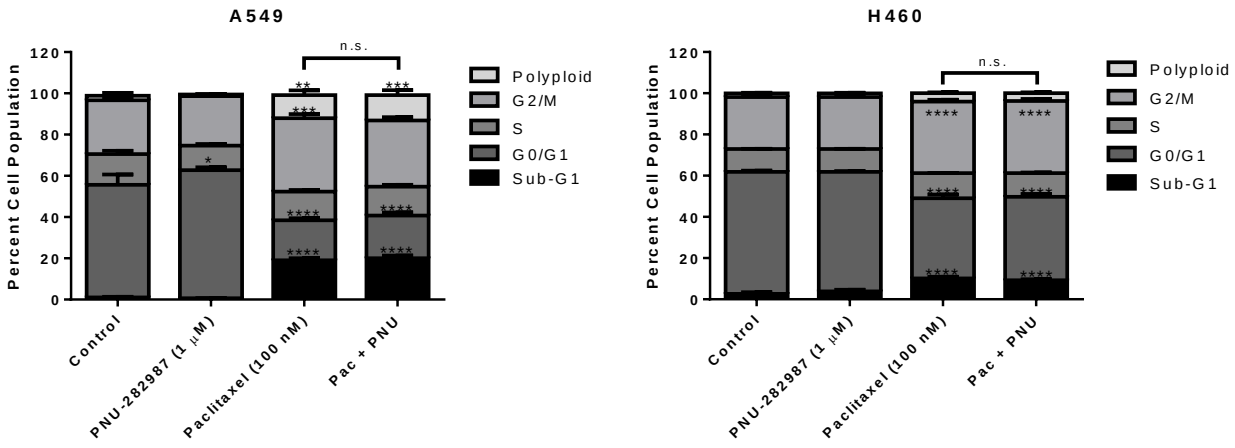

Figure 34. PNU-282987 can interfere with paclitaxel-induced G2/M arrest of A549 NSCLC cells. A549 (left) or H460 (right) cells were treated with PNU-282987, paclitaxel, or the combination for 48 hours. Cell cycle analysis was determined by propidium iodide staining and subsequent flow cytometry analysis. **P* < 0.05, ****P* < 0.001, *****P* < 0.0001 vs control. Data are expressed as the mean ± SEM of three independent experiments. n.s., not significant.

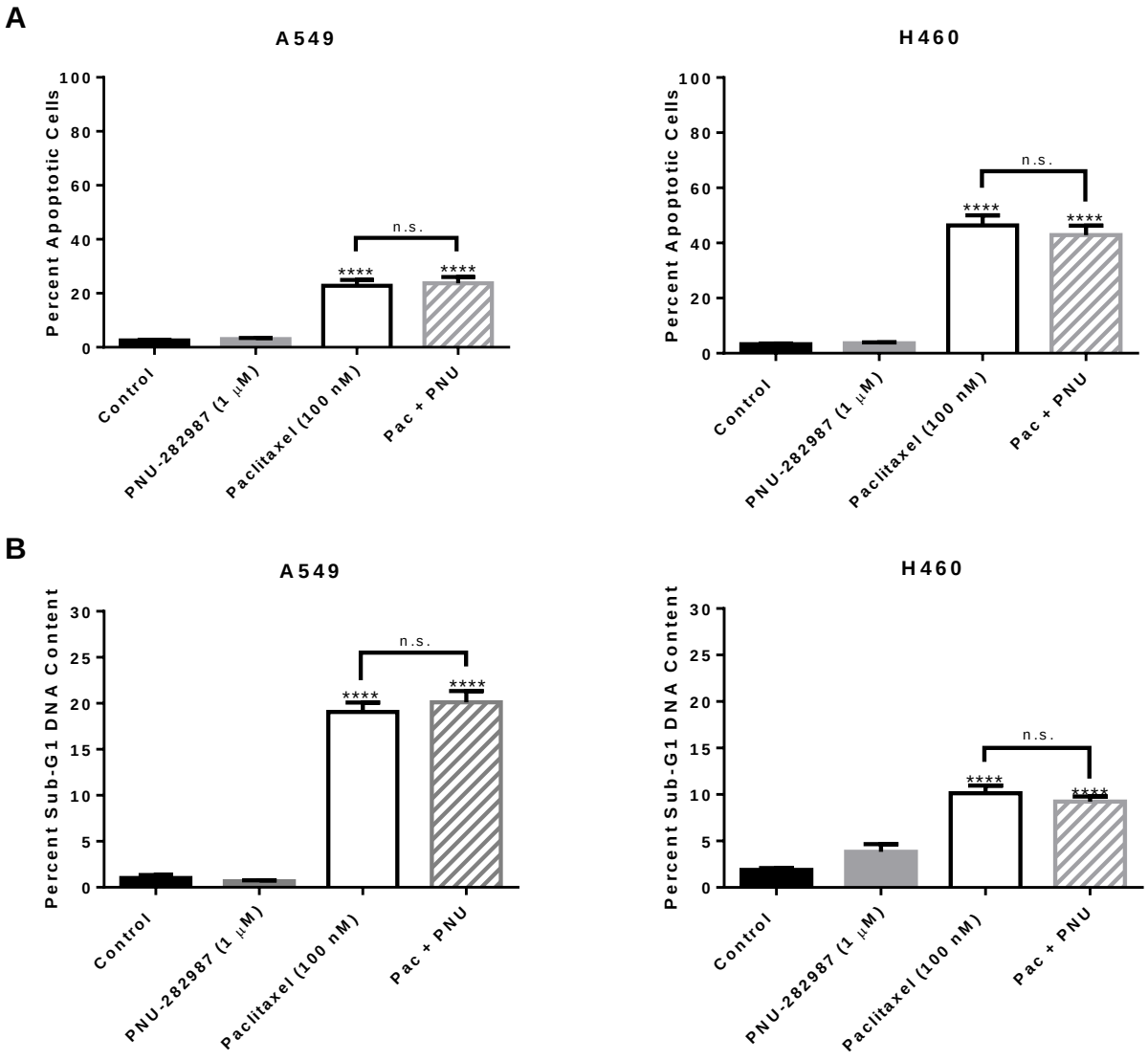

Figure 35. PNU-282987 fails to interfere with paclitaxel-induced apoptosis (A) and sub-G1 DNA content (B) of NSCLC cells. A549 and H460 cells were treated with PNU-282987 (1 μM), paclitaxel (100 nM), or the combination of paclitaxel and PNU-282987 for 48 h. Quantification of apoptotic cells and sub-G1 DNA content was determined by the Annexin V/PI assay and propidium iodide staining, respectively, followed by flow cytometry analysis. ****$P < 0.0001$ vs control; n.s., not significant. Data are expressed as mean + SEM of three independent experiments.

D. Discussion

This work is the first to investigate the effects of a nAChR silent agonist on lung cancer, particularly in combination with cancer chemotherapy as a potential treatment for CIPN. The Damaj laboratory has discovered that a silent agonist specific for the α7 nAChR, R-47, is capable of both reversing and preventing a sensory symptom of CIPN in mice, while also protecting the intra-epidermal nerve fibers of the hind paw from the neurotoxic effects of paclitaxel. These observations led us to investigate if R-47 would influence cancer progression before and/or during chemotherapy, especially considering the controversy surrounding the role of nicotine, a nAChR full agonist, in cancer growth.

Consistent with our previous work involving nicotine in **Chapters 2 and 3**, R-47 does not appear to promote lung cancer progression in our cell culture and tumor-bearing animal models. We aimed to mimic the conditions of the behavioral experiments involving R-47 by testing concentrations ranging above its IC_{50} value of 19 nM to levels that can lead to off-target binding (10 μM) (Clark *et al.*, 2014). We also referenced pharmacokinetic analyses of R-47 in mice to ensure that the *in vitro* concentrations would represent those that are achieved in the plasma. For example, mice receiving 5 mg/kg R-47 orally, a dose shown by the Damaj laboratory to reverse paclitaxel-induced mechanical allodynia, have a C_{max} of 324 ng/ml or 0.78 uM (Clark *et al.*, 2014), which is similar to our *in vitro* R-47 concentration of 1 μM. A higher dose of R-47 (10 mg/kg, p.o.) can both reverse and prevent said allodynia and was used in our tumor-bearing animals (data not shown; **Figure 30**). As for the α7 full agonist, we chose to test PNU-282987 concentrations of 1 to 10 μM due to its EC_{50} value of 154 nM and no detectable agonist activity at other nAChRs with concentrations up to 100 μM (Bodnar *et al.*, 2005).

Although the results of the *in vitro* assays show no effects of R-47 on NSCLC cells, the tumor-bearing animal study revealed a potential antitumor property of the drug. Even though the tumor volume and tumor weight measurements of the paclitaxel + water- and paclitaxel + R-47-treated mice were not significantly different, there was an enhanced decrease in both outcomes with the drug combination. R-47 alone did not induce significant decreases in tumor growth, yet it appears to be playing an antitumor role, especially in the presence of paclitaxel. One possible explanation is that persistent desensitization of the α7 nAChR on endothelial cells (ECs) is enhancing the antiangiogenic effect of paclitaxel, which is primarily characterized by a downregulation in vascular endothelial growth factor (VEGF) (Bocci *et al.*, 2013). α7 nAChRs are expressed on the surface of ECs and have been found to be the predominant nAChR subtype involved in angiogenesis (Heeschen *et al.*, 2002). ECs contain the components for acetylcholine synthesis, allowing for endogenous autocrine and/or paracrine nAChR activation, resulting in VEGF release and subsequent EC proliferation and migration in tumor angiogenesis (Cooke and Ghebremariam, 2008). This hypothesis could explain why the antiproliferative effect of R-47 was only observed *in vivo*. It is also possible that an active metabolite of R-47 has a greater half-life than the parent compound and contributes to the *in vivo* tumor response as well.

In contrast, the positive control PNU-282987 significantly increased NSCLC growth, both alone and in the presence of paclitaxel. However, these observations raise the question of why an α7 nAChR full agonist would promote lung cancer growth when nicotine, a nAChR agonist that can bind to the α7 subtype, does not. It is possible that the differences in affinity for and/or efficacy at the α7 nAChR are responsible for

heightened activation with PNU-282987 (K_i = 26 nM, EC_{50} = 154 nM in rat hippocampus) as opposed to relatively lower receptor activation with nicotine (EC_{50} = 113.34 μM for human receptor expressed in *Xenopus* oocyte) (Chavez-Noriega *et al.*, 1997; Bodnar *et al.*, 2005).

Collectively, these data demonstrate that the α7 nAChR silent agonist R-47 does not promote NSCLC growth. Most importantly, R-47 did not interfere with paclitaxel-induced growth arrest or apoptosis, and it even enhanced the antitumor effect of the chemotherapy *in vivo*. On the contrary, the α7 nAChR full agonist significantly enhanced NSCLC colony formation and attenuated paclitaxel-induced growth arrest. These observations indicate that the duration of α7 nAChR activation and the subsequent responses, including an influx of calcium and/or stimulation of various downstream signaling pathways, play a role in how these agonists influence lung cancer progression and chemosensitivity.

DISCUSSION

A. Summary

Our work demonstrates that a clinically relevant paclitaxel regimen induces the development and maintenance of multiple hallmarks of CIPN in mice, including both mechanical and cold allodynia, as well as transient negative affective-related symptoms such as anxiety- and depression-like behaviors. In this model, nicotine, an agonist of nicotinic acetylcholine receptors (nAChRs), is capable of preventing and reversing paclitaxel-induced mechanical allodynia and intra-epidermal nerve fiber loss. Nicotine cannot produce this antiallodynic effect in the presence of mecamylamine, a nonselective nAChR antagonist, or MLA, an α7 nAChR antagonist, indicating that the α7 nAChR is mediating this property of nicotine. Similarly, R-47, a silent agonist of the α7 nAChR, can also prevent and reverse paclitaxel-induced peripheral neuropathy, while causing no preference in vehicle-treated mice, suggesting that the drug may not possess the same abuse liability as nicotine.

Furthermore, both nicotine and R-47 failed to significantly promote lung cancer growth or interfere with the effectiveness of an antitumor drug, paclitaxel, in lung cancer cell lines and in lung tumor-bearing mice. Although the controversy surrounding nicotine and cancer remains, our data consistently demonstrates that nicotine does not influence lung tumor cell viability, colony formation, or proliferation, nor the growth arrest, apoptosis, or DNA fragmentation induced by paclitaxel under clinically relevant conditions. Most importantly, tumor-bearing mice revealed that nicotine, whether administered for 7 days

in conjunction with paclitaxel or for 1 month prior to paclitaxel, does not enhance human A549 NSCLC tumor volume or tumor weight.

The α7 silent agonist R-47 produced similar results in these experiments, thereby shedding light specifically on the relationship between the α7 nAChR and tumor response. Currently, the α7 nAChR is thought to play the greatest role in nAChR-mediated promotion of cancer cell proliferation and survival. For example, Mucchietto *et al.*, (2017) have shown that 100 nM nicotine significantly increases A549 cell number after 48 hours of treatment, which is inhibited by the α7 nAChR antagonists α-bungarotoxin and MLA. In addition, Tu *et al.*, (2016) showed that AGS gastric cancer cells with a knockdown of the α7 nAChR undergo greater levels of G2/M arrest and apoptosis following exposure to ixabepilone, a microtubule poison, than wild-type cells. These outcomes suggest that the blockade or absence of α7 nAChRs hinders tumor cell proliferation and enhances sensitivity to chemotherapy. Although the full mechanism of action of R-47 is currently unknown, we can presume that the silent agonist is desensitizing the α7 nAChRs and preventing endogenous acetylcholine from binding, thereby serving as an antagonist after the initial receptor response and presenting no detectable inhibition of paclitaxel's antitumor effects. Overall, our experimental findings suggest that nAChRs, especially the α7 subtype, are promising therapeutic targets for CIPN. Yet, it remains unclear how nAChRs are involved in protecting neurons and/or alleviating the pain associated with nerve damage, specifically that induced by cancer chemotherapy.

B. The Role of nAChRs in Treating CIPN

The mechanism(s) for the development of CIPN, specifically paclitaxel-induced peripheral neuropathy, are not completely understood. However, research has led to multiple hypotheses as to which physiological processes may be responsible, including the dysfunction of mitochondria and the presence of an inflammatory state. It has been reported that nicotinic acetylcholine receptors play a modulatory role in both of these responses to paclitaxel and may provide an explanation for the neuroprotective effect of nicotine and R-47.

B.1. nAChRs, Mitochondrial Dysfunction, and Autophagy

Nicotine has been shown to be a competitor of the cofactor NADH, specifically at mitochondrial complex I of the electron transport chain, thereby decreasing mitochondrial respiration and superoxide anion generation (Cormier *et al.*, 2001). In brain mitochondria, nicotine prevented mitochondrial swelling, ROS generation, and cytochrome c release into the cytosol, and decreased the mitochondrial membrane potential, suggesting that nicotine can inhibit opening of the mPTP (Xie *et al.*, 2005). The presence of nAChRs on the outer mitochondrial membrane has been observed in various tissue types, including the brain, and α7-containing nAChRs have been found to play a role in regulating the formation of the mPTP via downstream intramitochondrial kinases, such as the PI3K/Akt pathway (Lykhmus *et al.*, 2014).

In addition to direct activity at the mitochondrial membrane, nicotine may also resolve mitochondrial dysfunction indirectly via autophagy. When cells undergo stress that leads to mitochondrial dysfunction, the homeostatic process of autophagy, or self-

eating, is induced to promote mitochondrial turnover (Lee *et al.*, 2012). It is possible that paclitaxel is causing the development of atypical mitochondria while also inhibiting autophagy since paclitaxel has been shown to block initiation of autophagosome formation in mitotic cells and interfere with autophagosome movement and maturation in non-mitotic cells (Veldhoen *et al.*, 2012). These consequences of paclitaxel exposure could be combated by a drug that induces an autophagic response, which has been shown to protect neurons. For example, autophagic flux during prion-mediated mitochondrial toxicity in SH-SY5Y neuroblastoma cells proved to enhance survival, an effect that was mediated by α7 nAChRs as shown by the inhibition of neuroprotection with methyllycaconitine (MLA), an α7 nAChR antagonist (Jeong and Park, 2015). Likewise, knockdown of the autophagy-related 5 gene caused a decrease in PNU-282987 (α7 nAChR agonist)-induced activation of autophagy, as well as protection from mitochondrial dysfunction and apoptosis. Similarly, nicotine induced autophagy in SH-SY5Y cells, thereby inhibiting ROS formation and apoptosis after amyloid-β protein exposure; knockdown of the α7 nAChR significantly increased neuronal cell death in this system (Hung *et al.*, 2009). Lastly, nicotine, a stimulator of the PI3K pathway (Huang *et al.*, 2012), may be promoting mitochondrial turnover since autophagic degradation of the mitochondria is inhibited by 3MA, a PI3K inhibitor (Doménech *et al.*, 2015).

Our preliminary studies have shown that nicotine significantly increases acridine orange (AO) staining, an indicator of autophagic vesicles, in N2a neuroblastoma cells within 48 hours, but this effect dissipates at 72 hours post-treatment (**Supplementary Fig. 16 in Appendix 3A**). Surprisingly, we did not observe any alterations in autophagosome vesicle formation (AO staining) or autophagic flux (LC3 conversion) with

paclitaxel (**Supplementary Fig. 16 in Appendix 3A**). Therefore, we concluded that nicotine's transient promotion of autophagy may not be the primary mechanism responsible for its protective effect in paclitaxel-induced neurotoxicity and shifted our focus toward how nicotine may be attenuating paclitaxel-induced inflammation.

B.2. nAChRs, Macrophages, and Pro-Inflammatory Cytokine Release

It has been found that human macrophages express mRNA for the α1, α7, and α10 nAChR subunits, and that the α7 subunit is necessary for nicotine- and acetylcholine-mediated inhibition of TNF release from primary human macrophages (Wang *et al.*, 2003). Also, in α7 nAChR-containing primary rat brain microglia, nicotine inhibits LPS-induced p38 MAPK activation (Suzuki *et al.*, 2006). These studies suggest that nicotine, and possibly R-47, can stimulate the α7 nAChR downstream signaling pathways in macrophages to suppress pro-inflammatory cytokine synthesis and release. This hypothesis is strengthened by preliminary data in the Damaj laboratory demonstrating that R-47, the α7 nAChR silent agonist, can attenuate paclitaxel-induced changes in microglia morphology, a hypertrophic phenotype with shortened processes and an enlarged cell body suggestive of activation, in the dorsal horn of the spinal cord in mice (data not shown; Zheng *et al.*, 2011).

In regards to neuroprotection, it has been shown that agents which interfere with microtubule function can upregulate phosphorylated JNK (p-JNK) and p38 MAPK (p-p38) and induce cell death in primary rat cortical neurons (Huang *et al.*, 2012). Nicotine abrogates these effects by reducing the increase in p-JNK and p-p38, and by significantly increasing neuron viability; these actions of nicotine are blocked by α-bungarotoxin, an

α7 nAChR antagonist, and LY294002, a PI3K inhibitor. Nicotine has also been shown to protect against beta-amyloid-enhanced glutamate neurotoxicity in a model of Alzheimer's Disease via the α7 nAChR, an effect that was inhibited by α-bungarotoxin and LY294002 (Kihara *et al.*, 2001). In both *in vitro* and *in vivo* models of spinal cord injury, nicotine protected neurons from apoptosis by upregulating the phosphorylation of ERK1/2 via the α7 nAChR, as determined by inhibition with α-bungarotoxin or U0126, a specific ERK1/2 inhibitor (Toborek *et al.*, 2007). These findings suggest that nicotine can also protect neurons from various forms of toxicity via the MAPK and PI3K pathways downstream from the α7 nAChR. Lastly, nicotine may also be protecting neurons from degeneration due to its role in upregulating nerve growth factor (NGF) mRNA and protein expression, as well as mRNA of the receptor for NGF, tyrosine receptor kinase A (trkA), in spinal cord neurons (Garrido *et al.*, 2003). Overall, nAChR activation and downstream signaling appear to combat pro-inflammatory responses and may be the mechanism through which nicotine and R-47 are preventing the development of CIPN.

C. Future Studies

The literature demonstrates that nicotine can protect neurons from various sources of toxicity via activation of the α7 nAChR subtype. Therefore, future studies will determine if nicotine is neuroprotective in a mouse model of paclitaxel-induced peripheral neuropathy via the α7 nAChR. Wild-type and α7 nAChR knockout mice will be treated with paclitaxel and/or nicotine followed by an assessment of mechanical allodynia with the von Frey test and of intra-epidermal nerve fiber loss with confocal microscopy. Subsequently, the site of nicotine-mediated α7 nAChR activation will be investigated with

Cre//*ox*-mediated macrophage-specific knockout of the α7 nAChR. These mice will also be treated with paclitaxel and/or nicotine, then tested for mechanical allodynia and analyzed for pro-inflammatory cytokines via an ELISA in various sensory tissues, including the dorsal root ganglia and spinal cord. After identifying the involvement of the α7 nAChR in the protective role of nicotine, the pro-inflammatory effects of paclitaxel and potential anti-inflammatory role of nicotine will be further investigated by evaluating macrophage infiltration/microglial activation via immunohistochemistry. Our future work may reveal that this site of therapeutic intervention is common to some or all neuropathy-inducing chemotherapy drugs, including vincristine, platinum compounds, and bortezomib. If so, selective agonists for the α7 nAChR, such as R-47, can be further investigated to increase efficacy and minimize any potential side effects in cancer patients being treated for CIPN.

In order to test our hypothesis that nicotine can alleviate the neuropathic pain associated with CIPN, we plan to perform a double-blind, randomly-ordered, within-subjects clinical study. The patients recruited for this study will have completed their cancer chemotherapy regimen (paclitaxel or oxaliplatin), be deemed treatment-stable (cancer is in remission), and be diagnosed with CIPN above grade 1 (asymptomatic or mild symptoms including paresthesia; NIH Common Terminology Criteria for Adverse Events) and a pain score above 4 (scale of 0-10 on Brief Pain Inventory-Short Form) that has persisted for at least 3 months. To eliminate extraneous factors, patients with other chronic diseases will not be eligible, as well as those who are currently using any nicotine or tobacco products and/or other investigative drugs for CIPN, such as antidepressants and anticonvulsants. The patients will wear a de-identified transdermal patch releasing 0,

7, or 14 mg of nicotine daily for 14 days with a 1-week washout period between conditions; each patient will receive every dose in a random order. The patients' pain scores and daily function (walking, housework, etc.) will be evaluated before, during, and after patch use to test the efficacy of nicotine in alleviating neuropathic pain. If nicotine is found to significantly reduce pain scores and increase the patients' ability to complete daily tasks, then the patch can be tested in a larger clinical trial in order to be approved for this indication in addition to smoking cessation. The FDA-approved use of nicotine patches for the treatment of CIPN symptoms will allow for former and current cancer patients experiencing CIPN to achieve pain relief while other *preventative* investigative treatments, such as R-47, are further tested and developed as novel CIPN therapies.

D. The Ongoing Conversation Regarding Nicotine and Cancer

An emerging area of interest in the nicotine-cancer debate is the use of e-cigarettes, or electronic nicotine delivery systems (ENDS), that heat and aerosolize nicotine. Although we are not advocating that cancer patients use ENDS for the treatment of CIPN, their recreational use is now being studied to better understand the effects of nicotine on cancer. In 2016, the FDA Center for Tobacco Products began regulating ENDS, but their influence on human health has not been investigated extensively. The work that has been done thus far focuses on the role of nicotine in carcinogenesis, a pre-existing topic regarding nicotine in the cancer field [see reviews by (Dang *et al.*, 2016; Haussmann and Fariss, 2016)].

The majority of e-cigarette liquids (e-liquid) contain nicotine in a vehicle of propylene glycol (PG) and/or glycerol, which are both included on the FDA's Generally

Regarded as Safe list (Rowell and Tarran, 2015); yet, these classifications were based upon oral consumption, not inhalation of aerosolized particles. It has been reported in non-asthmatic patients that occupational exposure to PG mist can result in upper respiratory irritation (Wieslander *et al.*, 2001). In addition, heating of glycerol or vegetable glycerin (VG) is known to produce DNA-damaging aldehydes, such as acrolein, at temperatures known to be reached during e-cigarette use (Rowell and Tarran, 2015). The majority of chemical carcinogens damage DNA either directly by forming adducts, such as 8-oxo-2'-deoxyguanosine, or indirectly by interfering with DNA repair pathways. Therefore, these observations with e-liquid components suggest that the nicotine vehicle can produce toxicity alone. However, it is important to compare this level of toxicity to other nicotine delivery systems that are approved by the FDA.

Multiple reports have demonstrated that e-liquid can contain similar levels of carcinogenic nitrosamines (NNN, NNK, NAT, NAB) when compared to nicotine replacement therapy (NRT). For example, Nicorette gum (4 mg nicotine) contains 2 ng nitrosamines/piece, whereas the NicoDerm CQ patch (4 mg nicotine) has 8 ng/patch, similar to that of the 8.18 ng/g observed in 16 mg nicotine e-liquid, all of which are 500 to over 1,000-fold lower than the 3365-9290 ng/g nitrosamine levels in cigarettes (Cahn and Siegel, 2011). It has also been shown that former smokers now using NRT or e-cigarettes with similar levels of nicotine and derivatives in their urine (121.6 and 126.9 nM/mg of creatinine, respectively) have significantly less NNAL, a tobacco-derived nitrosamine, in their urine (11.6 and 2.5 pq/mg of creatinine, respectively) than cigarette smokers (51.1-81.2 pq/mg of creatinine) (Shahab *et al.*, 2017). Likewise, this analysis also revealed that NRT and e-cigarette users had significantly lower levels of volatile organic compounds,

including acrolein (35.3 and 33.3 ng/mg of creatinine, respectively) in their urine, when compared to cigarette smokers (91.2-107.1 ng/mg of creatinine). These studies suggest that e-cigarettes produce similar levels of nitrosamines and DNA-damaging aldehydes as FDA-approved NRT products. However, we do have to consider that the form of nicotine (aerosolized particles versus drug being ingested orally or absorbed transdermally) and organ distribution (lung, oral cavity, bloodstream) vary. For instance, aerosol particle size influences deposition patterns in the lungs (Bennett *et al.*, 2002).

Initial investigations regarding the role of e-cigarette exposure in animal models appears to be consistent thus far (**Table 9**). Mice exposed to e-liquid aerosols containing nicotine for 4 weeks exhibited deoxyguanosine adducts in multiple organs, including the lung, as well as reductions in DNA-repair activity and proteins in the lung (Lee *et al.*, 2018). Likewise, Canistro *et al.*, (2017) observed that rats exposed to e-liquid aerosols for 12 weeks display oxygen free radical formation and DNA oxidation in the lung. However, both reports lacked a vehicle treatment that consisted of exposure to *only* PG-VG aerosol particles (no nicotine). This control group is of great importance according to the *in vitro* literature. Both Ganapathy *et al.*, (2017) and Yu *et al.*, (2016) observed significant DNA damage following treatment with PG-VG (no nicotine) e-cigarette aerosol extracts in oral squamous cell carcinoma cells, and in both non-cancerous keratinocytes and head and neck squamous cell carcinoma, respectively; similar degrees of DNA damage were observed with various concentrations of nicotine in PG-VG. These data suggest that the vehicle itself could be toxic to both healthy and cancerous cells, regardless of nicotine content.

On the other hand, some argue that nicotine can damage DNA, inhibit DNA-repair, and enhance carcinogenesis in healthy lung and bladder cells (Lee *et al.*, 2018). Yet, it must be noted that those studies involved nicotine, not nicotine aerosols, at fairly high concentrations (1 μM – 5 mM in bladder cells and 50 μM – 25 mM in lung cells). Although it may be possible to achieve these high levels of nicotine in the lung, the drug is known to be rapidly absorbed into the bloodstream (Benowitz *et al.*, 2009). For example, Rose *et al.*, (2010) discovered that the half-life of lung nicotine washout ranges from approximately 20-90 seconds in cigarette smokers. Lastly, Cervellati *et al.*, (2014) reported that e-liquid aerosol containing nicotine can cause cytotoxicity to both keratinocytes and non-small cell lung cancer cells, but the e-liquid also contained a flavor that by itself produced significant decreases in cell viability. However, the study did reveal that e-cigarette vapor without flavor or nicotine did not have an effect on viability; it is not clear if the vapor contained PG-VG particles. Overall, the e-cigarette field has only just begun to grow and it is difficult to compare the current observations due to differences in methodology, including treatment concentrations, and both route (e-liquid aerosol extract versus direct contact with aerosols) and duration of exposure. Future studies will allow for a better understanding of e-cigarette safety, but in the meantime, it appears that e-liquid aerosols may be harmful *irrespective* of nicotine. This observation is consistent with our findings in **Chapters 2 and 3** that nicotine does not play a significant role in cancer progression.

Animal/ Cell Line	Control	Treatment	Exposure	Results (compared to control)	Reference
Male, FVBN Mouse	Filtered air	E-liquid aerosol (10 mg/ml nicotine in PG-VG)	35 ml puff for 4 s at 30-s intervals for 3 h/d, 5 d/w, for 12 w	Induced deoxyguanosine adducts in lung, bladder, and heart; Reduced DNA-repair activity and proteins in lung	(Lee *et al.*, 2018)
Male, Sprague Dawley Rat	Non-exposed	E-liquid aerosol (18 mg/ml nicotine in PG-VG; 1 ml/day)	Puff for 17 s (6 s on, 5 s off, 6 s on) at 20-min intervals for 11 cycles each day, 5 d/w, for 4 w	Induction of CYP enzymes, increase in oxygen free radical formation, and DNA oxidation (8-hydroxy-2'-deoxyguanosine) in lung	(Canistro *et al.*, 2017)
UM-SCC-1 (oral squamous cell carcinoma)	Untreated	E-liquid aerosol *extract* (equivalent to 10 puffs/5L) from 0, 12, or 18 mg/ml nicotine in PG-VG	Extract added to medium for 1 h	All extracts significantly increased DNA damage within p53 and induced 8-oxo-deoxyguanosine lesions	(Ganapathy *et al.*, 2017)
UROtsa (human bladder epithelial), BEAS-2B (human lung epithelial)	Untreated	Nicotine: 1-5 μM (UROtsa), 50-200 μM (BEAS-2B)	Drug added to medium for 1 h	Induced deoxyguanosine adducts; Reduced DNA-repair activity and proteins	(Lee *et al.*, 2018)
	Untreated	Nicotine: 5 mM (UROtsa), 25 mM (BEAS-2B)	Drug added to medium for 1 h	Enhanced mutational susceptibility and tumorigenic transformation	
HaCaT (keratinocyte), UMSCC10B (metastatic head and neck squamous cell carcinoma), NH30 (primary head and neck squamous cell carcinoma)	Untreated	1% e-liquid aerosol *extract* from 0 or 12 mg/ml nicotine in PG-VG; Nicotine (0.5 nM)	Extract added to medium for 1 w (UMSCC10B, HN30) or 8 w (HaCaT)	All conditions significantly increased DNA strand breaks	(Yu *et al.*, 2016)
HaCaT (keratinocytes), A549 (NSCLC)	Serum-free medium w/ filtered air	E-liquid aerosol from balsamic flavor w/ or w/o nicotine) or e-cig vapor w/o flavor or nicotine	Serum-free medium, then e-cig aerosol for 50 min, then growth for 24 h in media w/ 10% FBS	Only e-cig aerosols from e-liquid (flavor w/ or w/o nicotine) significantly increased in LDH release and decreased viability	(Cervellati *et al.*, 2014)

Table 9. Preclinical safety studies for e-cigarette use. Abbreviations: d, days; h, hours; LDH, lactate dehydrogenase; NSCLC, non-small cell lung cancer; PG-VG, propylene glycol-vegetable glycerin; s, seconds; w, weeks.

E. Conclusion

CIPN continues to interfere with the treatment of cancer and quality of life of cancer survivors. The preclinical findings in this work suggest that nicotine will not significantly enhance lung cancer growth or interfere with chemosensitivity in patients. However, our studies are designed to establish the basic principle that activation of nicotinic

acetylcholine receptors can mitigate CIPN; to this end, we have a library of selective agents that are specific for particular nAChR subtypes, including the α7 nAChR silent agonist R-47, which can be developed to overcome any concerns relating to the use of nicotine. Still, nicotine shows great promise as a potential therapy for those patients who are currently suffering from CIPN. Furthermore, if nicotine patches are found to produce favorable outcomes in cancer patients with no risk, our battery of *in vitro* and *in vivo* tests will be verified as translatable and can be used to screen nicotine and other novel CIPN therapies against various neuropathy-inducing cancer chemotherapy agents, such as vincristine, platinum compounds, and bortezomib.

REFERENCES

Al-Wadei HAN, Al-Wadei MH, and Schuller HM (2012) Cooperative regulation of non-small cell lung carcinoma by nicotinic and beta-adrenergic receptors: A novel target for intervention. *PLoS One* **7**.

Alirezaei M, Kemball CC, and Whitton JL (2011) Autophagy, inflammation and neurodegenerative disease. *Eur J Neurosci* **33**:197–204.

Alotaibi M, Sharma K, Saleh T, Povirk LF, Hendrickson EA, and Gewirtz DA (2016) Radiosensitization by PARP Inhibition in DNA Repair Proficient and Deficient Tumor Cells: Proliferative Recovery in Senescent Cells. *Radiat Res* **185**:229–245.

AlSharari SD, Akbarali HI, Abdullah RA, Shahab O, Auttachoat W, Ferreira GA, White KL, Lichtman AH, Cabral GA, and Damaj MI (2013) Novel insights on the effect of nicotine in a murine colitis model. *J Pharmacol Exp Ther* **344**:207–17.

AlSharari SD, Carroll FI, McIntosh JM, and Damaj MI (2012) The antinociceptive effects of nicotinic partial agonists varenicline and sazetidine-A in murine acute and tonic pain models. *J Pharmacol Exp Ther* **342**:742–9.

Alsharari SD, King JR, Nordman JC, Muldoon PP, Jackson A, Zhu AZX, Tyndale RF, Kabbani N, and Damaj MI (2015) Effects of menthol on nicotine pharmacokinetic, pharmacology and dependence in mice. *PLoS One* **10**:1–16.

Bagdas D, AlSharari SD, Freitas K, Tracy M, and Damaj MI (2015) The role of alpha5 nicotinic acetylcholine receptors in mouse models of chronic inflammatory and

neuropathic pain. *Biochem Pharmacol* **97**:590–600, Elsevier Inc.

Bagdas D, Ergun D, Jackson A, Toma W, Schulte MK, and Damaj MI (2017) Allosteric modulation of α4β2* nicotinic acetylcholine receptors: Desformylflustrabromine potentiates antiallodynic response of nicotine in a mouse model of neuropathic pain. *Eur J Pain* 1–10.

Bagdas D, Muldoon PP, Zhu AZX, Tyndale RF, and Damaj MI (2014) Effects of methoxsalen, a CYP2A5/6 inhibitor, on nicotine dependence behaviors in mice. *Neuropharmacology* **85**:67–72, Elsevier Ltd.

Beijers AJM, Jongen JLM, and Vreugdenhil G (2012) Chemotherapy-induced neurotoxicity: The value of neuroprotective strategies. *Neth J Med* **70**:18–25.

Bennett GJ, Liu GK, Xiao WH, Jin HW, and Siau C (2011) Terminal arbor degeneration - a novel lesion produced by the antineoplastic agent paclitaxel. *Eur J Neurosci* **33**:1667–1676.

Bennett WD, Brown JS, Zeman KL, Hu S, Scheuch G, Sommerer K, and Al BET (2002) Lung Regions. *J Aerosol Med* **15**:179–188.

Benowitz NL, Hukkanen J, and III PJ (2009) Nicotine Chemistry, Metabolism, Kinetics and Biomarkers, in *Nicotine Psychopharmacology* pp 29–60.

Benowitz NL, Jacob P, and Savanapridi C (1987) Determinants of nicotine intake while chewing nicotine polacrilex gum. *Clin Pharmacol Ther* **41**:467–473.

Blagosklonny M V., and Fojo T (1999) Molecular effects of paclitaxel: Myths and reality (a critical review). *Int J Cancer* **83**:151–156.

Bocci G, Di Paolo A, and Danesi R (2013) The pharmacological bases of the antiangiogenic activity of paclitaxel. *Angiogenesis* **16**:481–492.

Bodnar AL, Cortes-Burgos L a, Cook KK, Dinh DM, Groppi VE, Hajos M, Higdon NR, Hoffmann WE, Hurst RS, Myers JK, Rogers BN, Wall TM, Wolfe ML, and Wong E (2005) Discovery and structure-activity relationship of quinuclidine benzamides as agonists of alpha7 nicotinic acetylcholine receptors. *J Med Chem* **48**:905–908.

Bodnoff SR, Suranyi-Cadotte B, Aitken DH, Quirion R, and Meaney MJ (1988) The effects of chronic antidepressant treatment in an animal model of anxiety. *Psychopharmacology (Berl)* **95**:298–302, GERMANY, WEST.

Boehmerle W, Huehnchen P, Peruzzaro S, Balkaya M, and Endres M (2014) Electrophysiological, behavioral and histological characterization of paclitaxel, cisplatin, vincristine and bortezomib-induced neuropathy in C57Bl/6 mice. *Sci Rep* **4**:6370.

Bogdanova O V, Kanekar S, Anci KED, and Renshaw PF (2013) Physiology & Behavior Factors in fl uencing behavior in the forced swim test. *Physiol Behav* **118**:227–239, Elsevier Inc.

Brown KC, Perry HE, Lau JK, Jones D V., Pulliam JF, Thornhill BA, Crabtree CM, Luo H, Chen YC, and Dasgupta P (2013) Nicotine induces the up-regulation of the α7-nicotinic receptor (α7-nAChR) in human squamous cell lung cancer cells via the Sp1/GATA protein pathway. *J Biol Chem* **288**:33049–33059.

Cahn Z, and Siegel M (2011) Electronic cigarettes as a harm reduction strategy for tobacco control: A step forward or a repeat of past mistakes? *J Public Health Policy*

32:16–31.

Canistro D, Vivarelli F, Cirillo S, Marquillas CB, Buschini A, Lazzaretti M, Marchi L, Cardenia V, Rodriguez-Estrada MT, Lodovici M, Cipriani C, Lorenzini A, Croco E, Marchionni S, Franchi P, Lucarini M, Longo V, Croce CM Della, Vornoli A, Colacci A, Vaccari M, Sapone A, and Paolini M (2017) E-cigarettes induce toxicological effects that can raise the cancer risk. *Sci Rep* **7**:1–9.

Carlisle DL, Liu X, Hopkins TM, Swick MC, Dhir R, and Siegfried JM (2007) Nicotine activates cell-signaling pathways through muscle-type and neuronal nicotinic acetylcholine receptors in non-small cell lung cancer cells. *Pulm Pharmacol Ther* **20**:629–641.

Catassi A, Servent D, Paleari L, Cesario A, and Russo P (2008) Multiple roles of nicotine on cell proliferation and inhibition of apoptosis: Implications on lung carcinogenesis. *Mutat Res - Rev Mutat Res* **659**:221–231.

Cervellati F, Muresan X, Sticozzi C, Gambari R, Montagner G, Forman H, Torricelli C, Maioli E, and Valacchi G (2014) Comparartive effects between electronic and cigarette smoke in human keratinocytes and epithelial lung cells. *Toxicol Vitr* **28**:999–1005.

Chaplan SR, Bach FW, Pogrel JW, Chung JM, and Yaksh TL (1994) Quantitative assessment of tactile allodynia in the rat paw. *J Neurosci Methods* **53**:55–63, NETHERLANDS.

Charan J, and Kantharia ND (2013) How to calculate sample size in animal studies ? **4**.

Chavez-Noriega LE, Crona JH, Washburn MS, Urrutia A, Elliott KJ, and Johnson EC (1997) Pharmacological Characterization of Recombinant Human Neuronal Nicotinic Acetylcholine Receptors Expressed in Xenopus Oocytes. *J Pharm Exp* **280**:346–356.

Chen GQ, Lin B, Dawson MI, and Zhang XK (2002) Nicotine modulates the effects of retinoids on growth inhibition and RARβ expression in lung cancer cells. *Int J Cancer* **99**:171–178.

Chernyavsky AI, Shchepotin IB, Galitovkiy V, and Grando SA (2015) Mechanisms of tumor-promoting activities of nicotine in lung cancer: synergistic effects of cell membrane and mitochondrial nicotinic acetylcholine receptors. *BMC Cancer* **15**:152.

Clark RB, Lamppu D, Libertine L, McDonough A, Kumar A, LaRosa G, Rush R, and Elbaum D (2014) Discovery of novel 2-((pyridin-3-yloxy)methyl)piperazines as alpha7 nicotinic acetylcholine receptor modulators for the treatment of inflammatory disorders. *J Med Chem* **57**:3966–3983.

Cooke JP, and Ghebremariam YT (2008) Endothelial Nicotinic Acetylcholine Receptors and Angiogenesis. *October* **18**:247–253.

Cormier a, Morin C, Zini R, Tillement JP, and Lagrue G (2001) In vitro effects of nicotine on mitochondrial respiration and superoxide anion generation. *Brain Res* **900**:72–9.

Crawley J, and Goodwin FK (1980) Preliminary report of a simple animal behavior model for the anxiolytic effects of benzodiazepines. *Pharmacol Biochem Behav*

13:167–170, UNITED STATES.

Czyzykowski R, Polowinczak-Przybylek J, and Potemski P (2016) Nicotine-induced resistance of non-small cell lung cancer to treatment - possible mechanisms. *Postep Hig Med Dosw* **70**:186–193.

Dalakas MC, Semino-Mora C, and Leon-Monzon M (2001) Mitochondrial alterations with mitochondrial DNA depletion in the nerves of AIDS patients with peripheral neuropathy induced by 2'3'-dideoxycytidine (ddC). *Lab Invest* **81**:1537–1544, United States.

Damaj MI, Carroll FI, Eaton JB, Navarro HA, Blough BE, Mirza S, Lukas RJ, and Martin BR (2004) Enantioselective effects of hydroxy metabolites of bupropion on behavior and on function of monoamine transporters and nicotinic receptors. *Mol Pharmacol* **66**:675–682.

Damaj MI, Siu ECK, Sellers EM, Tyndale RF, and Martin BR (2007) Inhibition of nicotine metabolism by methoxysalen: Pharmacokinetic and pharmacological studies in mice. *J Pharmacol Exp Ther* **320**:250–257.

Dang N, Meng X, and Song H (2016) Nicotinic acetylcholine receptors and cancer. *Biomed Reports* **4**:515–518.

Dasgupta P, Kinkade R, Joshi B, DeCook C, Haura E, and Chellappan S (2006) Nicotine inhibits apoptosis induced by chemotherapeutic drugs by up-regulating XIAP and survivin. *Proc Natl Acad Sci* **103**:6332–6337.

Dasgupta P, Rizwani W, Pillai S, Davis R, Banerjee S, Hug K, Lloyd M, Coppola D,

Haura E, and Chellappan SP (2011) ARRB1-mediated regulation of E2F target genes in nicotine-induced growth of lung tumors. *J Natl Cancer Inst* **103**:317–333.

Dasgupta P, Rizwani W, Pillai S, Kinkade R, Kovacs M, Rastogi S, Banerjee S, Carless M, Kim E, Coppola D, Haura E, and Chellappan S (2009) Nicotine induces cell proliferation, invasion and epithelial-mesenchymal transition in a variety of human cancer cell lines. *Int J Cancer* **124**:36–45.

Davis R, Rizwani W, Banerjee S, Kovacs M, Haura E, Coppola D, and Chellappan S (2009) Nicotine promotes tumor growth and metastasis in mouse models of lung cancer. *PLoS One* **4**:1–9.

Deng L, Guindon J, Cornett BL, Makriyannis A, Mackie K, and Hohmann AG (2015) Chronic cannabinoid receptor 2 activation reverses paclitaxel neuropathy without tolerance or cannabinoid receptor 1-dependent withdrawal. *Biol Psychiatry* **77**:475–487, Elsevier.

Di Cesare Mannelli L, Zanardelli M, and Ghelardini C (2013) Nicotine is a pain reliever in trauma- and chemotherapy-induced neuropathy models. *Eur J Pharmacol* **711**:87–94, Elsevier.

Doménech E, Maestre C, Esteban-Martínez L, Partida D, Pascual R, Fernández-Miranda G, Seco E, Campos-Olivas R, Pérez M, Megias D, Allen K, López M, Saha AK, Velasco G, Rial E, Méndez R, Boya P, Salazar-Roa M, and Malumbres M (2015) AMPK and PFKFB3 mediate glycolysis and survival in response to mitophagy during mitotic arrest. *Nat Cell Biol* **17**:1304–1316.

Dranitsaris G, Yu B, King J, Kaura S, and Zhang A (2015) Nab-paclitaxel, docetaxel, or

solvent-based paclitaxel in metastatic breast cancer: A cost-utility analysis from a Chinese health care perspective. *Clin Outcomes Res* **7**:249–256.

Efimova E V., Mauceri HJ, Golden DW, Labay E, Bindokas VP, Darga TE, Chakraborty C, Barreto-Andrade JC, Crawley C, Sutton HG, Kron SJ, and Weichselbaum RR (2010) Poly(ADP-ribose) polymerase inhibitor induces accelerated senescence in irradiated breast cancer cells and tumors. *Cancer Res* **70**:6277–6282.

Egleton RD, Brown KC, and Dasgupta P (2008) Nicotinic acetylcholine receptors in cancer: multiple roles in proliferation and inhibition of apoptosis. *Trends Pharmacol Sci* **29**:151–158.

Elgoyhen AB, Johnson DS, Boulter J, Vetter DE, and Heinemann S (1994) α9: An acetylcholine receptor with novel pharmacological properties expressed in rat cochlear hair cells. *Cell* **79**:705–715.

Emery SM, Alotaibi MR, Tao Q, Selley DE, Lichtman AH, and Gewirtz DA (2014) Combined Antiproliferative Effects of the Aminoalkylindole WIN55,212-2 and Radiation in Breast Cancer Cells. *J Pharmacol Exp Ther* **348**:293–302.

Ettinger DS, Akerley W, Bepler G, Blum MG, Chang A, Cheney RT, Chirieac LR, D'Amico TA, Demmy TL, Ganti AKP, Govindan R, Grannis FWJ, Jahan T, Jahanzeb M, Johnson DH, Kessinger A, Komaki R, Kong F-M, Kris MG, Krug LM, Le Q-T, Lennes IT, Martins R, O'Malley J, Osarogiagbon RU, Otterson GA, Patel JD, Pisters KM, Reckamp K, Riely GJ, Rohren E, Simon GR, Swanson SJ, Wood DE, and Yang SC (2010) Non-small cell lung cancer. *J Natl Compr Canc Netw* **8**:740–801, United States.

Fant R V., Henningfield JE, Shiffman S, Strahs KR, and Reitberg DP (2000) A pharmacokinetic crossover study to compare the absorption characteristics of three transdermal nicotine patches. *Pharmacol Biochem Behav* **67**:479–482.

Ferrea S, and Winterer C (2009) Neuroprotective and neurotoxic effects of nicotine. *Pharmacopsychiatry* **42**:255–265.

Fidanboylu M, Griffiths LA, and Flatters SJL (2011) Global inhibition of reactive oxygen species (ROS) inhibits paclitaxel-induced painful peripheral neuropathy. *PLoS One* **6**.

Flatters SJL, and Bennett GJ (2006) Studies of peripheral sensory nerves in paclitaxel-induced painful peripheral neuropathy: Evidence for mitochondrial dysfunction. *Pain* **122**:245–257.

Flood P, and Damaj MI (2014) Nicotine is out: Nicotinic agonists may have utility as analgesics. *Anesth Analg* **119**:232–233.

Flood P, and Daniel D (2004) Intranasal nicotine for postoperative pain treatment. *Anesthesiology* **101**:1417–1421.

Fornasari D (2012) Pain mechanisms in patients with chronic pain. *Clin Drug Investig* **32**:45–52.

Freitas K, Ghosh S, Ivy Carroll F, Lichtman AH, and Imad Damaj M (2013) Effects of alpha 7 positive allosteric modulators in murine inflammatory and chronic neuropathic pain models. *Neuropharmacology* **65**:156–164, Elsevier Ltd.

Ganapathy V, Manyanga J, Brame L, McGuire D, Sadhasivam B, Floyd E, Rubenstein

DA, Ramachandran I, Wagener T, and Queimado L (2017) Electronic cigarette aerosols suppress cellular antioxidant defenses and induce significant oxidative DNA damage. *PLoS One* **12**:1–20.

Gangloff A, Hsueh W-A, Kesner AL, Kiesewetter DO, Pio BS, Pegram MD, Beryt M, Townsend A, Czernin J, Phelps ME, and Silverman DHS (2005) Estimation of paclitaxel biodistribution and uptake in human-derived xenografts in vivo with (18)F-fluoropaclitaxel. *J Nucl Med* **46**:1866–1871.

Gao T, Zhou X-L, Liu S, Rao C-X, Shi W, and Liu J-C (2016) In vitro effects of nicotine on the non-small-cell lung cancer line A549. *J Pak Med Assoc* **66**:368–72.

Garrido R, King-pospisil K, Won K, Hennig B, and Toborek M (2003) Nicotine upregulates nerve growth factor expression and prevents apoptosis of cultured spinal cord neurons. **47**:349–355.

Giacinti C, and Giordano A (2006) RB and cell cycle progression. *Oncogene* **25**:5220–5227.

Gong WYI, Wu JF, Liu BJ, Zhang HY, Cao YUX, Sun J, Lv YUB, Wu X, and Dong JC (2014) Flavonoid components in Scutellaria baicalensis inhibit nicotine-induced proliferation, metastasis and lung cancer-associated inflammation in vitro. *Int J Oncol* **44**:1561–1570.

Grando S a (2014) Connections of nicotine to cancer. *Nat Rev Cancer* **14**:419–429, Nature Publishing Group.

Greenland S, Satterfield MH, and Lanes SF (1998) A meta-analysis to assess the

incidence of adverse effects associated with the transdermal nicotine patch. *Drug Saf* **18**:297–308, New Zealand.

Guo J, Kim D, Gao J, Kurtyka C, Chen H, Yu C, Wu D, Mittal A, Beg A, Chellappan S, Haura E, and Cheng J (2013) IKBKE is induced by STAT3 and tobacco carcinogen and determines chemosensitivity in non-small cell lung cancer. *Oncogene* **32**:151–159.

Gustorff B, Dorner T, Likar R, Grisold W, Lawrence K, Schwarz F, and Rieder A (2008) Prevalence of self-reported neuropathic pain and impact on quality of life: A prospective representative survey. *Acta Anaesthesiol Scand* **52**:132–136.

Habib AS, White WD, El Gasim MA, Saleh G, Polascik TJ, Moul JW, and Gan TJ (2008) Transdermal Nicotine for Analgesia after Radical Retropubic Prostatectomy. *Anesth Analg* **107**:999–1004.

Hajnoczky G, Csordas G, and Yi M (2002) Old players in a new role: mitochondria-associated membranes, VDAC, and ryanodine receptors as contributors to calcium signal propagation from endoplasmic reticulum to the mitochondria. *Cell Calcium* **32**:363–377, Scotland.

Hama A, and Takamatsu H (2016) Chemotherapy-Induced Peripheral Neuropathic Pain and Rodent Models. *CNS Neurol Disord Drug Targets* **15**:7–19.

Haussmann H-J, and Fariss MW (2016) Comprehensive review of epidemiological and animal studies on the potential carcinogenic effects of nicotine *per se*. *Crit Rev Toxicol* **46**:701–734.

Heeschen C, Jang JJ, Weis M, Pathak A, Kaji S, Hu RS, Tsao PS, Johnson FL, and Cooke JP (2001) Nicotine stimulates angiogenesis and promotes tumor growth and atherosclerosis. *Nat Med* **7**:833–839.

Heeschen C, Weis M, Aicher A, Dimmeler S, and Cooke JP (2002) A novel angiogenic pathway mediated by non-neuronal nicotinic acetylcholine receptors. *J Clin Invest* **110**:527–536.

Hershman DL, Lacchetti C, Dworkin RH, Lavoie Smith EM, Bleeker J, Cavaletti G, Chauhan C, Gavin P, Lavino A, Lustberg MB, Paice J, Schneider B, Smith M Lou, Smith T, Terstriep S, Wagner-Johnston N, Bak K, and Loprinzi CL (2014) Prevention and management of chemotherapy-induced peripheral neuropathy in survivors of adult cancers: American Society of Clinical Oncology clinical practice guideline. *J Clin Oncol* **32**:1941–1967, United States.

Huang L-C, Lin C-L, Qiu J-Z, Lin C-Y, Hsu K-W, Tam K-W, Lee J-Y, Yang J-M, and Lee C-H (2017) Nicotinic Acetylcholine Receptor Subtype Alpha-9 Mediates Triple-Negative Breast Cancers Based on a Spontaneous Pulmonary Metastasis Mouse Model. *Front Cell Neurosci* **11**:1–14.

Huang X, Cheng Z, Su Q, Zhu X, Wang Q, Chen R, and Wang X (2012) Neuroprotection by nicotine against colchicine-induced apoptosis is mediated by PI3-kinase--Akt pathways. *Int J Neurosci* **122**:324–32.

Hung SY, Huang WP, Liou HC, and Fu WM (2009) Autophagy protects neuron from Aβ-induced cytotoxicity. *Autophagy* **5**:502–510.

Improgo MR, Soll LG, Tapper AR, and Gardner PD (2013) Nicotinic acetylcholine

receptors mediate lung cancer growth. *Front Physiol* **4 SEP**:1–6.

Improgo MR, Tapper AR, and Gardner PD (2011) Nicotinic acetylcholine receptor-mediated mechanisms in lung cancer. *Biochem Pharmacol* **82**:1015–1021.

Iskandar AR, Liu C, Smith DE, Hu K, Choi S, Ausman LM, and Wang X (2013) b - Cryptoxanthin Restores Nicotine-Reduced Lung SIRT1 to Normal Levels and Inhibits Nicotine-Promoted Lung Tumorigenesis and Emphysema in A / J Mice. **6**:309–321.

Jarzynka MJ, Gou P, Bar-Joseph I, Hu B, and Cheng SY (2006) Estradiol and nicotine exposure enhances A549 bronchioloalveolar carcinoma xenograft growth in mice through the stimulation of angiogenesis. *Int J Oncol* **28**:337–344.

Jeong JK, and Park SY (2015) Melatonin regulates the autophagic flux via activation of alpha-7 nicotinic acetylcholine receptors. *J Pineal Res* 24–37.

Jin S-X, Zhuang Z-Y, Woolf CJ, and Ji R-R (2003) p38 Mitogen-Activated Protein Kinase Is Activated After a Spinal Nerve Ligation in Spinal Cord Microglia and Dorsal Root Ganglion Neurons and Contributes To the Generation of Neuropathic Pain. *J Neurosci* **23**:4017–4022.

Jin Z, Gao F, Flagg T, and Deng X (2004) Nicotine induces multi-site phosphorylation of Bad in association with suppression of apoptosis. *J Biol Chem* **279**:23837–23844.

Jones KR, Elmore LW, Jackson-Cook C, Demasters G, Povirk LF, Holt SE, and Gewirtz DA (2005) P53-Dependent Accelerated Senescence Induced By Ionizing Radiation in Breast Tumour Cells. *Int J Radiat Biol* **81**:445–458.

Jordan MA, Wendell K, Gardiner S, Jordan MA, Wendell K, Gardiner S, Derry WB, Copp H, and Wilson L (1996) Mitotic Block Induced in HeLa Cells by Low Concentrations of Paclitaxel (Taxol) Results in Abnormal Mitotic Exit and Apoptotic Cell Death Mitotic Block Induced in HeLa Cells by Low Concentrations of Paclitaxel (Taxol) Results in Abnormal Mitotic Exit. *Cancer Res* **56**:816–825.

Jordan MA, and Wilson L (2004) Microtubules as a target for anticancer drugs. *Nat Rev Cancer* **4**:253–265.

Kellar A, Egan C, and Morris D (2015) Preclinical Murine Models for Lung Cancer : Clinical Trial Applications. **2015**.

Kemper EM, Van Zandbergen AE, Cleypool C, Mos HA, Boogerd W, Beijnen JH, and Van Tellingen O (2003) Increased penetration of paclitaxel into the brain by inhibition of P-glycoprotein. *Clin Cancer Res* **9**:2849–2855.

Kihara T, Shimohama S, Sawada H, Honda K, Nakamizo T, Shibasaki H, Kume T, and Akaike A (2001) α7 Nicotinic Receptor Transduces Signals to Phosphatidylinositol 3-Kinase to Block A β-Amyloid-induced Neurotoxicity. *J Biol Chem* **276**:13541–13546.

Kilkenny C, Browne W, Cuthill IC, Emerson M, and Altman DG (2010) Animal research : Reporting in vivo experiments : The ARRIVE guidelines ABSTRACT. 1577–1579.

Kim HK, Park SK, Zhou J-L, Taglialatela G, Chung K, Coggeshall RE, and Chung JM (2004) Reactive oxygen species (ROS) play an important role in a rat model of neuropathic pain. *Pain* **111**:116–124.

Kim JH, Dougherty PM, and Abdi S (2015) Basic science and clinical management of painful and non-painful chemotherapy-related neuropathy. *Gynecol Oncol* **136**:453–459, Elsevier B.V.

Krukowski K, Nijboer CH, Huo X, Kavelaars A, and Heijnen CJ (2015) Prevention of chemotherapy-induced peripheral neuropathy by the small-molecule inhibitor pifithrin-[mu]. *Pain* **156**:2184–2192.

Kyte SL, Toma W, Bagdas D, Meade JA, Schurman LD, Lichtman AH, Chen Z-J, Del Fabbro E, Fang X, Bigbee JW, Damaj MI, and Gewirtz DA (2018) Nicotine prevents and reverses paclitaxel-induced mechanical allodynia in a mouse model of CIPN. *J Pharmacol Exp Ther* **364**:110–119.

La Porta C, Lara-Mayorga IM, Negrete R, and Maldonado R (2016) Effects of pregabalin on the nociceptive, emotional and cognitive manifestations of neuropathic pain in mice. *Eur J Pain (United Kingdom)* 1–13.

Lam DC -l., Girard L, Ramirez R, Chau W -s., Suen W -s., Sheridan S, Tin VPC, Chung L -p., Wong MP, Shay JW, Gazdar AF, Lam W -k., and Minna JD (2007) Expression of Nicotinic Acetylcholine Receptor Subunit Genes in Non-Small-Cell Lung Cancer Reveals Differences between Smokers and Nonsmokers. *Cancer Res* **67**:4638–4647.

Ledeboer A, Jekich BM, Sloane EM, Mahoney JH, Langer SJ, Milligan ED, Martin D, Maier SF, Johnson KW, Leinwand LA, Chavez RA, and Watkins LR (2007) Intrathecal interleukin-10 gene therapy attenuates paclitaxel-induced mechanical allodynia and proinflammatory cytokine expression in dorsal root ganglia in rats.

Brain Behav Immun **21**:686–698.

Lee H-W, Park S-H, Weng M, Wang H-T, Huang WC, Lepor H, Wu X-R, Chen L-C, and Tang M (2018) E-cigarette smoke damages DNA and reduces repair activity in mouse lung, heart, and bladder as well as in human lung and bladder cells. *Proc Natl Acad Sci* **115**:E1560–E1569.

Lee J, Giordano S, and Zhang J (2012) Autophagy, mitochondria and oxidative stress: cross-talk and redox signalling. *Biochem J* **441**:523–540.

Li H, Wang S, Takayama K, Harada T, Okamoto I, Iwama E, Fujii A, Ota K, Hidaka N, Kawano Y, and Nakanishi Y (2015) Nicotine induces resistance to erlotinib via cross-talk between α 1 nAChR and EGFR in the non-small cell lung cancer xenograft model. *Lung Cancer* **88**:1–8, Elsevier Ireland Ltd.

Li Y, Zhang H, Kosturakis AK, Cassidy RM, Zhang H, Kennamer-Chapman RM, Jawad AB, Colomand CM, Harrison DS, and Dougherty PM (2015) MAPK signaling downstream to TLR4 contributes to paclitaxel-induced peripheral neuropathy. *Brain Behav Immun* **49**:255–266, Elsevier Inc.

Little, RJA and Rubin, DB (1987) Statistical Analysis with Missing Data. John Wiley & Sons, New York.

Liu C-C, Lu N, Cui Y, Yang T, Zhao Z-Q, Xin W-J, and Liu X-G (2010) Prevention of Paclitaxel-induced allodynia by Minocycline: Effect on loss of peripheral nerve fibers and infiltration of macrophages in rats. *Mol Pain* **6**:76, BioMed Central Ltd.

Liu W, Yi D, Guo J, Xiang Z, Deng L, and He L (2015) Nuciferine , extracted from

Nelumbo nucifera Gaertn , inhibits tumor-promoting effect of nicotine involving Wnt / β -catenin signaling in non-small cell lung cancer. *J Ethnopharmacol* **165**:83–93, Elsevier.

Los M, Mozoluk M, Ferrari D, Stepczynska A, Stroh C, Renz A, Herceg Z, Wang Z-Q, and Schulze-Osthoff K (2002) Activation and Caspase-mediated Inhibition of PARP: A Molecular Switch between Fibroblast Necrosis and Apoptosis in Death Receptor Signaling. *Mol Biol Cell* **13**:978–988.

Lykhmus O, Gergalova G, Koval L, Zhmak M, Komisarenko S, and Skok M (2014) Mitochondria express several nicotinic acetylcholine receptor subtypes to control various pathways of apoptosis induction. *Int J Biochem Cell Biol* **53**:246–252, Elsevier Ltd.

Ma X, Jia Y, Zu S, Li R, Jia Y, Zhao Y, Xiao D, Dang N, and Wang Y (2014) Alpha5 Nicotinic acetylcholine receptor mediates nicotine-induced HIF-1α and VEGF expression in non-small cell lung cancer. *Toxicol Appl Pharmacol* **278**:172–179, Elsevier Inc.

Maier CR, Hollander MC, Hobbs EA, Dogan I, and Dennis PA (2011) Nicotine does not enhance tumorigenesis in mutant K-Ras-driven mouse models of lung cancer. *Cancer Prev Res (Phila)* **4**:1743–1751.

Majithia N, Temkin SM, Ruddy KJ, Beutler AS, Hershman DL, and Loprinzi CL (2016) National Cancer Institute-supported chemotherapy-induced peripheral neuropathy trials: outcomes and lessons. *Support Care Cancer* **24**:1439–1447.

Maneckjee R, and Minna JD (1990) Opioid and nicotine receptors affect growth

regulation of human lung cancer cell lines. *Proc Natl Acad Sci U S A* **87**:3294–3298.

Marrero MB, Bencherif M, Lippiello PM, and Lucas R (2011) Application of alpha7 nicotinic acetylcholine receptor agonists in inflammatory diseases: An overview. *Pharm Res* **28**:413–416.

Martínez-García E, Irigoyen M, González-Moreno Ó, Corrales L, Teijeira Á, Salvo E, and Rouzaut A (2010) Repetitive nicotine exposure leads to a more malignant and metastasis-prone phenotype of SCLC: A molecular insight into the importance of quitting smoking during treatment. *Toxicol Sci* **116**:467–476.

Massie MJ (2004) Prevalence of depression in patients with cancer. *J Natl Cancer Inst Monogr* **10021**:57–71.

Matta SG, Balfour DJ, Benowitz NL, Boyd RT, Buccafusco JJ, Caggiula AR, Craig CR, Collins AC, Damaj MI, Donny EC, Gardiner PS, Grady SR, Heberlein U, Leonard SS, Levin ED, Lukas RJ, Markou A, Marks MJ, McCallum SE, Parameswaran N, Perkins KA, Picciotto MR, Quik M, Rose JE, Rothenfluh A, Schafer WR, Stolerman IP, Tyndale RF, Wehner JM, and Zirger JM (2007) Guidelines on nicotine dose selection for in vivo research. *Psychopharmacology (Berl)* **190**:269–319.

Mattes MJ (2007) Apoptosis assays with lymphoma cell lines: Problems and pitfalls. *Br J Cancer* **96**:928–936.

Mehnert A, Brahler E, Faller H, Harter M, Keller M, Schulz H, Wegscheider K, Weis J, Boehncke A, Hund B, Reuter K, Richard M, Sehner S, Sommerfeldt S, Szalai C, Wittchen HU, and Koch U (2014) Four-week prevalence of mental disorders in

patients with cancer across major tumor entities. *J Clin Oncol* **32**:3540–3546.

Mucchietto V, Fasoli F, Pucci S, Moretti M, Benfante R, Maroli A, Di Lascio S, Bolchi C, Pallavicini M, Dowell C, Mcintosh M, Clementi F, and Gotti C (2017) α9- and α7-containing receptors mediate the pro-proliferative effects of nicotine in the A549 adenocarcinoma cell line. *Br J Pharmacol*, doi: 10.1111/bph.13954.

Murphy SE, von Weymarn LB, Schutten MM, Kassie F, and Modiano JF (2011) Chronic nicotine consumption does not influence 4-(methylnitrosamino)-1-(3-pyridyl)-1-butanone induced lung tumorigenesis. *Cancer Prev Res (Phila)* **4**:1752–1760.

Murray RP, Connett JE, and Zapawa LM (2009) Does nicotine replacement therapy cause cancer? Evidence from the Lung Health Study. *Nicotine Tob Res* **11**:1076–1082.

Nair S, Bora-Singhal N, Perumal D, and Chellappan S (2014) Nicotine-mediated invasion and migration of non-small cell lung carcinoma cells by modulating STMN3 and GSPT1 genes in an ID1-dependent manner. *Mol Cancer* **13**:173.

Nakada T, Kiyotani K, Iwano S, Uno T, Yokohira M, Yamakawa K, Fujieda M, Saito T, Yamazaki H, Imaida K, and Kamataki T (2012) Lung tumorigenesis promoted by anti-apoptotic effects of cotinine, a nicotine metabolite through activation of PI3K/Akt pathway. *J Toxicol Sci* **37**:555–563.

Neelakantan H, Ward SJ, and Walker EA (2016) Effects of paclitaxel on mechanical sensitivity and morphine reward in male and female C57Bl6 mice. *Exp Clin Psychopharmacol* **24**:485–495.

Negus SS, Neddenriep B, Altarifi AA, Carroll FI, Leitl MD, and Miller LL (2015) Effects of ketoprofen, morphine, and kappa opioids on pain-related depression of nesting in mice. *Pain* **156**:1153–1160, United States.

Nieto FR, Entrena JM, Cendan CM, Pozo E Del, Vela JM, and Baeyens JM (2008) Tetrodotoxin inhibits the development and expression of neuropathic pain induced by paclitaxel in mice. *Pain* **137**:520–531.

Nishioka T, Guo J, Yamamoto D, Chen L, Huppi P, and Chen CY (2010) Nicotine, through upregulating pro-survival signaling, cooperates with NNK to promote transformation. *J Cell Biochem* **109**:152–161.

Nishioka T, Luo L-Y, Shen L, He H, Mariyannis A, Dai W, and Chen C (2014) Nicotine increases the resistance of lung cancer cells to cisplatin through enhancing Bcl-2 stability. *Br J Cancer* **110**:1785–1792.

Ogburn PL, Hurt RD, Croghan IT, Schroeder DR, Ramin KD, Offord KP, and Moyer TP (1999) Nicotine patch use in pregnant smokers: nicotine and cotinine levels and fetal effects. *Am J Obstet Gynecol* **181**:736–43.

Otrubova K, Brown M, McCormick MS, Han GW, O'Neal ST, Cravatt BF, Stevens RC, Lichtman AH, and Boger DL (2013) Rational design of fatty acid amide hydrolase inhibitors that act by covalently bonding to two active site residues. *J Am Chem Soc* **135**:6289–6299, United States.

Paleari L, Catassi A, Ciarlo M, Cavalieri Z, Bruzzo C, Servent D, Cesario A, Chessa L, Cilli M, Piccardi F, Granone P, and Russo P (2008) Role of α7-nicotinic acetylcholine receptor in human non-small cell lung cancer proliferation. *Cell Prolif*

41:936–959.

Papke RL, Stokes C, Damaj MI, Thakur GA, Manther K, Treinin M, Bagdas D, Kulkarni AR, and Horenstein NA (2017) Persistent activation of α7 nicotinic ACh receptors associated with stable induction of different desensitized states. *Br J Pharmacol* 1–17.

Park E-S, Gao X, Chung JM, and Chung K (2006) Levels of mitochondrial reactive oxygen species increase in rat neuropathic spinal dorsal horn neurons. *Neurosci Lett* **391**:108–111.

Pelissier-Rota MA, Pelosi L, Meresse P, and Jacquier-Sarlin MR (2015) Nicotine-induced cellular stresses and autophagy in human cancer colon cells: A supportive effect on cell homeostasis via up-regulation of Cox-2 and PGE<inf>2</inf> production. *Int J Biochem Cell Biol* **65**:239–256, Elsevier Ltd.

Pillai S, Rizwani W, Li X, Rawal B, Nair S, Schell MJ, Bepler G, Haura E, Coppola D, and Chellappan S (2011) ID1 Facilitates the Growth and Metastasis of Non-Small Cell Lung Cancer in Response to Nicotinic Acetylcholine Receptor and Epidermal Growth Factor Receptor Signaling □. **31**:3052–3067.

Pillai S, Trevino J, Rawal B, Singh S, Kovacs M, Li X, Schell M, Haura E, Bepler G, and Chellappan S (2015) β-Arrestin-1 mediates nicotine-induced metastasis through E2F1 target genes that modulate epithelial-mesenchymal transition. *Cancer Res* **75**:1009–1020.

Polomano RC, Mannes AJ, Clark US, and Bennett GJ (2001) A painful peripheral neuropathy in the rat produced by the chemotherapeutic drug, paclitaxel. *Pain*

94:293–304.

Pratesi G, Cervi S, Balsari A, Bondiolotti G, and Vicentini LM (1996) Effect of serotonin and nicotine on the growth of a human small cell lung cancer xenograft. *Anticancer Res* **16**:3615–3619, Greece.

Puliyappadamba VT, Cheriyan VT, Thulasidasan AKT, Bava S V, Vinod BS, Prabhu PR, Varghese R, Bevin A, Venugopal S, and Anto RJ (2010) Nicotine-induced survival signaling in lung cancer cells is dependent on their p53 status while its down-regulation by curcumin is independent. *Mol Cancer* **9**:220.

Pyter LM, Pineros V, Galang JA, McClintock MK, and Prendergast BJ (2009) Peripheral tumors induce depressive-like behaviors and cytokine production and alter hypothalamic-pituitary-adrenal axis regulation. *Proc Natl Acad Sci U S A* **106**:9069–74.

Reagan-Shaw S, Nihal M, and Ahmad N (2008) Dose translation from animal to human studies revisited. *FASEB J* **22**:659–661.

Richardson EJ, Ness TJ, Redden DT, Stewart CC, and Richards JS (2012) Effects of nicotine on spinal cord injury pain vary among subtypes of pain and smoking status: Results from a randomized, controlled experiment. *J Pain* **13**:1206–1214, Elsevier Ltd.

Roberson RS, Kussick SJ, Vallieres E, Cells LC, Cancers L, Chen SJ, and Wu DY (2005) Escape from Therapy-Induced Accelerated Cellular Senescence in p53-Null Lung Cancer Cells and in Human Lung Cancers. *Cancer Res* **65**:2795–2803.

Rock ML, Karas AZ, Rodriguez KBG, Gallo MS, Pritchett-Corning K, Karas RH, Aronovitz M, and Gaskill BN (2014) The time-to-integrate-to-nest test as an indicator of wellbeing in laboratory mice. *J Am Assoc Lab Anim Sci* **53**:24–8.

Rollema H, Coe JW, Chambers LK, Hurst RS, Stahl SM, and Williams KE (2007) Rationale, pharmacology and clinical efficacy of partial agonists of α4β2nACh receptors for smoking cessation. *Trends Pharmacol Sci* **28**:316–325.

Romero HK, Christensen SB, Di Cesare Mannelli L, Gajewiak J, Ramachandra R, Elmslie KS, Vetter DE, Ghelardini C, Iadonato SP, Mercado JL, Olivera BM, and McIntosh JM (2017) Inhibition of α9α10 nicotinic acetylcholine receptors prevents chemotherapy-induced neuropathic pain. *Proc Natl Acad Sci* 201621433, National Academy of Sciences.

Rose JE, Mukhin AG, Lokitz SJ, Turkington TG, Herskovic J, Behm FM, Garg S, and Garg PK (2010) Kinetics of brain nicotine accumulation in dependent and nondependent smokers assessed with PET and cigarettes containing 11C-nicotine. *Proc Natl Acad Sci* **107**:5190–5195.

Rosner M, Schipany K, and Hengstschläger M (2013) Merging high-quality biochemical fractionation with a refined flow cytometry approach to monitor nucleocytoplasmic protein expression throughout the unperturbed mammalian cell cycle. *Nat Protoc* **8**:602–626.

Rowbotham MC, Rachel Duan W, Thomas J, Nothaft W, and Backonja MM (2009) A randomized, double-blind, placebo-controlled trial evaluating the efficacy and safety of ABT-594 in patients with diabetic peripheral neuropathic pain. *Pain* **146**:245–

252, International Association for the Study of Pain.

Rowell PP, Hurst HE, Marlowe C, and Bennett BD (1983) Oral administration of nicotine: its uptake and distribution after chronic administration to mice. *J Pharmacol Methods* **9**:249–61.

Rowell TR, and Tarran R (2015) Will chronic e-cigarette use cause lung disease? *Am J Physiol - Lung Cell Mol Physiol* **309**:L1398–L1409.

Rowley TJ, Payappilly J, Lu J, and Flood P (2008) The Antinociceptive Response to Nicotinic Agonists in a Mouse Model of Postoperative Pain. *Anesth Analg* **107**:1052–1057.

Schaal C, and Chellappan SP (2014) Nicotine-mediated cell proliferation and tumor progression in smoking related cancers. *Mol Cancer Res* **12**:14–23.

Scholz J, and Woolf CJ (2007) The neuropathic pain triad: neurons, immune cells and glia. *Nat Neurosci* **10**:1361–1368.

Seidman AD, Berry D, Cirrincione C, Harris L, Muss H, Marcom PK, Gipson G, Burstein H, Lake D, Shapiro CL, Ungaro P, Norton L, Winer E, and Hudis C (2008) Randomized phase III trial of weekly compared with every-3-weeks paclitaxel for metastatic breast cancer, with trastuzumab for all HER-2 overexpressors and random assignment to trastuzumab or not in HER-2 nonoverexpressors: Final results of cancer and leu. *J Clin Oncol* **26**:1642–1649.

Seretny M, Currie GL, Sena ES, Ramnarine S, Grant R, Macleod MR, Colvin LA, and Fallon M (2014) Incidence, prevalence, and predictors of chemotherapy-induced

peripheral neuropathy: A systematic review and meta-analysis. *Pain* **155**:2461–2470, International Association for the Study of Pain.

Shahab L, Goniewicz ML, Blount BC, Brown J, McNeill A, Udeni Alwis K, Feng J, Wang L, and West R (2017) Nicotine, carcinogen, and toxin exposure in long-Term e-cigarette and nicotine replacement therapy users. *Ann Intern Med* **166**:390–400.

Shaw S, Bencherif M, and Marrero MB (2002) Janus kinase 2, an early target of α7 nicotinic acetylcholine receptor-mediated neuroprotection against Aβ-(1-42) amyloid. *J Biol Chem* **277**:44920–44924.

Shi J, Liu F, Zhang W, Liu X, Lin B, and Tang X (2015) Epigallocatechin-3-gallate inhibits nicotine-induced migration and invasion by the suppression of angiogenesis and epithelial-mesenchymal transition in non-small cell lung cancer cells. *Oncol Rep* **33**:2972–2980.

Slivicki RA, Ali YO, Lu H-C, and Hohmann AG (2016) Impact of Genetic Reduction of NMNAT2 on Chemotherapy-Induced Losses in Cell Viability In Vitro and Peripheral Neuropathy In Vivo. *PLoS One* **11**:e0147620, United States.

So WKW, Marsh G, Ling WM, Leung FY, Lo JCK, Yeung M, and Li GKH (2009) The symptom cluster of fatigue, pain, anxiety, and depression and the effect on the quality of life of women receiving treatment for breast cancer: a multicenter study. *Oncol Nurs Forum* **36**:E205-14.

Sokolova E, Matteoni C, and Nistri A (2005) Desensitization of neuronal nicotinic receptors of human neuroblastoma SH-SY5Y cells during short or long exposure to nicotine. *Br J Pharmacol* **146**:1087–1095.

St-Pierre S, Jiang W, Roy P, Champigny C, LeBlanc É, Morley BJ, Hao J, and Simard AR (2016) Nicotinic acetylcholine receptors modulate bone marrow-derived pro-inflammatory monocyte production and survival. *PLoS One* **11**:1–18.

Sun H, and Ma X (2015) α5-nAChR modulates nicotine-induced cell migration and invasion in A549 lung cancer cells. *Exp Toxicol Pathol* **67**:477–482, Elsevier GmbH.

Suzuki T, Hide I, Matsubara A, Hama C, Harada K, Miyano K, Andra M, Matsubayashi H, Sakai N, Kohsaka S, Inoue K, and Nakata Y (2006) Microglial a7 Nicotinic Acetylcholine Receptors Drive a Phospholipase C/IP3 Pathway and Modulate the Cell Activation Toward a Neuroprotective Role. *J Neurosci Res* **83**:1461–1470.

Thompson RD, and Grant C V (1971) Automated Preference Testing Apparatus for Rating Palatability of Foods1. *J Exp Anal Behav* **15**:215–220.

Toborek M, Son KW, Pudelko A, King-Pospisil K, Wylegala E, and Malecki A (2007) ERK 1/2 signaling pathway is involved in nicotine-mediated neuroprotection in spinal cord neurons. *J Cell Biochem* **100**:279–292.

Togashi Y, Hayashi H, Okamoto K, Fumita S, Terashima M, de Velasco MA, Sakai K, Fujita Y, Tomida S, Nakagawa K, and Nishio K (2015) Chronic nicotine exposure mediates resistance to EGFR-TKI in EGFR-mutated lung cancer via an EGFR signal. *Lung Cancer* **88**:16–23, Elsevier Ireland Ltd.

Toma W, Kyte SL, Bagdas D, Alkhlaif Y, Alsharari SD, Lichtman AH, Chen Z-J, Del Fabbro E, Bigbee JW, Gewirtz DA, and Damaj MI (2017) Effects of paclitaxel on the development of neuropathy and affective behaviors in the mouse.

Neuropharmacology **117**:305–315, England.

Tsurutani J, Castillo SS, Brognard J, Granville CA, Zhang C, Gills JJ, Sayyah J, and Dennis PA (2005) Tobacco components stimulate Akt-dependent proliferation and NFkB-dependent survival in lung cancer cells. *Carcinogenesis* **26**:1182–1195.

Tu CC, Huang CY, Cheng WL, Hung CS, Chang YJ, and Wei PL (2016) Silencing A7-nAChR levels increases the sensitivity of gastric cancer cells to ixabepilone treatment. *Tumor Biol* **37**:9493–9501, Tumor Biology.

Turcott JG, Juarez-Hernandez E, De la Torre-Vallejo M, Sanchez-Lara K, Luvian-Morales J, and Arrieta O (2016) Value: Changes in the Detection and Recognition Thresholds of Three Basic Tastes in Lung Cancer Patients Receiving Cisplatin and Paclitaxel and Its Association with Nutritional and Quality of Life Parameters. *Nutr Cancer* **68**:241–249, United States.

Umana IC, Daniele CA, and McGehee DS (2013) Neuronal nicotinic receptors as analgesic targets: It's a winding road. *Biochem Pharmacol* **86**:1208–1214, Elsevier Inc.

Umana IC, Daniele CA, Miller BA, Gallagher K, and Brown MA (2017) Nicotinic Modulation of Descending Pain Control Circuitry. *Pain* **158**:1938–1950.

Van Maanen MA, Papke RL, Koopman FA, Koepke J, Bevaart L, Clark R, Lamppu D, Elbaum D, LaRosa GJ, Tak PP, and Vervoordeldonk MJ (2015) Two novel α7 nicotinic acetylcholine receptor ligands: In vitro properties and their efficacy in collagen-induced arthritis in mice. *PLoS One* **10**:1–20.

Veldhoen RA, Banman SL, Odsen R, Simmen T, Simmonds AJ, Underhill DA, and Goping IS (2012) The chemotherapeutic agent paclitaxel inhibits autophagy through two distinct mechanisms that regulate apoptosis. *Oncogene* **32**:736–746, Nature Publishing Group.

Wagener TL, Floyd EL, Stepanov I, Driskill LM, Frank SG, Meier E, Leavens EL, Tackett AP, Molina N, and Queimado L (2017) Have combustible cigarettes met their match? The nicotine delivery profiles and harmful constituent exposures of second-generation and third-generation electronic cigarette users. *Tob Control* **26**:e23–e28.

Wang H, Yu M, Ochani M, Amella CA, Tanovic M, Susarla S, Li JH, Wang H, Yang H, Ulloa L, Al-Abed Y, Czura CJ, and Tracey KJ (2003) Nicotinic acetylcholine receptor alpha7 subunit is an essential regulator of inflammation. *Nature* **421**:384–388.

Warren GW, Romano MA, Kudrimoti MR, Randall ME, McGarry RC, Singh AK, and Rangnekar VM (2012) Nicotinic modulation of therapeutic response *in vitro* and *in vivo*. *Int J Cancer* **131**:2519–2527.

Webster MR, Xu M, Kinzler KA, Kaur A, Appleton J, O'Connell MP, Marchbank K, Valiga A, Dang VM, Perego M, Zhang G, Slipicevic A, Keeney F, Lehrmann E, Wood W, Becker KG, Kossenkov A V., Frederick DT, Flaherty KT, Xu X, Herlyn M, Murphy ME, and Weeraratna AT (2015) Wnt5A promotes an adaptive, senescent-like stress response, while continuing to drive invasion in melanoma cells. *Pigment Cell Melanoma Res* **28**:184–195.

Wieslander G, Norbäck D, and Lindgren T (2001) Experimental exposure to propylene glycol mist in aviation emergency training: Acute ocular and respiratory effects. *Occup Environ Med* **58**:649–655.

Wilkerson JL, Ghosh S, Bagdas D, Mason BL, Crowe MS, Hsu KL, Wise LE, Kinsey SG, Damaj MI, Cravatt BF, and Lichtman AH (2016) Diacylglycerol lipase β inhibition reverses nociceptive behaviour in mouse models of inflammatory and neuropathic pain. *Br J Pharmacol* **173**:1678–1692.

Wu S, Lv Y, Lin B, Luo L, Lv S, Bi A, and Jia Y (2013) Silencing of periostin inhibits nicotine-mediated tumor cell growth and epithelial-mesenchymal transition in lung cancer cells. 875–880.

Xie YX, Bezard E, and Zhao BL (2005) Investigating the receptor-independent neuroprotective mechanisms of nicotine in mitochondria. *J Biol Chem* **280**:32405–32412.

Xin M, and Deng X (2005) Nicotine inactivation of the proapoptotic function of Bax through phosphorylation. *J Biol Chem* **280**:10781–10789.

Yagoubian B, Akkara J, Afzali P, Alfi DM, Olson L, Conell-Price J, Yeh J, Eisig SB, and Flood P (2011) Nicotine Nasal Spray as an Adjuvant Analgesic for Third Molar Surgery. *J Oral Maxillofac Surg* **69**:1316–1319.

Yalcin I, Bohren Y, Waltisperger E, Sage-Ciocca D, Yin JC, Freund-Mercier MJ, and Barrot M (2011) A time-dependent history of mood disorders in a murine model of neuropathic pain. *Biol Psychiatry* **70**:946–953, Elsevier Inc.

Yoo SS, Lee SM, Do SK, Lee WK, Kim DS, and Park JY (2014) Unmethylation of the CHRNB4 gene is an unfavorable prognostic factor in non-small cell lung cancer. *Lung Cancer* **86**:85–90, Elsevier Ireland Ltd.

Yu V, Rahimy M, Korrapati A, Xuan Y, Zou AE, Krishnan AR, Tsui T, Aguilera JA, Advani S, Crotty Alexander LE, Brumund KT, Wang-Rodriguez J, and Ongkeko WM (2016) Electronic cigarettes induce DNA strand breaks and cell death independently of nicotine in cell lines. *Oral Oncol* **52**:58–65, Elsevier Ltd.

Zeng F, Li YC, Chen G, Zhang YK, Wang YK, Zhou SQ, Ma LN, Zhou JH, Huang YY, Zhu WY, and Liu XG (2012) Nicotine inhibits cisplatin-induced apoptosis in NCI-H446 cells. *Med Oncol* **29**:364–373.

Zhang H, Boyette-Davis JA, Kosturakis AK, Li Y, Yoon SY, Walters ET, and Dougherty PM (2013) Induction of monocyte chemoattractant protein-1 (mcp-1) and its receptor ccr2 in primary sensory neurons contributes to paclitaxel-induced peripheral neuropathy. *J Pain* **14**:1031–1044, Elsevier Ltd.

Zhang H, Li Y, de Carvalho-Barbosa M, Kavelaars A, Heijnen CJ, Albrecht PJ, and Dougherty PM (2016) Dorsal root ganglion infiltration by macrophages contributes to paclitaxel chemotherapy induced peripheral neuropathy. *J Pain* 1–12, Elsevier Inc.

Zhang J, Kamdar O, Le W, Rosen GD, and Upadhyay D (2009) Nicotine induces resistance to chemotherapy by modulating mitochondrial signaling in lung cancer. *Am J Respir Cell Mol Biol* **40**:135–146.

Zhang Q, Tang X, Zhang Z-F, Velikina R, Shi S, and Le AD (2007) Nicotine Induces

Hypoxia-Inducible Factor-1α Expression in Human Lung Cancer Cells via Nicotinic Acetylcholine Receptor–Mediated Signaling Pathways. *Clin Cancer Res* **13**:4686–4694.

Zhao J, Xin M, Wang T, Zhang Y, and Deng X (2009) Nicotine Enhances the Antiapoptotic Function of Mcl-1 through Phosphorylation. *Mol Cancer Res* **7**:1954–1961.

Zheng FY, Xiao WH, and Bennett GJ (2011) The response of spinal microglia to chemotherapy-evoked painful peripheral neuropathies is distinct from that evoked by traumatic nerve injuries. *Neuroscience* **176**:447–454.

Zheng Y, Ritzenthaler JD, Roman J, and Han S (2007) Nicotine Stimulates Human Lung Cancer Cell Growth by Inducing Fibronectin Expression. *Am J Respir Cell Mol Biol* **37**:681–690.

APPENDIX 1

SUPPLEMENTAL DATA WITH NICOTINE IN LUNG CANCER CELLS

Appendix 1A: Nicotine and Lung Tumor Cell Dormancy

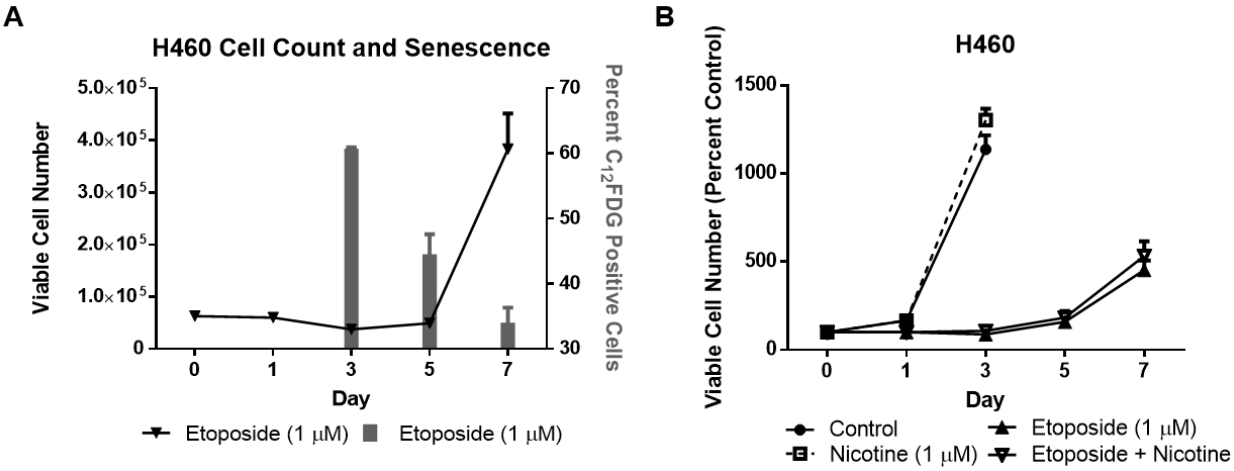

Supplementary Figure 8. Nicotine does not accelerate proliferative recovery of senescent/dormant H460 cells. A) The Gewirtz laboratory has shown that the cancer chemotherapy drug etoposide (1 μM), a topoisomerase II poison, can induce a transient, senescent growth arrest in H460 NSCLC cells (manuscript in preparation), which has also been reproduced here. H460 cells were treated with etoposide for 24 hours (Day 0 to Day 1), then the drug was removed and replaced with fresh medium. Viable cell number was determined via trypan blue exclusion (left y-axis) and percentage of senescent (C_{12}FDG-positive) cells was determined by flow cytometry (right y-axis). Data are expressed as the mean ± SEM of one experiment. B) The Day 0 time point represents the initial number of H460 cells after seeding. A 24-hour etoposide pretreatment period occurred from Day 0 to Day 1 for the etoposide and etoposide + nicotine conditions, then the nicotine and etoposide + nicotine samples were treated with nicotine for 24 hours from Day 1 to Day 2; no drugs were present after Day 2. The number of viable cells was determined via trypan blue exclusion. Data are expressed as the mean ± SEM of three independent experiments.

Appendix 1B: Nicotine Salt versus Nicotine Base

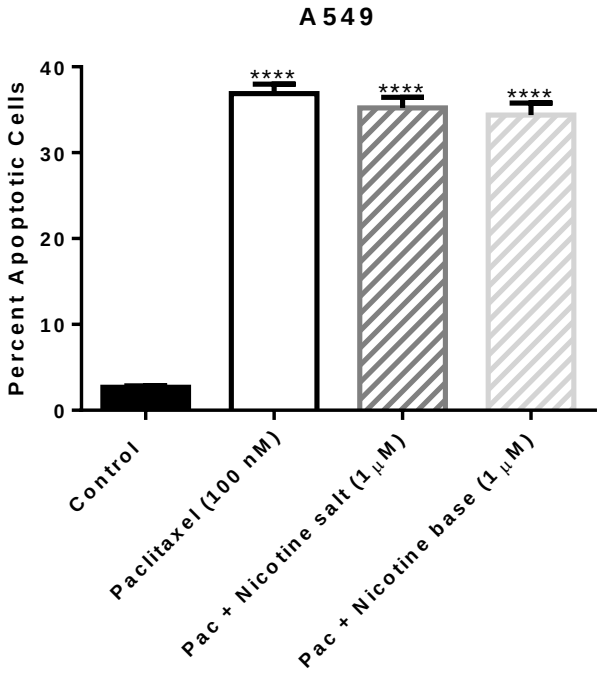

Supplementary Figure 9. Both nicotine hydrogen tartrate salt and nicotine free base fail to interfere with paclitaxel-induced apoptosis of A549 NSCLC cells. The free base formulation of nicotine is frequently used in cancer studies and was therefore tested here against the nicotine salt to ensure that this parameter does not influence the action of nicotine. A549 cells were treated with paclitaxel (100 nM) or the combination of paclitaxel and nicotine (1 μM) for 48 h. Quantification of apoptotic cells was determined by the Annexin V/PI assay and flow cytometry analysis. A one-way ANOVA was performed, followed by the Bonferroni post hoc test. ****$P <$ 0.0001 vs control; both combination treatments were found to not be significantly different from paclitaxel alone. Data are expressed as mean + SEM of one experiment.

Appendix 1C: The Effect of Nicotine on the Cell Cycle

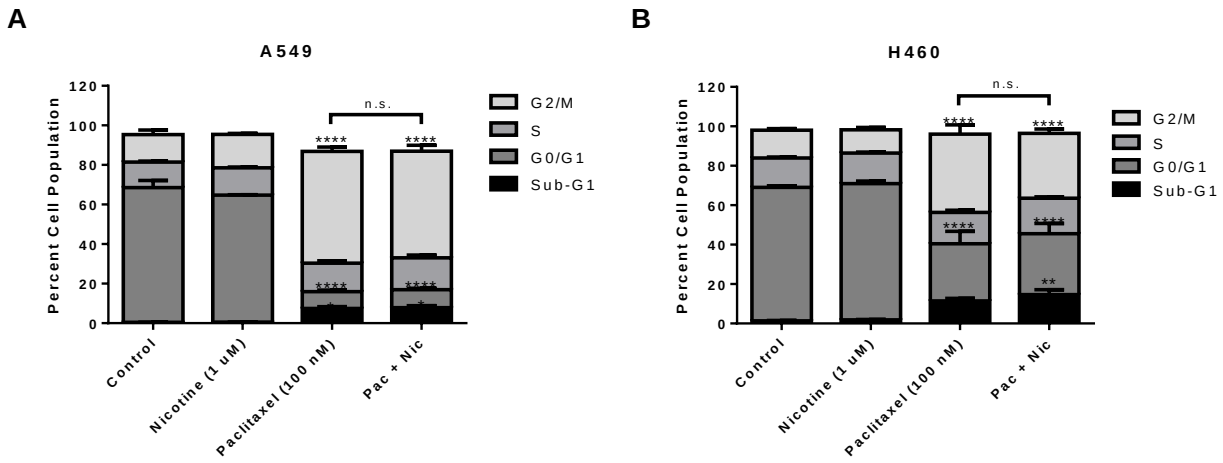

Supplementary Figure 10. Nicotine fails to interfere with paclitaxel-induced G2/M arrest of NSCLC cells. A549 (left) or H460 (right) cells were treated with nicotine, paclitaxel, or the combination for 48 hours. Cell cycle analysis was determined by propidium iodide staining and subsequent flow cytometry analysis. A two-way ANOVA was performed, followed by the Bonferroni post hoc test. *P < 0.05, **P < 0.01, ****P < 0.0001 vs control. Data are expressed as the mean ± SEM of two independent experiments. Nic, nicotine; n.s., not significant.

APPENDIX 2

TUMOR-BEARING ANIMAL MODELS

Appendix 2A: Lewis Lung Carcinoma Cells are Resistant to Paclitaxel

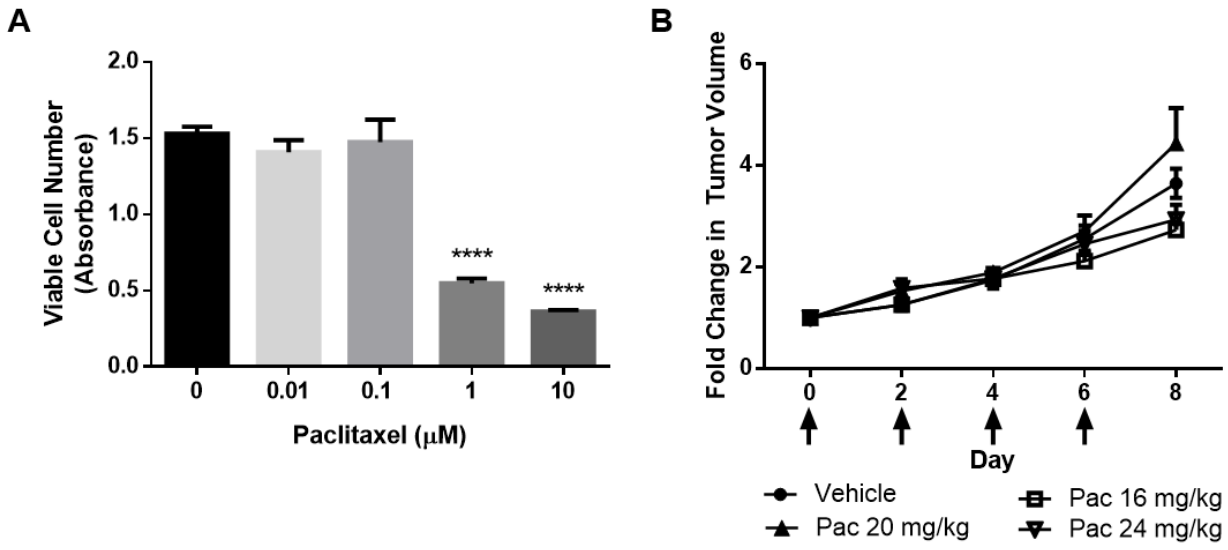

Supplementary Figure 12. Lewis lung carcinoma (LLC) cells are resistant to paclitaxel *in vitro* and *in vivo*. A) LLC were treated with various concentrations of paclitaxel for 24 hours, then allowed to grow for 24 hours before viability was assessed with the MTS assay. A one-way ANOVA was performed, followed by the Bonferroni post hoc test. ****$P < 0.0001$ vs control (0 μM paclitaxel). Data are expressed as mean + SEM of one experiment. B) C57BL/7J male mice were subcutaneously injected with 1.25×10^6 cells in each flank. Once tumors became palpable, mice were given paclitaxel (16-24 mg/kg, i.p.) every other day for a total of 4 injections, starting on day 0. The left and right flank tumor volumes (*l* x *w* x *h*) were determined with calipers and compared to the respective baseline tumor volumes to calculate fold change; the fold change values were averaged for each mouse. n = 7 mice per group. Data are expressed as mean + SEM. Pac, paclitaxel.

Appendix 2B: Mechanical Allodynia in Tumor-Bearing Mice

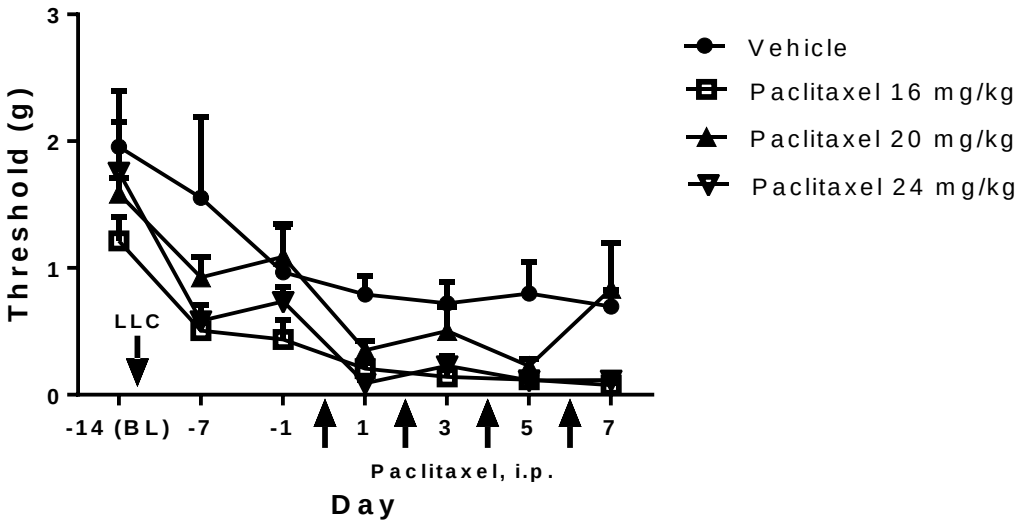

Supplementary Figure 13. Mice exhibit mechanical allodynia following Lewis lung carcinoma (LLC) inoculation and vehicle or paclitaxel injections. C57BL/7J male mice were subcutaneously injected with 1.25 x 10^6 cells in each flank on day -13. Once tumors became palpable, mice were given paclitaxel (16-24 mg/kg, i.p.) every other day for a total of 4 injections, starting on day 0. Mechanical threshold was determined with von Frey filaments and is described in grams of force. A two-way ANOVA was significant for time ($P < 0.0001$) and treatment ($P < 0.0001$), but there was no significant interaction between the two ($P = 0.8947$). n = 7 mice per group. Data are expressed as mean + SEM. BL, baseline.

Appendix 2C: Dose-response of Paclitaxel in NOD *scid* gamma (NSG) Mice

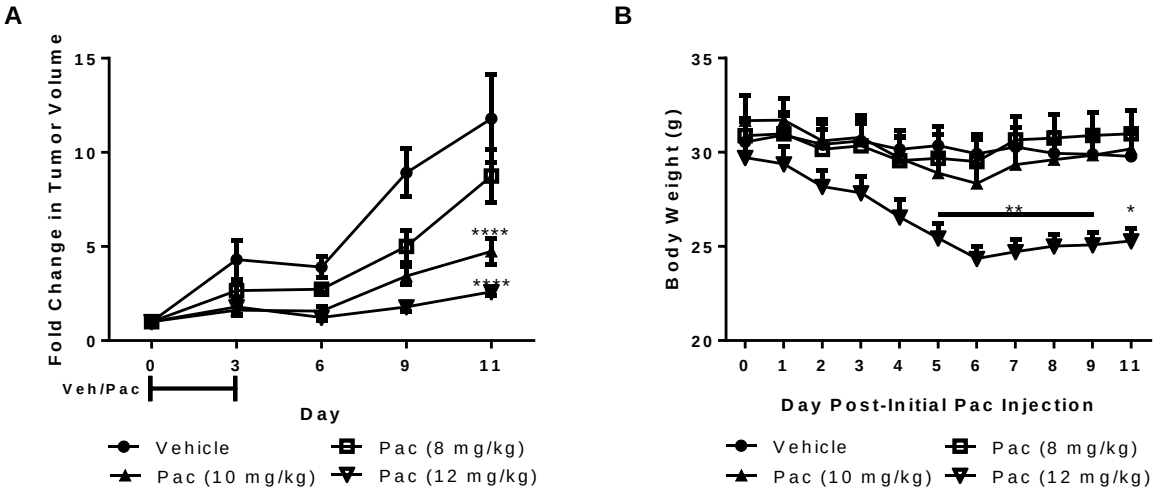

Supplementary Figure 14. Paclitaxel dose-dependently decreases A549 NSCLC tumor volume in NSG mice. Mice were subcutaneously injected with 1.5 x 10^6 cells in each flank. Once tumors became palpable, mice were given paclitaxel (8-12 mg/kg, i.p.) daily for 4 days starting on day 0. A) The left and right flank tumor volumes (*l* x *w* x *h*) were determined with calipers and compared to the respective baseline tumor volumes to calculate fold change; the fold change values were averaged for each mouse. B) Body weight was monitored before, during, and after paclitaxel administration. Two-way ANOVAs were performed, followed by Bonferroni post hoc tests. **P* < 0.05, ***P* < 0.01, *****P* < 0.0001 vs Vehicle. n = 5 mice per group. Data are expressed as mean + SEM. Veh, vehicle; Pac, paclitaxel.

Appendix 2D: Oral Gavage Induces Weight Loss in NSG Mice

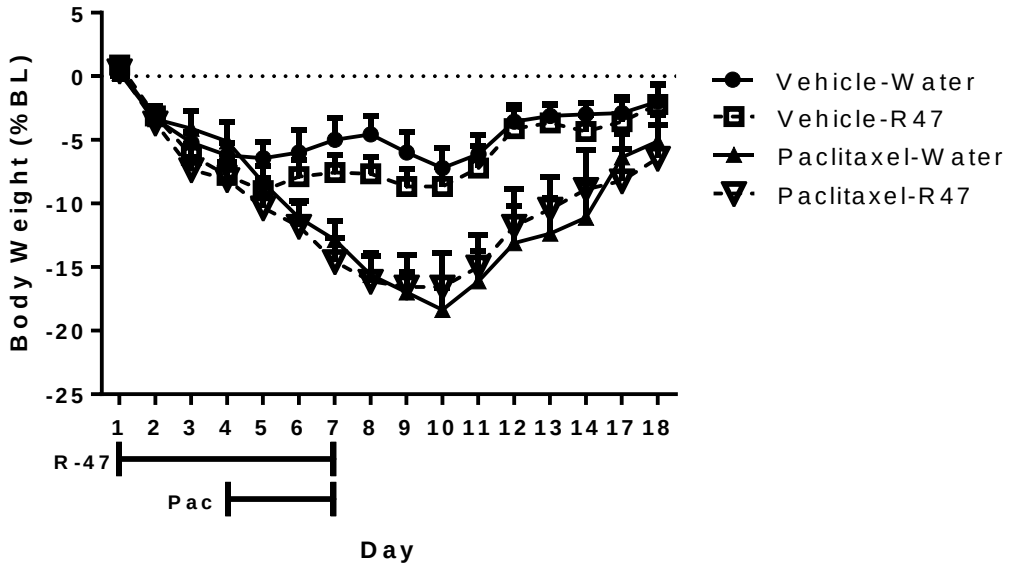

Supplementary Figure 15. Oral gavage induced weight loss in NSG mice. Mice received water or R-47 via oral gavage twice a day for 3 days, starting on day 1, and daily for 4 days, starting on day 4. Body weight was monitored before (baseline), during, and after drug administration. A two-way ANOVA was performed, followed by Bonferroni post hoc tests, to reveal no significant differences between Vehicle-Water vs Vehicle-R47 and Paclitaxel-Water vs Paclitaxel-R47, indicating that R-47 is not causing weight loss. n = 8-9 mice per group. Data are expressed as mean + SEM. BL, baseline; Pac, paclitaxel.

APPENDIX 3

SUPPLEMENTAL DATA WITH NICOTINE IN NEUROBLASTOMA CELLS

Appendix 3A: The Effect of Nicotine on Autophagy

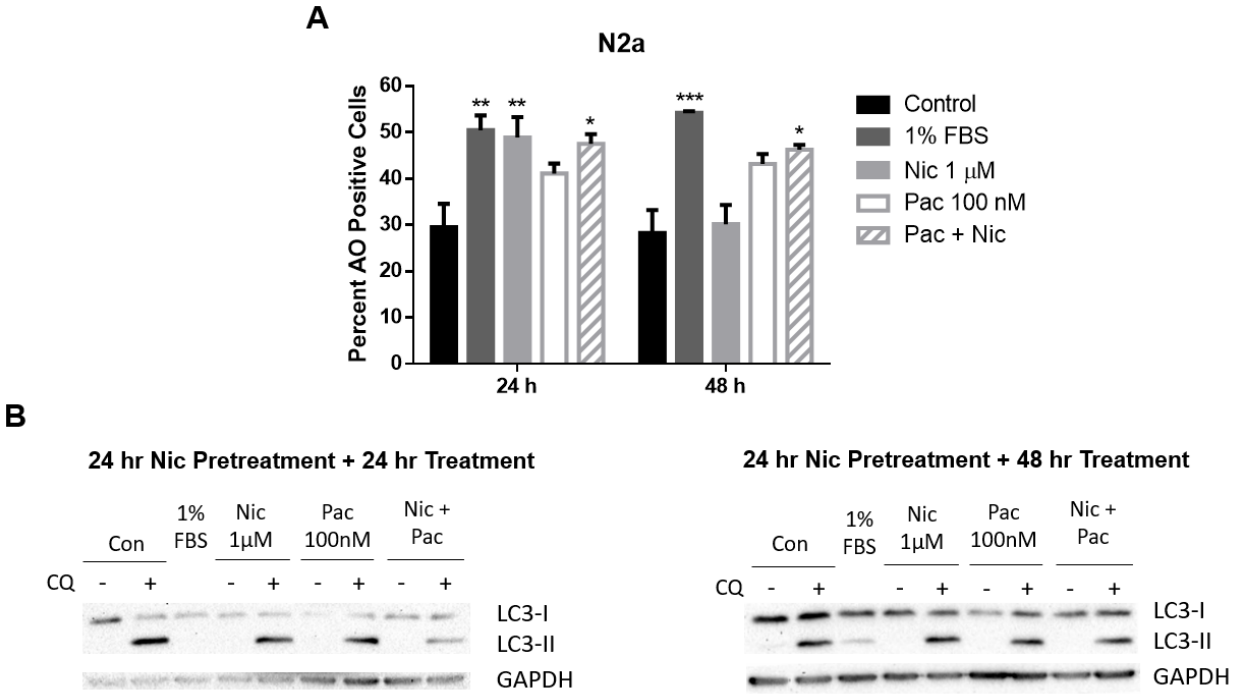

Supplementary Figure 16. Nicotine transiently increases autophagic vesicle formation, but both nicotine and paclitaxel appear to reduce autophagic flux in N2a neuroblastoma cells. The nicotine- and paclitaxel + nicotine-treated cells were exposed to nicotine (1 μM) for 24 hours. Then the paclitaxel- and nicotine + paclitaxel-treated cells were exposed to paclitaxel (100 nM) for 24 or 48 hours. Serum deprivation (1% FBS as opposed to 10% FBS used in the other conditions) was tested as a positive control. A) Cells were stained with acridine orange, a marker of acidic vesicles, then analyzed via flow cytometry. A two-way ANOVA was performed, followed by a Bonferroni post hoc test. **P* < 0.05, ***P* < 0.01, ****P* < 0.001 vs control. Data are expressed as mean ± SEM of one experiment. B) For the western blot analysis, one sample of each condition was treated with chloroquine (50 μM) for 4 hours prior to protein collection in order to inhibit fusion of the autophagosome with the lysosome. LC3-I is cytoplasmic and LC3-II is expressed on the surface of autophagosomes, then degraded upon fusion of the autophagosome with the lysosome. GAPDH was used as a loading control. AO, acridine orange; Con, control; CQ, chloroquine; FBS, fetal bovine serum; Nic, nicotine; Pac, paclitaxel.

VITA

Sarah Lauren Kyte was born on April 27, 1993 in Henrico County, Virginia and is an American citizen. She graduated from Powhatan High School in Powhatan, Virginia in 2011. She received her Bachelor of Science in Chemistry from Christopher Newport University in Newport News, Virginia in 2014. In the fall of 2014, she entered the Biomedical Sciences Doctoral Portal in the School of Medicine at Virginia Commonwealth University and joined the laboratory of Dr. David A. Gewirtz in the summer of 2015.

Education

Aug 2014 – Aug 2018
Virginia Commonwealth University (VCU), Richmond, VA
Doctor of Philosophy, Pharmacology and Toxicology

Aug 2011 – May 2014
Christopher Newport University (CNU), Newport News, VA
Bachelor of Science, *magna cum laude*, Chemistry

Research Experience

Mar 2015 – Aug 2018
Graduate Researcher, Dr. David A. Gewirtz, VCU

- Collected and analyzed data while investigating the pharmacological action of novel therapeutic agents for chemotherapy-induced peripheral neuropathy, a toxic side effect of cancer chemotherapy, with 6 *in vitro* assays and 2 mouse models of cancer
- Contributed to the preparation of 10 research grants, 2 of which I was the sole author, that resulted in $1,100,000 of research funding, including an F31 award
- Prepared 7 manuscripts and 2 book chapters, including 5 first-author/co-first-author publications
- Interpreted data of >50 publications regarding my dissertation project in order to write a comprehensive review article (currently under review)
- Presented data at 8 local and international conferences, including an oral presentation at the American Association for Cancer Research Annual Meeting in 2017
- Peer reviewed 6 research articles for multiple scientific journals, including: Cancer Letters, Pharmacological Research, International Journal of Nanomedicine, Journal of Pain Research, and Neuroscience Letters
- Taught cell culture and animal study procedures to 3 graduate students and mentored 1 undergraduate student
- Managed the laboratory: ordered supplies, prepared for inspections, wrote/edited IACUC animal protocols, etc. from Jan 2016-Aug 2018

Jan 2015 – Mar 2015
Graduate Researcher (Lab Rotation), Dr. M. Imad Damaj, VCU

- Characterized the acute and chronic behavioral effects of cancer chemotherapy drugs in mice
- Learned and performed 5 routes of drug administration, including osmotic minipump implantation, and 5 behavioral tests in mice

Sept 2014 – Nov 2014
Graduate Researcher (Lab Rotation), Dr. Matthew C.T. Hartman, VCU

- Learned and conducted 4 protein cyclization, validation, and purification techniques

Jan 2014 – Apr 2014
Undergraduate Researcher, Dr. Arunkumar K. Sharma, CNU

- Computationally simulated protein-protein interactions involved in Alzheimer's Disease

Sept 2012 – Apr 2013
Undergraduate Researcher, Dr. Jeffrey M. Carney, CNU

- Synthesized biologically active compounds utilizing organic chemistry

Grants

Jan 2018 – Jan 2021
F31 Ruth L. Kirschstein National Research Service Award

Distinctions

Jun 2017
Best Student Presentation Award Honorable Mention, Virginia Academy of Science

Jun 2016
Best Student Presentation Award, Virginia Academy of Science

Mar 2016
Charles C. Clayton Fellowship, Virginia Commonwealth University

Apr 2014
ACS Outstanding Chemistry Student Award, American Chemical Society

Professional Organizations

Jan 2018 – Present
Member, Society for Research on Nicotine and Tobacco

Aug 2017 – May 2018
Secretary, Pharmacology and Toxicology Student Organization at VCU

Jan 2017 – Aug 2018
Professional Development Chair and Member, Neuroscience Interest Group at VCU

Jan 2016 – Present
Secretary of Medical Sciences Section (2017-18) and Member, Virginia Academy of Science

Dec 2015 – Present
Member, American Association for Cancer Research

Courses

July 2016
National Institutes of Health Clinical and Translational Research for PhD Students

Community Service

Feb 2018-Aug 2018
Bible Study Group Leader, Passion Community Church, Midlothian, VA

Feb 2017
Science Fair Judge, Al Madina School of Richmond, Midlothian, VA

Aug 2013
Volunteer, Mary Washington Healthcare, Fredericksburg, VA

Publications

Bagdas D, **Kyte SL**, Toma W, Damaj MI. "Targeting Nicotinic Acetylcholine Receptors for the Treatment of Pain." *Neuroscience of Nicotine: Mechanisms and Treatments.* Elsevier, 2018; (in press).

Kyte SL and Gewirtz DA (2018). The influence of nicotine on lung tumor growth, cancer chemotherapy, and chemotherapy-induced peripheral neuropathy. *Journal of Pharmacology and Experimental Therapeutics*, 366: 303-313.

Curry ZA, Wilkerson JL, Bagdas D, **Kyte SL**, Patel N, Niphakis MJ, Hsu K, Cravatt BF, Gewirtz DA, Damaj MI, Lichtman AH (2018). Monoacylglycerol lipase inhibitors reverse paclitaxel-induced nociceptive behavior and proinflammatory markers in a mouse model of chemotherapy-induced neuropathy. *Journal of Pharmacology and Experimental Therapeutics*, 366: 169-183.

Cudjoe EK*, **Kyte SL***, Saleh T*, Landry JW, Gewirtz DA. "Autophagy Inhibition and Chemosensitization in Cancer Therapy." *Targeting Cell Survival Pathways to Enhance Response to Chemotherapy, Volume 3.* Ed. Daniel E. Johnson. Elsevier, 2018. pp. 260-275. *These authors contributed equally to this work.

Kyte SL*, Toma W*, Bagdas D, Meade JA, Schurman LD, Lichtman AH, Chen Z, Del Fabbro E, Fang X, Bigbee JW, Damaj MI, Gewirtz DA (2018). Nicotine prevents and reverses paclitaxel-induced mechanical allodynia in a mouse model of CIPN. *Journal of Pharmacology and Experimental Therapeutics*, 364: 110-119. *These authors contributed equally to this work.

Toma W*, **Kyte SL***, Bagdas D, Alkhlaif Y, Alsharari SD, Lichtman AH, Chen Z, Del Fabbro E, Bigbee J, Gewirtz DA, Damaj MI (2017). Effects of paclitaxel on the development of neuropathy and affective behaviors in the mouse. *Neuropharmacology*, 117: 305-315. *These authors contributed equally to this work.

Presentations

Kyte SL, Toma W, Thakur G, Damaj MI, Gewirtz DA. The α7 nicotinic acetylcholine receptor silent agonist R-47 prevents and reverses paclitaxel-induced peripheral neuropathy without enhancing the proliferation of lung cancer cells or interfering with paclitaxel-induced antitumor activity. **Poster presented at: American Association for Cancer Research Annual Meeting 2018; 2018 April 15; Chicago, IL.**

Kyte SL, Toma W, Thakur G, Bigbee JW, Damaj MI, Gewirtz DA. Are nicotinic acetylcholine receptors possible targets for the treatment of chemotherapy-induced peripheral neuropathy? **Poster presented at: Society for Research on Nicotine and Tobacco 24th Annual Meeting: 2018 Feb 24; Baltimore, MD.**

Kyte SL, Toma W, Damaj MI, Gewirtz DA. Targeting Nicotinic Acetylcholine Receptors for the Prevention and Reversal of Chemotherapy-Induced Peripheral Neuropathy. **Oral presentation at: Virginia Academy of Science 95th Annual Meeting; 2017 May 18; Richmond, VA.**

Kyte SL, Toma W, Damaj MI, Gewirtz DA. Targeting Nicotinic Acetylcholine Receptors for the Prevention and Reversal of Chemotherapy-Induced Peripheral Neuropathy. **Oral presentation at: American Association for Cancer Research Annual Meeting 2017; 2017 April 2; Washington, D.C.**

Kyte SL, Toma W, Damaj MI, Fang X, Gewirtz DA. Nicotine Prevents Chemotherapy-Induced Peripheral Neuropathy *in vivo*, and Fails to Stimulate the Growth of Lung Cancer Cells or Interfere with the Effectiveness of Chemotherapy *in vitro*. **Poster presented at: Virginia Academy of Science 94th Annual Meeting; 2016 May 19; Fredericksburg, VA.**

Kyte SL, Toma W, Damaj MI, Fang X, Gewirtz DA. Nicotine Prevents Chemotherapy-Induced Peripheral Neuropathy *in vivo*, and Fails to Stimulate the Growth of Lung Cancer Cells or Interfere with the Effectiveness of Chemotherapy *in vitro*. **Poster presented at: AACR Annual Meeting 2016; 2016 April 19; New Orleans, LA.**

Kyte SL, Toma W, Damaj MI, Gewirtz DA. Nicotinic Acetylcholine Receptor Agonists Fail to Stimulate Growth of Non-Small Cell Lung Cancer Cells or Interfere with the Effectiveness of Chemotherapy. **Poster presented at: VCU Massey Cancer Center 2015 Cancer Research Retreat; 2015 May 22; Richmond, VA.**